1998

Clay mineralogy, hydrochemistry and sedimentological history of the quaternary sediments of the St. Clair delta area (Michigan, Ontario).

Jamilh Mohammad. Mohsan
University of Windsor

INFORMATION TO USERS

This manuscript has been reproduced from the microfilm master. UMI films the text directly from the original or copy submitted. Thus, some thesis and dissertation copies are in typewriter face, while others may be from any type of computer printer.

The quality of this reproduction is dependent upon the quality of the copy submitted. Broken or indistinct print, colored or poor quality illustrations and photographs, print bleedthrough, substandard margins, and improper alignment can adversely affect reproduction.

In the unlikely event that the author did not send UMI a complete manuscript and there are missing pages, these will be noted. Also, if unauthorized copyright material had to be removed, a note will indicate the deletion.

Oversize materials (e.g., maps, drawings, charts) are reproduced by sectioning the original, beginning at the upper left-hand corner and continuing from left to right in equal sections with small overlaps.

Photographs included in the original manuscript have been reproduced xerographically in this copy. Higher quality 6" x 9" black and white photographic prints are available for any photographs or illustrations appearing in this copy for an additional charge. Contact UMI directly to order.

Bell & Howell Information and Learning
300 North Zeeb Road, Ann Arbor, MI 48106-1346 USA
800-521-0600

Clay Mineralogy, Hydrochemistry and Sedimentological History of the Quaternary Sediments of the St. Clair Delta Area

By

Jamilh Mohammad Mohsan

A thesis

Submitted to the

Faculty of Graduate Studies and Research

through the Department of Earth Sciences

in partial fulfillment of the requirements

for the degree of Master of Science

at the University of Windsor

Windsor, Ontario, Canada

1997

ABSTRACT

The St. Clair River delta, the largest in the Great Lakes area, is located astride the border between Michigan, United State of America (U.S.A), and Ontario Canada. It resembles a classic river-dominated delta system, with a typical "birds foot" morphology. The St. Clair River delta consists of six islands, from west to east: Seaway, Bassett, Squirrel, Walpole, the artificial Pottowatamie, and St. Anne. This study is performed on three continuous vertical sediments cores. The cores were taken along a north-south transect of Walpole island.

The St. Clair River delta is composed of a premodern and modern sediments. Sediments of the premodern delta were deposited from 3 500 to 5 000 B.P. at an elevated lake level. The sedimentation of modern sediments started about 3 500 B.P. and continues to this day. Beneath the delta, lacustrine and glaciolacustrine sediments are found. The lacustrine and glaciolacustrine sediments were deposited during the late Wisconsinan ice age. The advance and the retreat of the Laurentide Ice Sheet resulted in the formation of the lacustrine and glaciolacustrine sediments. These sediments are characterized by either varve-like or massive sediments.

The clay minerals of the clay fraction are determined to identify the glacial detrital sources, the sedimentary processes and the past environmental changes. The less than 2 μm clay fractions are dominated by illite, followed by chlorite, kaolinite, illite/smectite and smectite. The non-clay minerals of the less than 2μm clay fractions are dominated by quartz and sporadic trace amounts of plagioclase, K-feldspar, calcite, siderite and pyrite.

Two sites for shallow groundwater sampling were selected in the centre of Walpole Island to evaluate the environmental impact of the landfill and surficial disposal. Both sites were operated as an open garbage dumps for many years. Chemical analyses were performed on water samples to identify major ion concentrations, trace metals and ^{18}O and ^{13}C isotopic composition. Anomalous values were found for chloride, iron, manganese and arsenic. Groundwater flow direction is toward southeast of the study area and the data from the analysis delineate a young recharge (< 10 000 B.P.) similar to the present-day rainfall. Other possible sources may be the infiltration of St. Clair River or the infiltration from deeper geologic formations. The source of dissolved inorganic carbon in the water is related to C3 plant or Calvin photosynthetic cycles.

This work is dedicated to Hadi and Ali,
my husband and my son

ACKNOWLEDGMENT

I, first of all, would like to express my gratitude to Dr. Ihsan Al-Aasm, my thesis supervisor, for supervising my work on the St. Clair Delta. His assistance and support made this thesis possible. I am extremely thankful to Dr. W.H. Blackburn, my thesis co-supervisor who always found time to assist me.

I also wish to thank other people, Joanne Shwetz for her assistance during fieldwork, Ingrid Churchill for her help with the major ion and trace metal analyses, Julie Clark for her help with the isotopic extraction procedures, and Michelle Racz for her help with the sample preparation techniques for clay minerals.

My family, particularly my husband Dr. Hadi Al-Kahby gave me full encouragement and love. Without his understanding and guidance this project would not have been completed. Thanks to my sister Amal Abo-Jwhar, who helped me by watching my baby during my long working hours. Without her support and patience this work would have been postponed.

TABLE OF CONTENTS

LIST OF FIGURES

LIST OF TABLES

CHAPTER 1

INTRODUCTION

Background

Physiographically, the Province of Ontario is distinguished by two major regions: the Precambrian Canadian Shield and the Phanerozic borderlands (Fig. 1). The Canadian Shield has been subdivided from west to east into 3 divisions: the Severn Upland, which includes both the Nipigon plain and the Port Arthur hills, the Abitibi Upland, which comprises of the Cobalt plain and the Peneokean sudbury hills, and finally, the Laurentian highland which includes the Ottawa-Bonnechere Graben. The Ottawa-Bonnechere Graben, which is part of the St. Lawrance Graben, extends along the Ontario-Quebec border and is about 60 km wide. The Canadian Shield comprises Precambrian bedrock which was exposed to erosional episodes before the Paleozoic deposition took place about 570-250 million years ago (Johnson *et al.* 1992). Weathering episodes that followed the Paleozoic deposition during the Cretaceous (130-65 M.A). Periods of Quaternary glaciation were the principal agents that eroded the Precambrian rocks.

The borderlands of the province of Ontario can be defined as Lowlands bordering the Canadian Shield of Ontario. They have been subdivided into the Hudson Bay lowland and the St. Lawrence Lowland. In addition to these main divisions, the Moose River and the Appalachian basins are evident. These basins are shallow, gently dipping and have an elevation of 60 to 120 m with unconsolidated and organic-rich sedimentary rock sequences of Paleozoic age. The northwestern and the southeastern portion of the

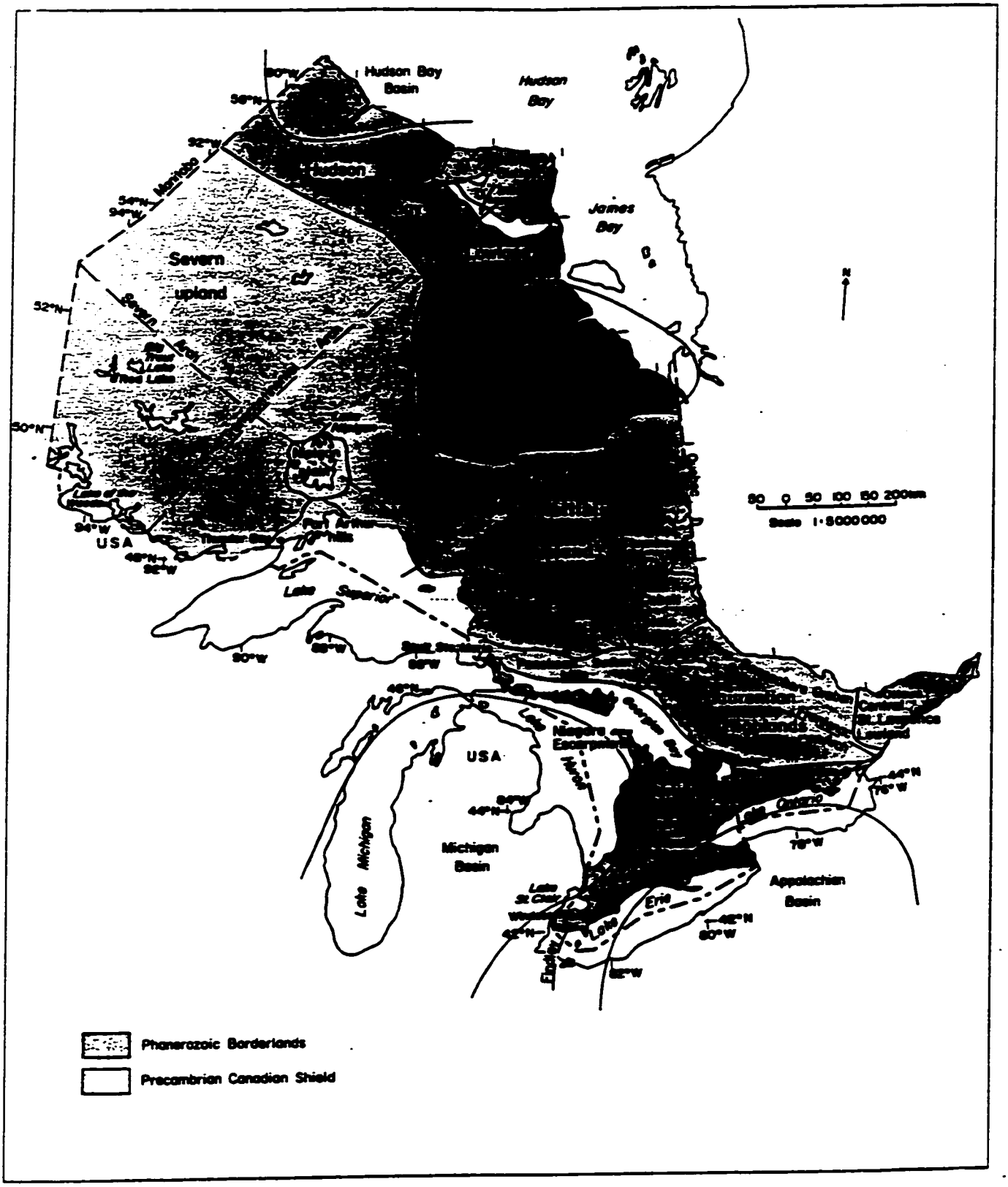

Fig. 1. Map of Ontario showing the physiographic regions (from Bostock 1970).

Hudson Bay Lowland are separated by the transcontinental Arch. The St. Lawrence Lowland border is divided into Western, Central and Eastern parts; only two parts (the Western and Central) occur within the Province of Ontario. Paleozoic and Mesozoic depositional and erosional successions occurred due to epicontinental sea invasion and withdrawal. The resultant sedimentary sequences include carbonate rocks, siliciclastic and evaporite deposits and the nondepositional gaps representing marine withdrawal. The approximate area that was covered by these sequences is 320 000 km^2 of the surface of Ontario.

The recent history of the Province of Ontario is related to the Quaternary Period, which started 1.8 million years ago (Barnett, 1992). The province of Ontario, and much of the Canadian landmass and that of the northern United States was covered by glacial ice. The consequences of the Quaternary glaciation played a role in removing sediment and soil, erosion of the bedrock and reshaping the surface by depositing a variety of sediments such as till, gravel, silt, and sand.

The Quaternary Period is represented by Pleistocene and Holocene epochs. The Pleistocene Epoch include the final glaciation and Holocene Epoch include the time 10 000 B.P. to the present (Barnett, 1992). Southwestern Ontario is covered by the Late Wisconsinan (as a last stage of Pleistocene) and Holocene sediments (Barnett, 1992). Because of the climatic fluctuations of Late Wisconsinan three stades (Port Bruce, Port Huron and Greaklakean), were generated by the advancing ice. They were separated by periods of retreating ice interstade (Mackinaw and Tow Creeks) (Fig. 2). The sediments deposited by advancing-retreating ice sheet are thick sequences of clayey, silt and sandy

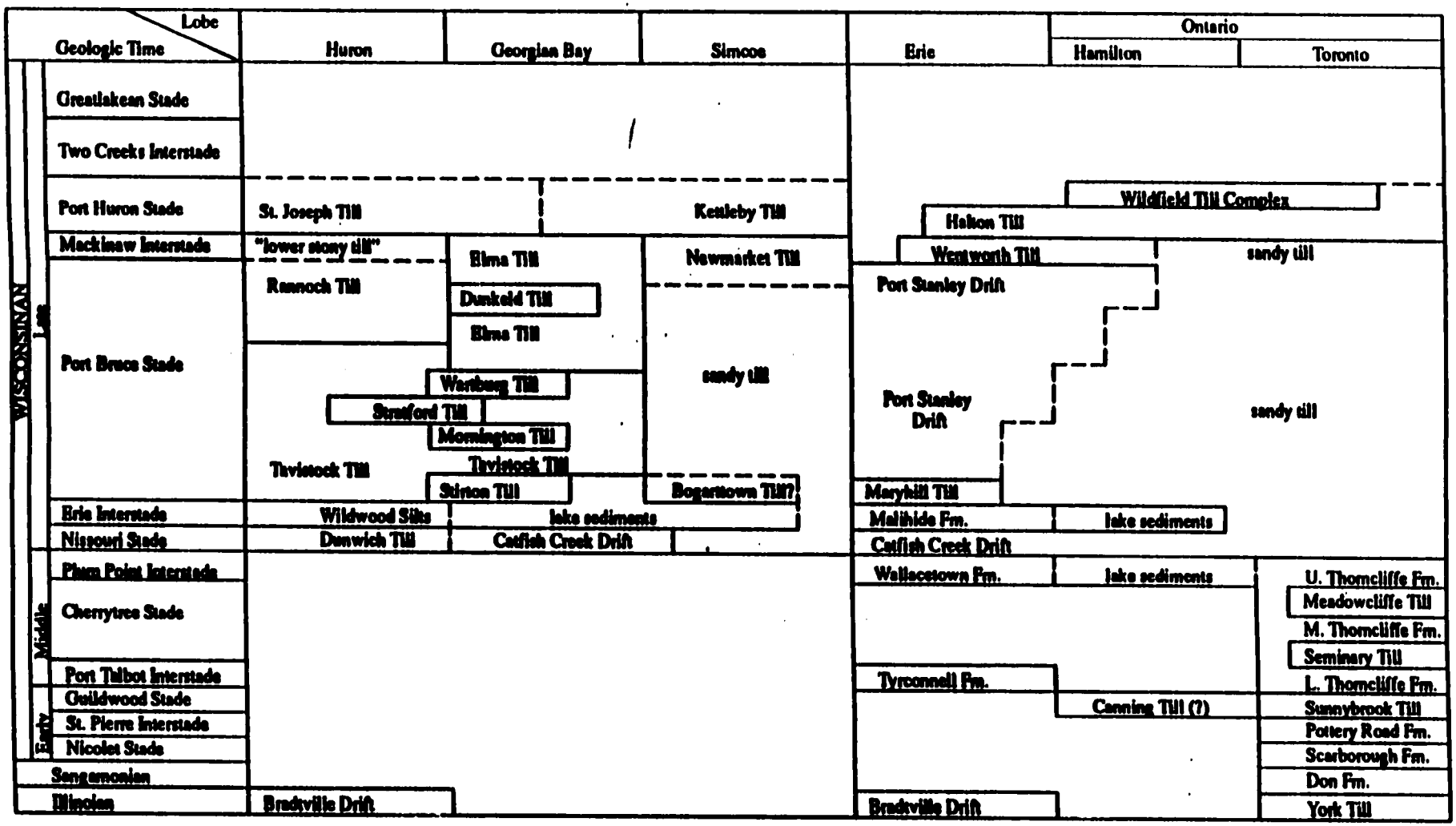

Fig. 2. Correlation chart for Southwestern Ontario (from Karrow 1989).

rhythmites, which were separated by the retreat ice laid down in a series of post glacial lakes. Lake Maumee IV was the only glacial lake that covered the present-day St. Clair Delta region (Bernett 1992) in the Port Bruce Stade. This was followed by Glacial Lake Arkona of the Mackinaw interstade. Glacial Lakes Whittlesey, Warren, Grassmere and Lundy of the Port Huron Stade were then succeively formed and, finally, Lake Algonquin of the Two Greeks Interstade (Hough 1958). The Holocene records contain various events such as the isostatic rebound of North Bay, which reduces water level in the great lakes by flow through the Ottawa River, occurred at the begining of this epoch and isostatic uplift took place about 5 000 Befor Present (B.P.). The Holocene uplift caused a closure of the North Bay outlet which increased the water level in Great Lakes and formed the Nipissing Great Lakes. During the Nipissing Great Lakes period, the St. Clair Delta deposits first began accumulating (Dorr and Eschman 1971; Flint 1971). Water budget reduction of the Great Lakes caused the upper 12 m of the St. Clair clay plain to be overconsolidated (Soderman and Kim 1970). The deposition of modern St. Clair sediments started about 3500 years ago.

Oxygen and deuterium isotopic data in ice cores and marine sediment have been used to study climatic evolution of the Quaternary. Oxygen isotope data obtained from the foraminifera shells of deep-sea cores represent the composition of ocean water in which they lived. The Quaternary period can be subdivided into 63 stages of various water compositions. The deuterium content of ice cores give an indication of the Quaternary period temperature as well as the changes in atmospheric composition through

Oxygen Isotope Stage *	Vostock Ice Core Stage *	Approximate Age (ka)	Classification following Dreimanis and Karrow (1972)		Approximate Radiocarbon Age
1	A		Holocene		
		10			
				Port Huron Stade	13
				Mackinaw Interstade	13.4
2	B		Late Wisconsinan	Port Bruce Stade	14.8
				Erie Interstade	15.5
				Nissouri Stade	20
		30			
				Plum Point Interstade	22+
3	C		Middle Wisconsinan	Cherryvue Stade	
				Port Talbot Interstade	>40
		60			
4	D			Guildwood Stade	
		75			
5a, b, c	E		Early Wisconsinan	St. Pierre Interstade	75
		105			
5d	F			Nicolet Stade	
		115			
5e	G		Sangamonian		
		135			
6	H		Illinoian		
		190			

* from Jouzel et al. 1989
* from Porter 1989

Fig. 3. Subdivision of Onrtario's Quaternary deposits (from Barnett 1992).

time. The first six youngest stages (Fig. 3) represent the Quaternary period of Ontario or the last 190 000 years ago (Barnett 1992).

Statements and Goals of the Project

The nature of clay transported by glaciers and then deposited as glacial, glacio-fluvial, glacio-lacustrine or glacio-marine sediment depends on the nature of the source rocks. Because the clay tills and glacial tills of the St. Clair Delta have never been exposed to industrial pollution knowledge of these tills and the chemistry of shallow groundwater around the garbage dump site, are the primary goals of this work. Three continuous cores were sampled along Walpole Island to identify the sedimentologic and stratigraphic sequence. Clay minerals and shallow groundwater were studied:

(1) To use clay minerals to interpret the geologic history and paleoenvironment of the area during the Quaternary time and

(2) To evaluate the environmental impact of the landfill on shallow groundwater by: (a) examining and quantifying trace metal in shallow groundwater, (b) examining and quantifying major ion concentrations in shallow groundwater and (c) quantifying and interpreting variation in groundwater ^{18}O and $^{13}C_{DIC}$.

Thesis Structure

This thesis is divided into 7 chapters and two appendices. Chapter 1 is the introduction which discusses background, objectives and reasons for conducting this study.

Chapter 2 provides physical description of the St. Clair Delta and includes the geographic and geomorphologic setting of the delta, description of the delta in particular physiographically, structurally and historically, and related studies and methods used in the investigation. Chapter 3 reviews the basic concepts related to clay mineralogy and phyllosilicates, selected clay samples and preparation and identification of clay minerals. Chapter 4 presents results of the study including core description, and clay fraction mineralogy distribution. Chapter 5 provides discussion of the paleoenvironment, and mineralogic variation of the St. Clair Delta sediments. Chapter 6 deals with the geochemistry of groundwater including chemical evolution of natural groundwater with discussion on groundwater chemistry, stable isotope chemistry and trace metal chemistry, the results and discussion which include major ion distribution, stable isotope distribution and trace metal distribution. Chapter 7 provides conclusions and recommendations.

CHAPTER 2
THE ST. CLAIR DELTA

Geographic and Geomorphologic Setting of the Study Area

The study area, Walpole Island of the St. Clair Delta, is located at latitude 42°35' N, longitude 82°30' W on the international boundry between Ontario and Michigan (Fig. 4). The formation and structure of the St. Clair River Delta is related to water levels in the Great Lakes and the flow regime of the St. Clair River. The water levels of the Great Lakes fluctuated particularly in Lakes Erie and Huron due to the abandonment of the Great Lakes outlet, which was blocked by a series of moraines and lake plains deposits during the late Wisconsinan ice retreat at about 13 000 B.P. (Raphael and Jaworski 1982). The present level of Lake Erie was established about 4000 B.P. and was followed by the establishment of the present level of Lake Huron.

The recent fluctuation in Lake St. Clair levels reflects water budgets in the Great Lakes basins and has affected the establishment and the morphology of the St. Clair River Delta. Another factor that has affected the St. Clair River Delta morphology is the St. Clair River flow regime with average water discharge 177,000 cubic feet per second, flow velocities up to 2 miles per hour and annual sediment load of 20 000 cubic yards (Raphael and Joworski 1982). The St. Clair River can be described as a strait that connects two lake basins because it does not drain the Huron basin by tributary system. Therefore, the St. Clair River cannot be defined as "a true" alluvial system and most sediments are made up of coarse sand and gravel (Pezzetta 1973; Raphael and Joworski 1982).

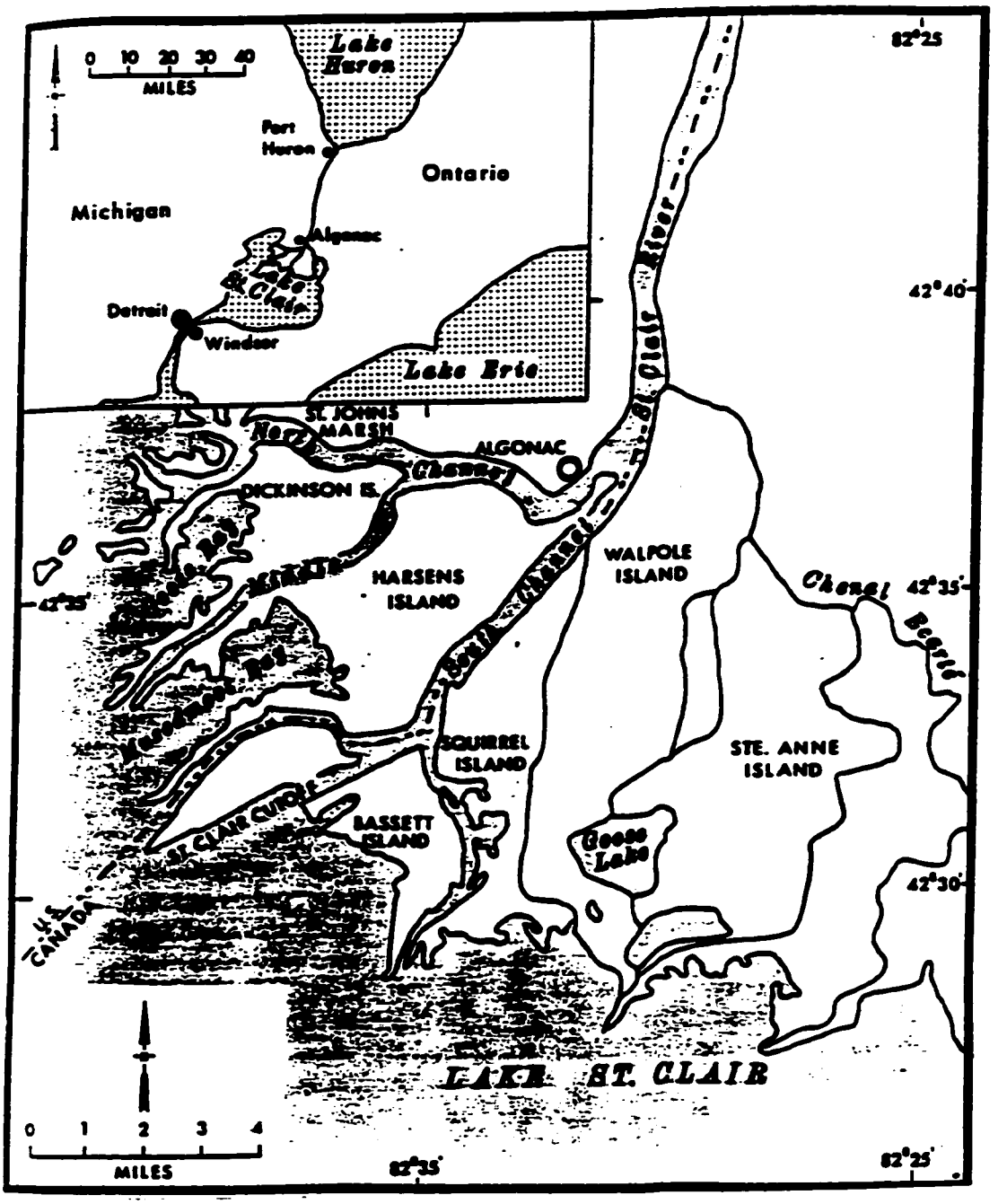

Fig. 4. The St. Clair River delta.

The most active distributary channels are the North, Middle and South Channels, Fig. 4, in the western part of the delta. These channels carry about 95% of the discharge. The only active channel in the eastern part is Chenal Écarté, which carries only 5% of the flow volume. The delta comprises six islands from west to east: Seaway, Bassett, Squirrel, Walpole, the artificial Pottowatamie, and St. Anne. Walpole Island is bounded to the east by the Chenal Ecarté, to the south by Lake St. Clair and to the west by St. Clair River. Walpole island covers 233 km^2 of uplands, marsh and water with 159 km^2 dry land (Ecologistics 1979). Walpole island is flat, low-lying and composed mostly of fine sandy soils. The ground level of the island is about 177 m above sea level; the highest ground occurs at Highbanks at the northern tip of Walpole Island and is 181 m above sea level. A high water table, at an elevation above lake level, is prevalent through out much of the island and results in poor drainage conditions (Wightman 1961).

Description of the St. Clair Delta

Physiography

The St. Clair deltaic plain is characterized by two distinctive sedimentary regions, an active portion which lies almost wholly within the U.S. territory and an inactive portion on the Canadian side of the international boundary (Pezzetta 1973).

The formation of a delta, according to Bhattacharya and Walker (1992), takes place "when a river of sediment-laden freshwater enters a standing body of water, loses its competence to carry sediment, and deposits it". The physical shape of a delta is

controlled by the density differences between the river and the standing body water, sediment grain size, coastal processes, climate, nature of the drainage basin, and the gradient of the shelf. The St. Clair Delta, which is located at the mouth of the St. Clair River, was formed by progradation of the north-eastern shoreline of Lake St. Clair. Progradation of the lake shoreline has created a modern, freshwater, lacustrine, birdfoot delta (Pezzetta 1973).

For descriptive purposes, deltas have been subdivided into: the delta plain, the delta front and the prodelta (Bhattacharya and Walker 1992). The delta plain, also known as the subaerial zone (Wightman 1961), is located behind the shoreline. As the main river enters this zone it may branch into small distributary channels that may meander. The meandering of the distributary channels may cause a deposition of well-sorted, upward-fining sand with cross-bedding. On both sides of the meandering stream levees composed of sands and silt are found. During spring floods, these levees may be breached resulting in the overflow of river water and the deposition of crevass splays in the interdistributary area. In the St. Clair Delta, because the water level fluctuates only 60 cm seasonally, levee deposits are poorly developed, and are less than 45 cm. in elevation (Raphael and Jaworski 1982).

The subaerial region of St. Clair Delta is a flat and featureless area (Pezzeta 1973). The highest portion is at the head of Walpole Island, where a bluff exists which is about 3.8 m above the level of Chenal Écarte (Wightman 1961). From these heights, the delta slopes gradually towards the south. The Canadian part of the St. Clair Delta consists of dry to slightly moist swamp areas and wet lands. The Chenal Ecarte and its

branch, Johnston Channel, are the main distributaries located along the eastern margin of the delta complex. The Chematogen and Bassett Channels lie along the western side of the delta (Pezzetta 1968). According to Wightman (1961), these distributaries are in equilibrium with the lake level and the present river gradient. Christensen (1993) concluded that the distributary channels, at certain intervals along their course, are up to six times deeper than the floor of the lake on the Canadian side of the delta and may be eleven times deeper than the lake depth on the U.S. side.

The delta front, known as the subaqueous delta (Wightman 1961), lies below the low-tide level. The delta front is the most active zone of the deltaic environment and is characterized by coarse sediments at the distibutary mouth and finer-grained sediments settling further offshore. The sediments of the delta front include both the sediments that were deposited at the distributary mouth and the sediment deposited further offshore. The distributary mouth sediments, or distributary mouth bars, are dominated by sands. The offshore sediments are called distal bars and are composed of very fine sands near the delta front and fine to silts and clays basinward. The repeated deposition at the mouth and distal bars results in a building of the delta front to open water so that coarser sediments of the mouth bar come to overlie finer sediments of the distal bar resulting in a general coarsening upward sequence (Tucker 1981). The most significant phenomenon of the St. Clair Delta is the fact that the distributary channels are much deeper than the lake basin (Pezzetta 1973; Rephael and Jaworski 1982; Christensen 1993). Christensen (1993) suggested a new model to explain this phenomenon, called the "burrowing-delta" model. The "burrowing-delta" model can

be defined as "a mechanism of delta progradation erosion at the channel-lake interface". The differential water densities of the St. Clair River as an outflow from Lake Huron and Lake St. Clair throughout the year are related to the temperature gradient of the flowing water. Lake Huron, St. Clair River and Lake St. Clair were investigated by Christensen (1993) in term of their water temperature. Christensen found that the water of Lake Huron is the coldest and as it flows south in the St. Clair River, toward the St. Clair Basin, it carries a sand-sized sediment load in traction. As this water enters the delta plain, it starts to flow into the distributary channels or 'burrow' channels, which encounters the Lake St. Clair with high velocity because of the shallow lake bed level. The resultant process is that the cooler, dense water produces an underflow current, which lies below the warmer upper layer of lake water. The underflow currents erode the lake bed to form a shallow underflow notch channel which progrades into the lake.

The prodelta is located in the basinward region; sediments which settle out in this zone mostly are in suspension and fine-grained material charactarizes of this region.

Structural Setting of the St. Clair Delta

The St. Clair Delta is situated astride the Algonquin Arch to the northeast; and the Findlay Arch to the southwest. Three significant structures are present in the St. Clair Delta region: the Electric and Dawn faults, and the Kimball-Colinvill monocline (Fig. 5). The Electric fault trends west to east through the southern part of the delta,

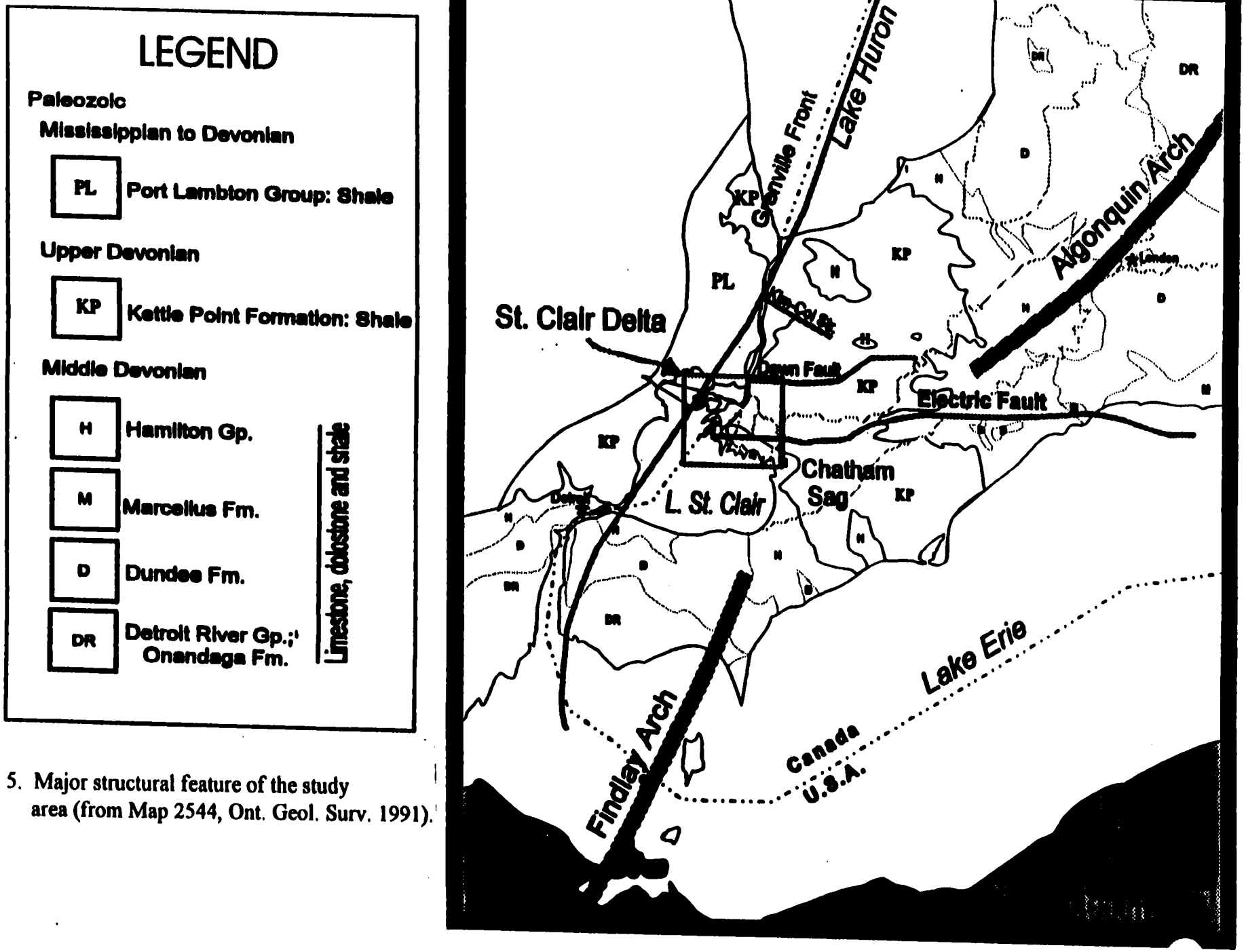

Fig. 5. Major structural feature of the study area (from Map 2544, Ont. Geol. Surv. 1991).

and extends eastward into Lake Erie. The Electric fault has a near vertical plane with a displacement of 84 m, downthrown to the south (Brigham 1971). The fault is Early Ordovician in age, with movement continuing through the Silurian (MacGregor 1980). The Dawn Fault is located north of the Electric Fault and parallel to it. Farther north is the Kimball-Colinville monoclinic structure, which has a displacement of 43 m, downthrown to the southwest (Brigham 1971).

Origin and Age of The Delta

The Late Wisconsinan ice age is characterized by three periods of ice advance and retreat due to climatic fluctuations. The ice advance periods, referred to as Nissouri, Port Bruce and Port Huron Stadials, were separated by three interstadial events: the Erie, the Mackinaw and the Two Creeks. The maximum retreat of the Laurentide Ice Sheet took place during the Two Creeks Interstadial Sediments (12000 B.P.) (Bernett 1992), or approximately since the time of formation of earliest Lake Algonquin (Pezzetta 1968). The earliest Lake Algonquin formation was as a result of the coalescence of the Lake Huron and Lake Michigan basins. Leverett and Taylor (1915) first suggested the possibility of two distinct periods of delta formation. Wightman (1961) concluded that the modern St. Clair delta is the second of a two stage phase of deltaic sedimentation within the St. Clair basin. The older stage (Delta 1) was formed during a time of high lake level in the St. Clair basin (late Main Algonquin 8000 B.P.). During the main Nippissing stage, conditions were suitable for the formation of a delta in the St. Clair basin which is considered to be the modern delta or Delta II of Wightman (1961).

The Nipissing Great Lakes basins has been divided into the Nipissing I, from 5500 to 4700 B.P. and the Nipissing II, from 4700 to 3700 B.P. (Lewis 1969). Lewis (1969, 1972) suggested the possibility of rising water level at the North Bay outlet and lowering water level at Port Huron during both Nipissing I and II. This resulted in a gradual water transfer and a consequent southward erosion. However, the high level at Port Huron lasted for a short period of time. With further falling of water level at about 3000 B.P. (Lewis 1969), Lake Algoma began to appear at about the present Great Lakes water level, i.e. about 181 m or 3 m below Nippissing water level (Hough 1958). Two periods of deltaic sedimentation, the premodern and modern, took place in the St. Clair basin (Table 1).

Table 1. Interpretation of the Events Related to the Origin of the St. Clair River Delta (Raphael and Jaworski 1982)

Approximate Date (B.P.)	Lake Stage	Event
3,500 to Present	Modern Lake St. Clair and Algoma Phase	Flow of Lake Huron continues outhward. Deposition of modern St. Clair River delta and dissection of premodern surface
3,500 to 5,000	Lake Nipissing	Deposition of premodren delta approximately five feet above present mean lake level.
5,000 to 10,500	Lake Stanley	Lake St. Clair basin exposed; outlet for upper Great Lakes via North Bay, Ontario.
10,500 to 12,500	Lake Algonquin and Post-Algonquin Phases	Valders Maximum.

Both the premodern and the modern deltaic sedimentation are underlain by approximately 30 m of clay till or lucustrine till. The tills of probable Wisconsinan age were deposited during the period of Lakes Whittlesey and Warren (Champman and Putnam 1951). The St. Clair basin till is typically either consolidated or overconsolidated, homogeneous and compressible (Soderman and Kim 1969). The clay deposits may reach 40% of the total glacial deposit. The lack of stratification and the scattering of pebbles are probably the result of periods of erosion and possible redeposition during more recent glacial acting on older lucustrine deposits (Dreimanis 1961). These tills are underlain by the Paleozoic limestones and black shales (Soderman and Kim 1969).

Review of Previous Work

Numerous scientific investigations have been conducted on the St. Clair Delta in general and on Walpole Island in particular. Cole (1903) concluded that the sandy deltaic deposits at the surface were underlain by deepwater, proglacial lake clays. Wightman (1961) proposed an approximate age for the formation of the delta and discussed the land-use and sediment discharge rate relative to the potential load which could be born by the hydrodynamics of the fluvial system. Pizzetta (1968) suggested that the sediments of the delta are derived from proximate source areas within a small drainage basin that is underlain by thick glacial deposits and that the delta is unique because it has formed at the mouth of a river which discharges from a large lake that is relatively free of sediment. Dominion Soil Investigations Inc. (1977a, 1977b) concluded that the water table throughout the delta is higher than the lake level. Ecologistics (1979) found that all the channels, ponds, bays and

shallow waters of Lake St. Clair have good water quality and are highly susceptible to pollution originating from upstream and other nearby sources. Raphael and Jaworski (1982) studied the geomorphology of the delta and established a relationship between landforms and vegetation. Jiwani (1983) investigated the quality of groundwater on Walpole Island and concluded that shallow water is characterized by poor drinking quality. Christensen (1993) mapped Chenal Ecarte and Bassett and Johnston channels using side-scan sonar, and formulated a 'borrowing delta' model to explain the progradation of these distributary channels into Lake St. Clair. White (1993) and Al-Aasm *et* al. (1995) examined the isotope chemistry of carbonates, and the mineralogy of fine fractions from the sediments of Goose Lake, Johnston Bay, and Lake St. Clair. Racz (1994) characterized the grain size distribution and mineralogy of sediments from Johnston Channel and Chenal Ecarte. MacFarlane (1995) studied the cores (HP, GD and DC cores) used in this thesis and conducted a grain size analysis of cores GD and DC. Cumming (1995) and Cumming and Al-Aasm (1996) also studied the sedimentology and porewater isotope chemistry of cores used in this study. They concluded that porewater ^{18}O and D concentrations for all cores are unaffected by secondary processes such as evaporation prior to or during infiltration and mineral exchanges with the host sediment. Porewater $^{13}C_{DIC}$ concentration profiles for cores HP and GD show that advecting mixing and displacement processes have occurred. Core GD porewater $^{13}C_{DIC}$ concentrations are enriched indicating that hydraulic conductivity is higher due to micro-fracturing during the Holocene. The DC core $^{13}C_{DIC}$ concentration profile shows a predominantly mineralized, St. Clair River $^{13}C_{DIC}$ value signature near the surface, with rapid depletion with depth due to increased biological

activity such as bacterial respiration within the fractures. Dwyer (1997) studied the mineralogy of the surface deltaic sedimentation of the western channels and concluded that the dominant clay minerals are illite followed by chlorite and kaolinite. The non-clay minerals of clay fractions are quartz, feldspar and calcite.

Methodology

The samples used in this study were selected from three vertical sediment cores taken along a 14 km north-south transect of Walpole Island (Fig. 6). Detailed field investigation and sampling were performed on the three cores by Cumming (1995). The Heritage Sand Pits (HP Core, 28.42 m depth) located to the north of the Island. More southerly is the Garbage Dump core (GD Core, 41.75 m depth), which is located next to an active reserve garbage dump in the centre of Walpole Island. The third core, the most southern, is the Dynamite Cut Road (DC Core, 21.41 m depth).

Fifty-one unevenly spaced samples were taken from the three cores. Samples were taken to represent probable mineralogic changes as manifested by changes in colour, texture or structure of the sediment as described by Cumming (1995). Seventeen samples were taken from the HP core, twenty four from the GD core and ten from the DC Core. X-ray diffraction was the principal method of mineralogical analysis, and both the qualitative and quantitative data of clay fractions based on the interpretation of the x-ray data.

Groundwater was sampled at two sites on Walpole Island next to Core-GD. Water samples were collected by using a Single Sample Disposable Teflon® Bailer with

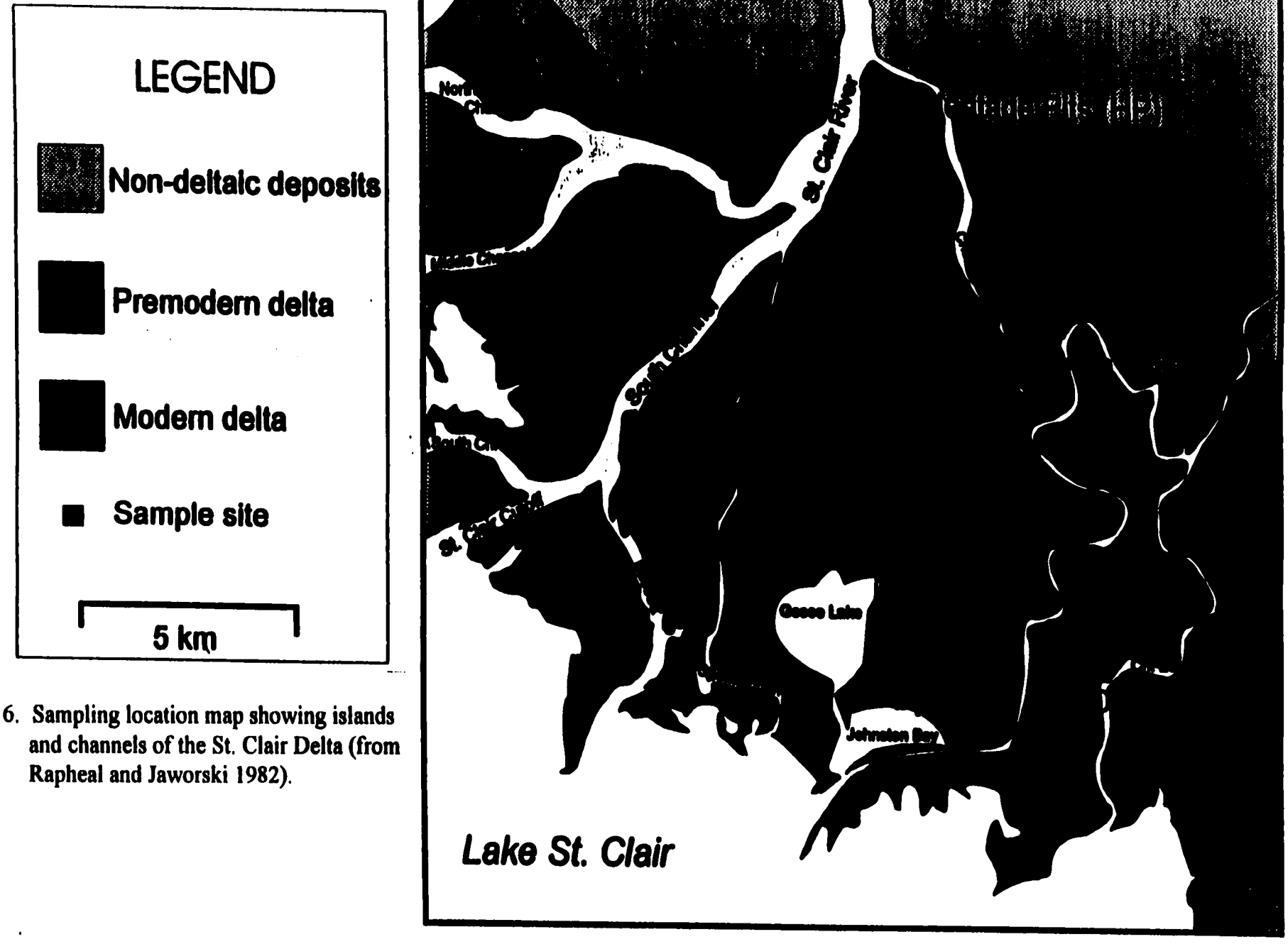

Fig. 6. Sampling location map showing islands and channels of the St. Clair Delta (from Rapheal and Jaworski 1982).

36" in length and 3" the interior diameter. The water samples were collected in pre-washed polyethylene bottles for the determination of stable isotopes (oxygen and carbon), major ions (carbonate, sulfate, chloride, calcium, magnesium, sodium and potassium) and trace metal (aluminum, arsenic, cadmium, cobalt, copper, iron, manganese, lead, vanadium, zinc, bismuth, chromium, nickel and antimony). Other parameters were such as the total dissolved solid, pH, and hydraulic conductivity measured in the field.

Groundwater $\delta^{18}O$ value determinations were made on CO_2 equilibrated with water at 25°C using a method outlined in Epstein and Mayeda (1953). CO_2 extraction was performed in the Stable Isotope Laboratory in the Department of Earth Sciences at the University of Windsor, while the actual $\delta^{18}O$ values were determined using mass spectrometry at the Isotope Laboratory of the Ottawa-Carleton Geoscience Centre at the University of Ottawa. The analytical precision for $\delta^{18}O$ analysis is better than 0.1‰.

Groundwater $\delta^{13}C_{DIC}$ values determination were made by using a method similar to that developed by Grabar and Aharon (1991) and the unpublished laboratory procedures of the Stable Isotope Laboratory at the Ottawa-Carleton Geoscience Centre at the University of Ottawa. Bicarbonate in solution is converted to CO_2 by adding water-free orthophosphoric acid. About 25 mL of water was required for each analysis. CO_2 extraction was performed in the Stable Isotope Laboratory at the University of Windsor, while the actual $\delta^{13}C_{DIC}$ values were determined at the Isotope Laboratory of the Ottawa-Carleton Geoscience Centre. The analytical precision for $\delta^{13}C_{DIC}$ analysis is better than 0.15‰.

The major dissolved cations in the groundwater (Ca^{2+}, Mg^{2+}, Na^{+} and K^{+}) and trace metals (Al, As, Cd, Co, Cu, Fe, Mn, Pb, V, Zn, Bi, Cr, Ni and Sb) were determined by ICP-OES ARL-Maxim and Graphite Furnace Atomic Absorption (GFAA) in the Great Lakes Institute for Environmental Research at the University of Windsor. The ICP data were taken for Ca, Fe, Mg, Mn, Na, V, Zn, Bi, Ni, Al, As and Sb. The precision of the ICP and GFAA of these elements are reported in the Appendix III, Table Al. The GFAA results were used for Al, Cd, Co, Cu, Pb and Cr.

Chloride concentrations were measured with an ORION 94-17B chloride electrode and Model 96-17B Combination Chloride Electrode Instruction Manual (see Appendix I for details).

Sulfate concentrations were determined by the Turbidimeteric Method using a PYE Unicam SP6-300 Spectrophotometer. Sulfate is precipitated by barium as $BaSO_4$ and the turbidity was measured on the spectrophotometer at 450 nm. The transmittance measurement of the sample is proportional to the SO_4^{2-} ion. The measurment procedure is reported in Appendix I.

And finally the alkalinity was determined according to the Standard Methods for the Examination of Water and Wastewater (APHA-AWWA-WPCF 1975). Appendix I contains the details.

CHAPTER 3
PHYLLOSILICATES STRUCTURE AND CLAY FRACTION MINERALOGY

Phyllosilicates and the Determination of Mineralogy of Clay Fraction

The sediments of the St. Clair Delta have been derived by glacial, fluvial and lacustrine erosion of Precambrian and Paleozoic rocks and Quaternary glacial sediments. Thus, the expected mineralogy of the sediments is the principal rock-forming minerals and their weathering products. The clay minerals of the clay-sized fraction are of special interest in this study because they can supply information on the glacial detrital sources, the sedimentary processes and past environmental changes.

The phyllosilicate mineral family can be defined as having silicon-, aluminum-, iron- or magnesium-coordinated layers stacked above each other. Clay minerals are a large subgroup of this family consisting of hydrous layer silicates. The characteristics which differentiate the various members of clay minerals are: the large ratio of surface area to volume and the platy morphology and perfect (001) cleavage (Moore and Reynolds 1989).

The structure of phyllosilicates consists of successive layers of Si-O tetrahedra in alteration with octahedral sheets. Each tetrahedron consists of a silicon located in the center and four oxygens occupying the corners. The tetrahedral sheet is connected with adjacent tetrahedra by sharing of its basal oxygens forming a hexagonal shape (Fig. 7a).

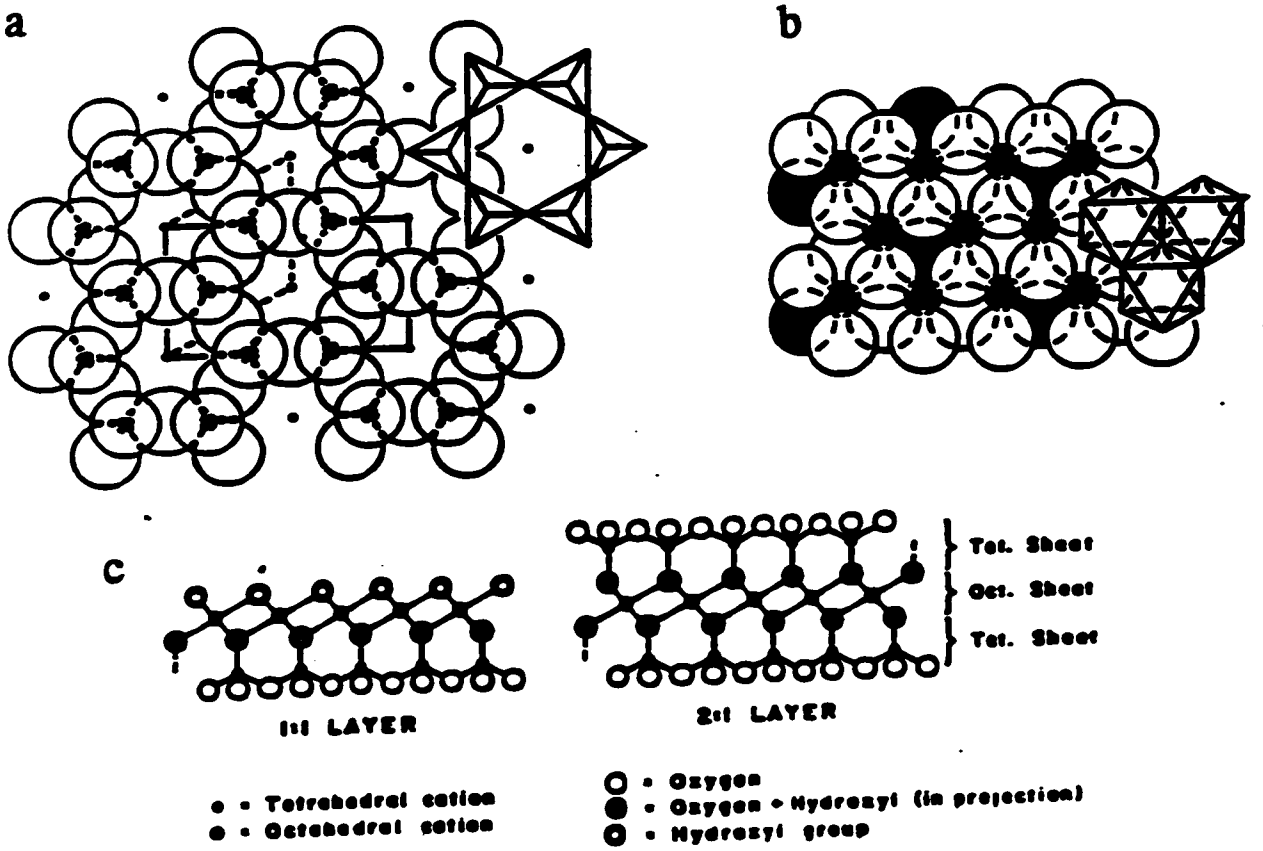

Fig. 7. A sketch showing (a) the tetrahedral sheet with hexagonal cells.
(b) the octahedral sheet with OH groups of lower anion plain.
(c) combination of sheets to form 1:1 and 2:1 layers (from Bailey 1980).

The apical oxygens point in a direction normal to the sheet to be shared with the adjacent octahedral sheet. The octahedral sheets comprise of Mg^{2+}, Fe^{2+} or Fe^{3+}, Al^{3+} at their centre and oxygens at the six corners. Each octahedral sheet connects with similar sheet in the opposite direction (Fig. 7b). Normally, the tetrahedral sheets are electrically neutral whereas the octahedral sheets can have a residual charge.

A minimum structure of an octahedra sheet consists of three octahedra and can be classified depending on the basis of the cation charge. Trioctahedral phyllosilicates have divalent cation such as Mg^{2+} or Fe^{2+} forming a complete structure with the hydroxyl ion being shared between the three octahedra. Trivalent cations such as Al^{3+} or Fe^{3+} form incomplete structures with each hydroxyl ion shared by two octahedra; such a structure is called dioctahedral.

A structure consisting of tetrahedral and octahedral sheets is called a layer structure and the main types of layer structure are tetrahedra-octahedra or T.O (1:1) structures and tetrahedra-octahedra-tetrahedra or T.O.T. (2:1) structures (Fig. 7c). The space between successive layers, called the interlayer, is either vacant when the structure is neutral or occupied by various cations such as K^+, Na^+, Mg^{2+} or Ca^{2+} for structures with a residual negative charge. Both the layer and interlayer comprise a structural unit with a thickness of 7 to 18 Å depending on the layer structure type.

Clay minerals may have layer charges on (001) surfaces and as a result of unsatisfied bonds on grain edges (Moore and Reynolds, 1989). These charges cause ions and molecules to be attracted to clay particles. Within the tetrahedral and octahedral layers, electrical charges may be the result of ionic substitution.

Substitution of trivalent for tetravalent, divalent for trivalent or univalent for divalent ions may generate layer charges. Interlayer cations or hydroxyl anions may satisfy the positive layer charge, and may result in disorder and instability. The substitution procedures give clay minerals a special characterization and properties such as adsorption, expandability and the formulation of organo-mineral complexes.

Clay minerals can be classified on the basis of layer structure and charge (Fig. 8). The kaolin-serpentine group has T.O. (1:1) layer structure with no or only a small layer charge. The tetrahedral sheet is occupied by Si^{4+} and the octahedral layer is based on Al^{3+} or Mg^{2+}. This group has no interlayer cation so the tetrahedral-octahedral layers have a special bonding to keep them together. Each layer has two surfaces: the basal oxygen of the silica tetrahedra and a surface of hydroxyls (different from the inner hydroxyl in the shared oxygen plane) which are part of the octahedra (Bailey 1988). The hydroxyl surface comes close to the basal oxygens of the adjacent layer, an arrangement that allows long hydrogen bonds to form between layers and gives structural stability.

As a main group, kaolin and serpentine contain a variety of species as a subgroup which differ in their orientation. Mineral species related to kaolin $Al_4Si_4O_{10}(OH)_8$ are kaolinite, dickite, nacrite, 7 Å-halloysite and 10 Å-halloysite. A negative charge can be found in this group because of interlayered smectite, vermiculite or mica. The serpentine minerals $(Mg,Fe)_3(Si_2O_5)(OH)_4$ are chrysotile, antigorite and lizardite. These minerals are often larger grain size than other clay minerals with silky (chrysotile) or platy (lizardite) habits (Moore and Reynolds 1989). 1989).

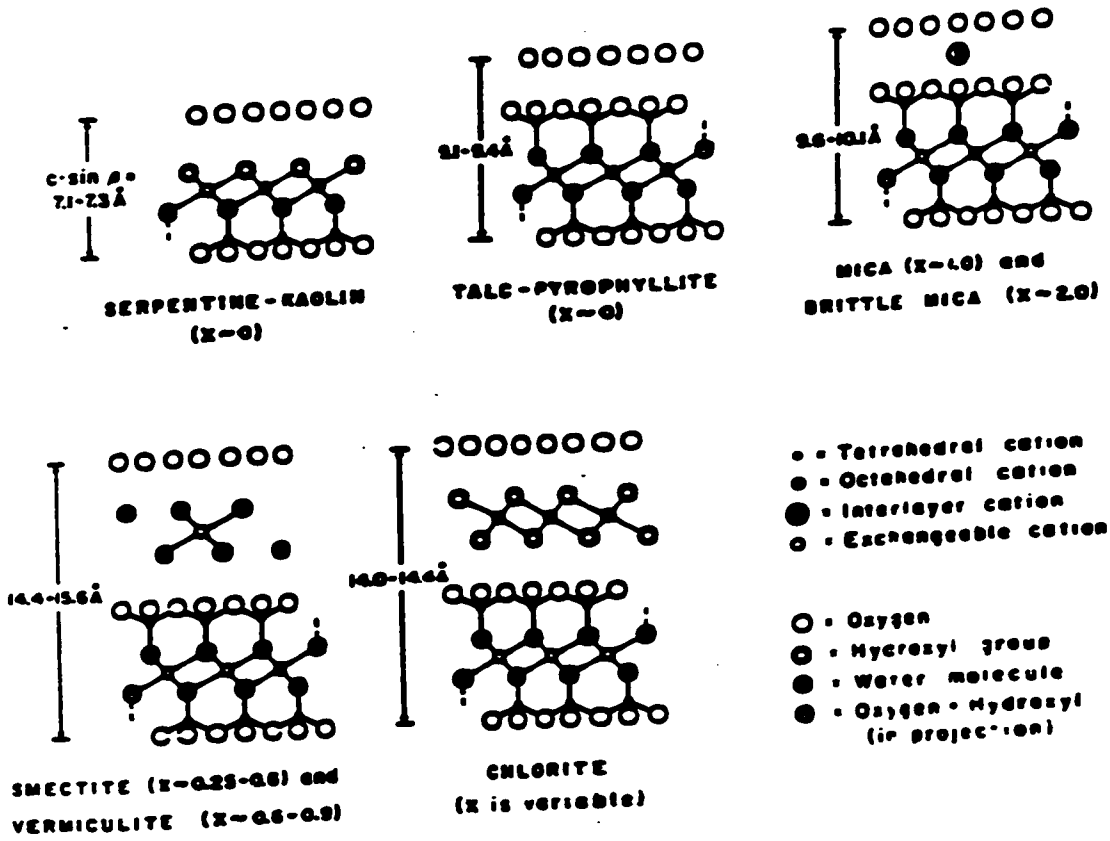

Fig. 8. A sketch showing the (010) view of structures of major clay mineral groups (from Bailey 1980).

Kaolinite is present in soil and permeable bedrock in warm, humid regions as a weathering product or a hydrothermal alteration of aluminosilicates such as feldspars and muscovite.

The structure of the pyrophyllite-talc group is 2:1 or T.O.T. layer formation with no charge or cation substitution. The pyrophyllite $Al_2Si_4O_{10}(OH)_2$-talc $Mg_3(Si_4O_{10}(OH)_2$ group exists as a stable structure and a product of hydrothermal or diagenetic processes (Chamley 1989).

The mica group is a 2:1 or T.O.T. layer structure with strong layer charge and cation substitution. The strong charge results from the substitution of trivalent ions for tetravalent ions in the tetrahedral sheet and divalent ions for trivalent ions in the octahedral sheets. The interlayer contains water molecules and univalent cations to neutralize the layer charge. The mica group has a trioctahedral subgroup with minerals such as muscovite, phengite, glauconite, and celadonite and a dioctahedral subgroup with minerals such as phlogopite and biotite. Mica group minerals are common in igneous and metamorphic rocks but also occur in the clay fraction of sedimentary rocks and soil.

As a member of the mica group, illite contains more Si, Mg, and H_2O, but less tetrahedral Al and less interlayer K than other ideal mica group mineral such as muscovite. Illite occurs in argillaceous sedimentary rock as clay-sized fraction and sometimes corresponds to a mixture of micaceous minerals of different origins (Chamley 1989). Illite is an end-member of a series, it may contain up to 5% of

interstratified material, which is generally smectite and sometimes vermiculite or chlorite (Moore and Reynolds 1989).

Vermiculite minerals have a 2:1 or T.O.T. structure layer with water and cations in the interlayer cations and a basal spacing of about 14 Å. The minerals of this group can be either trioctahedral or dioctahedral and result from pedogenesis or diagenesis (Chamley 1989).

Smectite group minerals can be defined as a large group of T.O.T. minerals characterized by swelling or expansion due to their small layer charge (< 0.6). The octahedral sheet of smectite consists of two planes of anions (O, and OH) which are closely packed. The tetrahedral sheets are composed of six-fold hexagonal rings of silica tetrahedra (Bailey 1988) and interlayer complexes with water and organic molecules. The swelling phenomenon is a function of both the size and the charge of the interlayer cation (Na, K, or Ca) present (Moore and Reynolds 1989). The basal spacing ranges between 10 to 18 Å with different shape according to the origin; flakes, curls and laths of different sizes can be found (Chamley 1989). Smectite minerals may form in different chemical environments, most of them surficial soil or sediments with a weathering environment characterized by very slow movement of water such as in swampy lowlands or arid to semiarid regions (Berner 1971). Smectite group members are montmorillonite, beidellite, nontronite, stevensite, saponite and hectorite.

The chlorite group minerals have T.O.T. structures and can be considered 2:1 layer silicates with a hydroxide interlayer, or as 2:1:1 layer. The chlorite standard structure consists of alteration between trioctahedral (negatively charged) and

octahedral (positively charged) sheets. The basal spacing is 14 Å and within a structure the layers and the interlayers are strongly bound. Because of substitution of Al^{3+} for Si^{4+} in the tetrahedral layer, a charge deficit occurs which is neutralized by an excess of charge in the octahedral sheet, generated by substitution of Al^{3+} and or Fe^{3+} for Fe^{2+} and Mg^{2+}. Chlorites originate by weathering of the ferromagnesian minerals of crystalline igneous or metamorphic rocks (Chamley 1989).

Mixed-layer clay minerals can be defined as a vertical arrangement of two or more types of single layers stacked along a line perpendicular to (001) (Moore and Reynolds 1989). Three mixed-layer types are recognized:

1- A periodic alteration of layers of two types e.g. illite/smectite.

2- A random alteration of each type of layer e.g. irregular illite-vermiculite.

3- Partially ordered structures.

Clay Samples Selection and Preparation

All samples were prepared for both qualitative and quantitative determination by x-ray diffraction analysis according to the general procedure of Moore and Reynolds (1989). The goal of this procedure is to obtain the less than 2μm fractions by using settling velocities predicted by Stokes' Law. Carbonates and organic matter were removed from each sample to avoid their interference and fluorescence upon x-ray analysis which increase the background in the low angle region and mask clay minerals peaks (Furlong 1968).

To remove the organic matter each sample was treated with NaOCl (bleach), heated in a water bath for 15 minutes, and centrifuged at 800 round per minute (rpm) for five minutes. The supernatant was discarded. The centrifugation was repeated until all organic matter was removed as indicated by changing color to gray, white or red. The removal of carbonate was accomplished by adding 250 mL buffer solution (82 g sodium acetate in 900 mL distilled water and 27 mL glacial acetic acid with a final pH of 5), stirring until the dissolution reaction diminished and heating the sample overnight. Each sample was dispersed by mixing with 100 mL distilled water, agitating in a blender for 2-3 minutes, centrifuging at 2000 rpm for three minutes, and decanting the clear water. The dispersion procedure was repeated until water became opalescent. To separate the less than 2μm fractions, sodium hexametaphosphate was added to the final 100 mL wash, mixing for 2-3 minutes, centrifuging at 1000 rpm for 2 minutes and 7 seconds, and decanting the supernatant (the < 2μm fractions) into clean beaker. An oriented slide was prepared for each sample by pouring 20-30 mL of clay suspension through a 0.22 μm Millipore vacuum filter funnel, and removing the filter paper when all the fluid passed through (Moore and Reynold 1989). The oriented less than 2μm fractions were then applied to a glass slide and stored in a dessicator using the technique of Drever (1973).

All x-ray diffraction scans employed CuKα radiation at 40 KV and 20 mA. Scanning was at 0.5° 2θ/minute from 3 to 35° 2θ with a scanning step size of 0.02°2θ. Each sample was scanned three times. The first scan used the air-dried sample. The second scans were made on samples which had been exposed to ethylene glycol vapour

at 60°C for at least eight hours. The third and the final scans were made following heating of the slides to 360°C for at least four hours.

The extant minerals of the clay fractions were identified using the peak patterns on the air-dried scans and observing peak position shift and peak position shift on the subsequent scans following glycolation and heating. Quantification measurements were made by a 5-point smoothing of the glycolated scan, stripping the background and measuring peak intensities. Quatification employed the mineral intensity correction factors (MIF) of Moore and Reynolds (1989) and Biscaye (1965) as given in Table 2.

Table 2. Peaks use for quantification and the mineral intensity factor (MIF) employed (after Biscaye 1965)

Mineral	Peak	MIF
Smectite	S(003)	0.79
Illite	I(002)	0.48
Chlorite	C(003)	1.12
Kaolinite	K(002)	2.18
Illite/Smectite	I(002)/S(003	0.63
Quartz	Q(100)	1.00

Identification of Clay Minerals

The clay minerals identified in all samples from the three cores are smectite, illite, chlorite, kaolinite, and illite/smectite. Illite dominated the clay fraction in all cores. Other clay minerals were found in varying amounts. In addition, quartz was present in significant amount in all samples, and plagioclase, K-feldspar, calcite,

siderite and pyrite were found in minor amounts. The presence of smectite was identified by the presence of the (001) peak at 5.4° 2θ and (003) peak at 15.7° 2θ. The (003) coincides at 16.2° 2θ with the illite reflection. Therefore, this reflection can not used for positive identification purposes. The 16.29 Å peak was not affected by glycolation because of the low concentration of smectite or heating because of the low heating level (Blackburn, personal communication, 1997).

The strongest diffraction peak of illite, I(001), (see Appendix II, Fig. 1A), occurs at 8.8° 2θ (10 Å) followed by the (002) at 17.7° 2θ (5 Å peak), the 020 diffraction peak at 19.8° 2θ(4.5 Å) and the final strong peak of illite (004) coincides with quartz (101) at 26.6° 2θ (3.34 Å). Therefore, the (004) peak can not be used for the quantitative analysis purpose. In general, the illite peaks were relatively broad signifying poorly crystalline material.

Chlorite was identified (see Appendix II, Fig. 1A) by the presence of the (001) diffraction peak of 16.29 Å at 6.2° 2θ and the (003) peak at 18.7° 2θ of 4.75 Å. The (002) diffraction peak of chlorite at 12.4° 2θ (7.13 Å) coincides with kaolinite (001) and the (004) peak at 25.1° 2θ (3.54Å) coincides with the 002 diffraction peak of kaolinite. The quantitative analysis peaks of chlorite were 001 and 003 .

Because both kaolinite peaks (001) at 12.4° 2θ(3.5 Å) and (002) at 25.1° 2θ (3.54Å) are coincident with chlorite 002 and 004 respectively, the presence of kaolinite was identified according to the following calculation (Biscaye 1965; Moore and Reynolds 1989):

(1) C (002) = 3.3 * C (003)

C (004) = 2 * C (003)

(2) K (001) = K [(001) + C (002)] - C (002)

K (002) = K [(002) + C (004)] - C (004)

The presence of mixed-layer illite /smectite was identified by the presence of an illite (002) and smectite (003) overlap peak at 16.4° 2θ (5.46 Å). Small amounts of mixed-layer clay were found in all samples.

All the non-clay minerals were identified from the relative position and intensities of their x-ray peaks on the diffraction tracing. The only non-clay minerals present in sufficient quantity to be identified were quartz, plagioclase, k-feldspar, calcite, siderite and pyrite.

The strongest diffraction peak of quartz (see Appendix II, Fig. 1A), the (101), at 26.6° 2θ (3.34 Å), coincides with the strong (004) illite peak. Positive identification of quartz is based on the (101) peak at 20.8° 2θ (4.27 Å). Plagioclase was identified from peak (002) which occurred at 27.4° 2θ (3.25 Å). K-feldspar was identified from the 220 peak at 27.8° 2θ (3.2 Å). The presence of the 104 calcite peak at 29.5° 2θ (3.02 Å) was used for its identification. Very small amounts of calcite were found in all samples eventhough an attempt was made to remove carbonates during slide preparation. Siderite was identified by the (104) diffraction peak occurring at 32° 2θ (2.79 Å). The identification of pyrite employed the (200) diffraction peak at 33° 2θ (2.7 Å).

CHAPTER 4
RESULTS

Core Description

The three cores of different depth of Walpole Island have been subdivided into units according to their grain size distributions, textures, and other sedimentological characterizations. More complete descriptions of the core sediments are given by Cumming (1995)

1) Sand : 0-3.5 m depth; unconsolidated sediments; well sorted; stratified with a visible bedding; quartz and carbonate are the dominant minerals; pale yellowish brown (10 YR 8/6) to greenish grey (5 GY 6/1).

2) Non-rhythmic clayey-silt: 3.5-5.5 m depth; well sorted and well rounded; carbonate-rich; light olive grey (5 Y 6/1) to greenish grey (5 GY 6/1).

3) Green clay: 3-4 m depth in Core-GD; unsorted and ungraded; pale olive green (10 Y 6/2); with ferrous iron staining. A one metre green clay layer is distinguishable a lack of silt-sized grains and carbonate minerals and existence of calcitic concretions at its base.

4) Rhythmically-stratified clayey silt: 5.5-14 m depth; well sorted; carbonate-rich; moist; rhythmically stratified. The laminations possibly seasonal, are characterized by two kinds particle sizes silt and clay.

5) Clayey-silt diamicton: 14-27.42, 14-40.75 and 14-40.41 m depth in Core-HP, GD and DC, respectively. These unsorted sediments are massive; dark yellowish brown

(10 YR 4/2) to brownish grey (5 YR 4/1); carbonate rich; moist to wet; with angular clasts.

6) **Silty-sand diamicton**: 27.42-28.42, 40.75-41.75, 20.41 - 21.41m depth in Core-HP, GD and DC, respectively. These sediments are coarse to very fine grained; angular;

unsorted; light olive grey (5 Y 6/1) to olive grey (5 Y 4/1). The sandy diamicton is generally about 1 m thick and lies just above bedrock. At the sediment-bedrock interface, it is generally coarse grained.

7) **Bedrock**: the bedrock is encountered in the GD Core at 40.75 m where it comprises Upper Devonian black shales. The Middle Devonian limestones are intersected in the DC Core at a depth of 20.45 m.

Clay Mineral Distribution

Five clay minerals were identified in the Walpole Island sediments. Illite is the major clay component in all samples; chlorite is second in abundance and was recognizable in all samples studied; kaolinite is third in abundance, and finally smectite and illite/smectite were found in minor and variable concentrations in all samples.

Clay Fraction Mineralogy in HP Core

Illite dominates the clay fraction mineralogy over the length of HP core (Table 3; Fig. 9). Although there is a general increase in illite concentration from about 56

Table 3. Normalized mineral concentration (%) in the clay-sized fraction of core-HP

Sample #	Core depth (m)	Smectite	Illite	Chlorite	Kaolinite	Illite/Smectite	Quartz
HP3	3.5	0.81	58.71	19.79	13.65	3.52	3.52
HP4	5.01	0.75	56.35	10.10	28.06	3.55	1.18
HP5	6.58	1.92	56.72	18.21	15.47	4.06	3.60
HP7	9.93	0.81	61.37	21.68	9.58	2.39	4.18
HP8	11.5	1.75	52.17	14.21	11.24	2.57	18.04
HP9	12.1	1.24	56.03	16.87	9.67	3.94	12.22
HP10	13.74	0.91	73.38	18.80	2.21	3.60	1.10
HP11	15.75	1.01	68.99	18.13	3.84	4.47	3.56
HP12	16.73	0.54	65.00	19.09	5.77	2.56	7.04
HP13	18.55	0.59	64.35	17.17	13.26	2.86	1.76
HP14	20.05	0.94	62.71	16.04	16.23	2.23	1.85
HP15	21.2	0.35	66.29	19.38	9.98	2.33	1.67
HP16	22.86	0.75	66.49	16.43	11.59	2.13	2.61
HP17	24.35	0.50	66.74	16.03	12.98	2.32	1.42
HP18	26.27	0.47	70.95	16.92	6.50	3.35	1.80
HP19	27.9	0.73	65.46	18.19	11.15	1.61	2.86

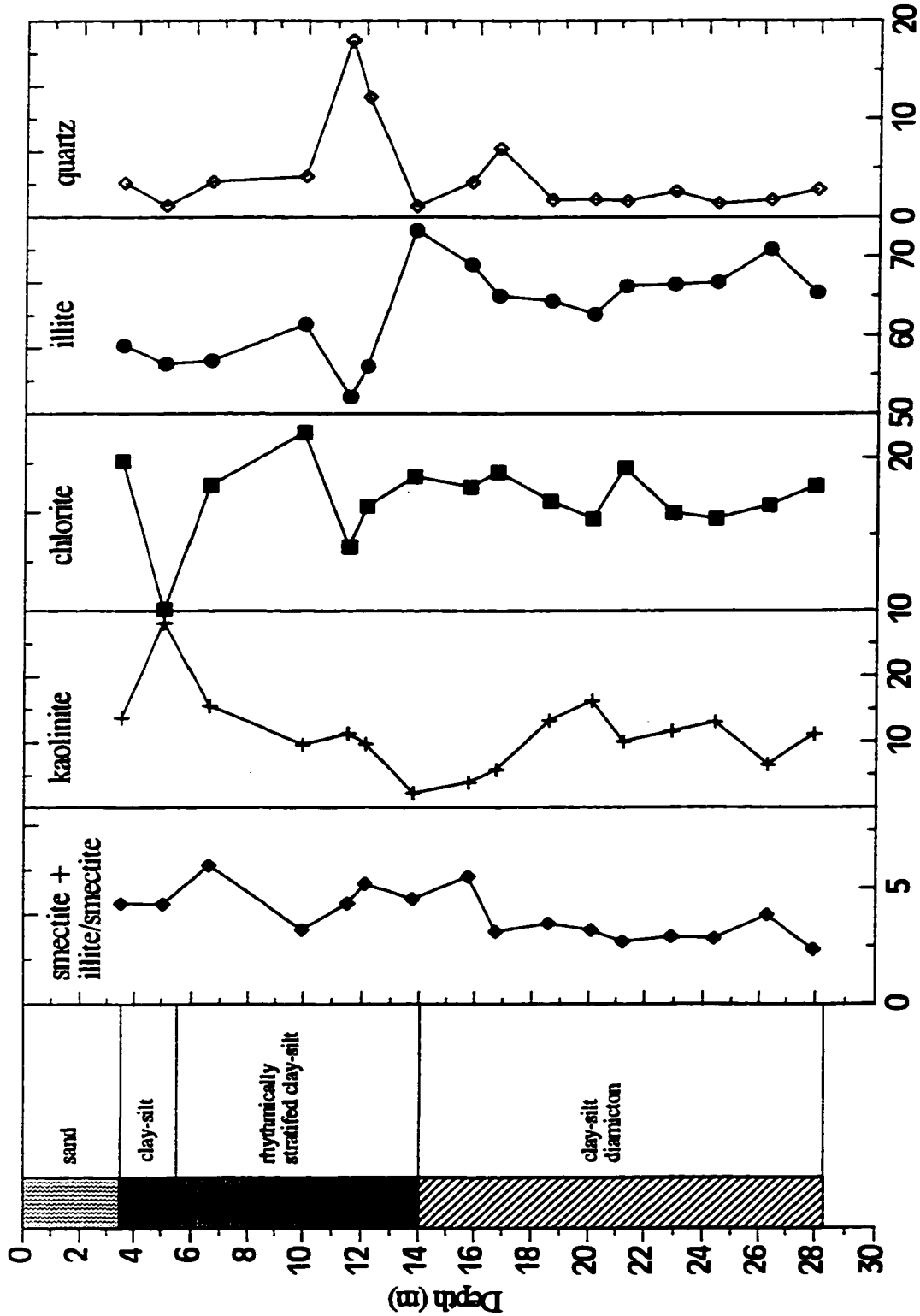

Fig. 9. Normalized mineral concentrations (%) in the clay-size fraction of core HP.

percent at the top of the core to about 65 percent at the bottom, there are actually two populations with a significant break at about 14 m. Above this depth, illite averages 57 percent; below the 14 m depth, illite averages 66 percent. The break at 14 m corresponds closely to substrates change from clayey silt-rhythmically stratified clayey silt to clayey-silt diamicton. Chlorite generally has a distribution that follows illite. Above 14 m, chlorite concentrations are highly variable with a distinct low concentration (10 percent) at about 5 m corresponding to the bottom of the clayey-silt sequence. Below this (5.5 to 14 m depth) is the rhythmically-stratified clayey silt which has variable chlorite values. Below the 14 m, where the clayey-silt diamicton unit starts, chlorite averages is 17 percent.

The highest kaolinite concentration is found above 14 m (28 percent) at the same depth where the lowest value of chlorite occurs within the clayey silt sediments. Below the clayey silt unit and within the rhythmically-stratified clayey silt, kaolinite values decrease to the change to the clay-silt diamicton (the 14 m depth). Within the clay-silt diamicton, a general increase in kaolinite values is observed to the bottom of the core with possible reversals at about 21 m and 27 m. Overall, kaolinite concentrations closely mirror chlorite concentrations.

Illite/smectite clay shows little variation with depth. Trace amounts of smectite are also found. Quartz dominates the non-clay fraction mineralogy with depth but generally at low concentrations. Significant high values of quartz were found (18 percent) within the rhythmically-stratified clayey silt (11.5 m depth) in the clay-silt diamicton (7 percent) at about 16.5 m. The other non-clay minerals, plagioclase, K-

feldspar, calcite, and siderite, were found only in trace amounts in the stratigraphic sequence.

X-ray diffraction patterns (see Appendix II, Fig. 2A and 3A) for both depths 11.5 and 13.74 m of the HP core illustrate the mineral composition at these depths.

Clay Fraction Mineralogy in the GD Core

Illite is the major clay component in the samples analyzed (Table 4; Fig. 10) and constitutes about 60 percent of the total clay over the length of the Core-GD. The distribution of illite along the vertical stratigraphic units maintains almost a constant concentration with few exceptions. Illite reaches the lowest concentrations (43 percent and 38 percent, respectively) at depths of about 8 m within the rhythmic stratified clay-silt and 24 m within the clay-silt diamicton. Illite highest concentration (72 percent) at about 17 m depth within the clay-silt diamicton.

Although, chlorite is second in abundance; it's concentrations are less than 20 percent. Chlorite follows almost same pattern of illite's in its distribution. The lowest chlorite concentration (8 percent) is found at the same depth of illite lowest concentration (38 percent at 24 m).

Kaolinite mirrors chlorite in its distibution. Kaolinite is absent near surface within the green clay and within the rhythmically-stratified clay-silt and it reaches the highest concentration at same depth (24 m) of illite and chlorite lowest concentrations. Otherwise, kaolinite keeps slightly variable values with depth. Mixed-layer illite/smectite and semectite display almost a constant low cocentrations with no major

Table 4. Normalized mineral concentration (%) in the clay-sized fraction of core-GD

Sample #	Core depth (m)	Smectite	Illite	Chlorite	Kaolinite	Illite/Smectite	Quartz
GD3	3.64	0.59	63.25	25.03	0.00	2.50	8.62
GD5	5.79	0.84	61.77	20.22	10.81	2.74	3.61
GD6	7.71	1.08	42.92	14.28	16.03	0.12	25.56
GD7	8.73	0.75	61.62	19.88	10.56	2.01	5.18
GD8	10.65	0.84	61.66	18.96	12.15	4.06	2.33
GD9	12.48	1.24	64.44	20.11	8.29	2.63	3.30
GD10	13.3	1.05	66.06	19.62	9.42	1.72	2.12
GD11	14.92	0.54	67.33	19.94	9.06	1.78	1.34
GD13	16.78	0.46	72.03	15.54	8.86	1.82	1.29
GD14	18.72	0.98	59.84	20.15	4.72	4.25	10.05
GD15	19.47	2.44	63.74	17.82	7.74	4.70	3.56
GD16	21.79	1.21	62.28	20.96	6.41	3.37	5.70
GD17	23.05	0.94	66.10	19.13	7.20	3.21	3.42
GD18	24.31	1.28	37.90	7.74	43.80	3.60	5.68
GD19	26.1	0.95	56.82	18.66	9.42	3.20	10.92
GD20	27.4	0.40	65.37	19.49	10.35	1.82	2.57
GD21	29.24	1.44	68.53	22.33	0.00	4.42	3.27
GD22a	30.75	1.92	65.80	11.46	11.39	8.44	0.98
GD23	32.09	0.50	69.49	18.87	8.63	1.21	1.29
GD24b	33.84	0.60	68.38	22.16	5.52	1.56	1.77
GD25	34.52	0.92	64.60	21.79	8.94	1.87	1.87
GD26	36.66	1.02	66.26	14.14	13.86	2.93	1.78
GD27	38.39	0.40	66.71	19.29	10.01	1.69	1.89
GD28	39.13	0.68	63.61	16.50	14.06	2.86	2.29

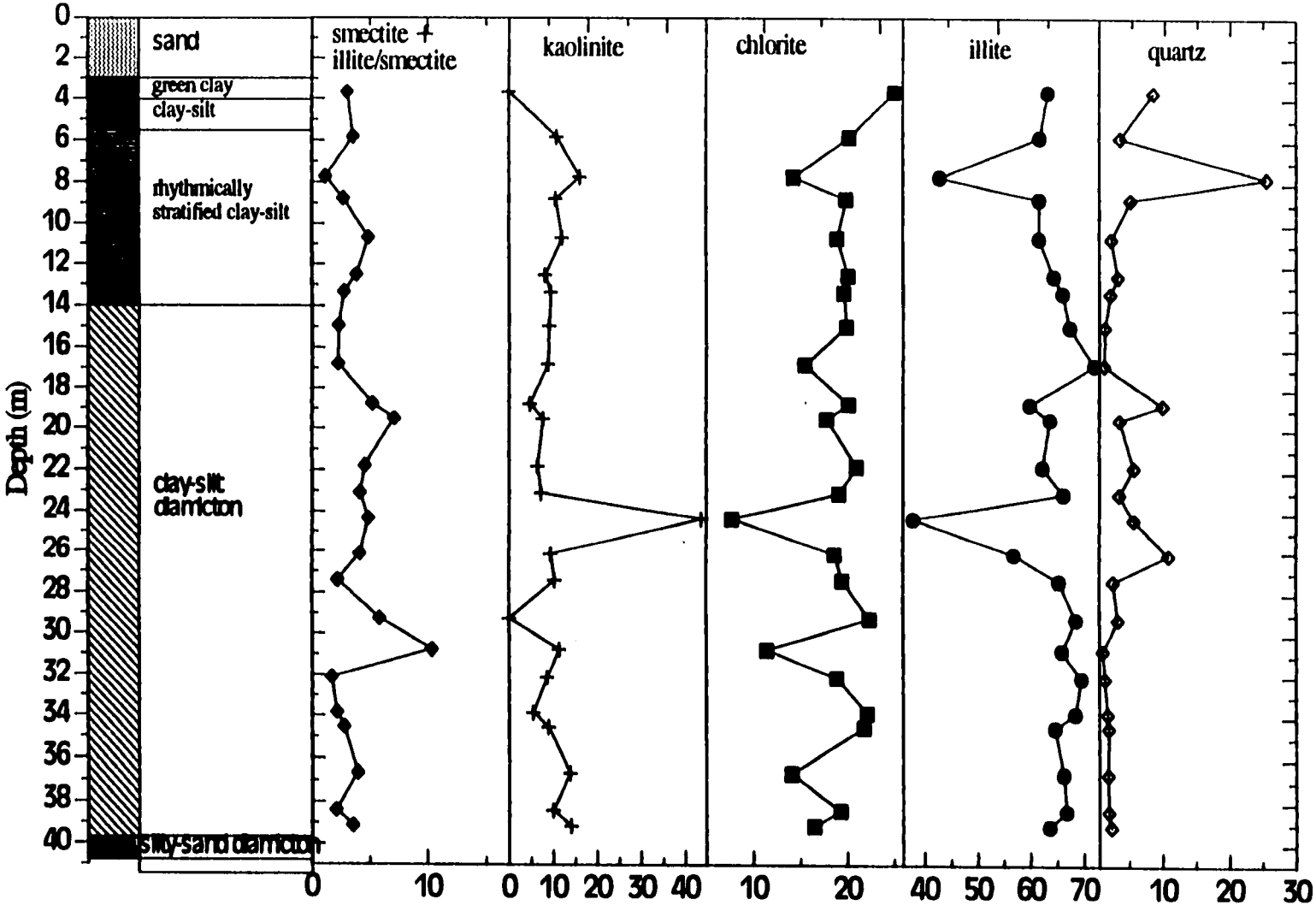

Fig. 10. Normalized mineral concentrations (%) in the clay-size fraction of core GD.

change over the length of the GD core. The illite/smectite and smectite clay fraction do not exceed 10 percent.

X-ray diffraction analysis of air-dried scan of the green clay unit illustrates a unique patterns of both illite and chlorite with broad peaks because of a probable enrichment of iron (Moore and Reynolds 1989). In the air-dried scan, all the clay minerals diffraction peaks are broad due to the heavy metal substitution and its different scattering power. The effect of Fe substitution on diffraction intensity is due to the great difference in scattering power between Fe and Al or Mg (Moore and Reynolds 1989). The air-dried scan shows a strong effect of Fe on the hydroxide sheet which produces a strong C (001) and C (003) peaks relative to the C (002) and C (004) peaks intensities, although kaolinite is absent and does not coincide with those later peaks. Upon heating some peaks shrink to low intensities as in C (001), C (002), C (003) and C (004) as well as I(002). The x-ray diffraction patterns of the clay-silt diamicton (16.78 m) (see Appendix II, Fig. 6A) illustrate very sharp peaks with high intensities of illite and chlorite. X-ray diffraction patterns of the 24.31 m (see Appendix II, Fig. 7A) contain thick crystallites of illite and chlorite (sharp peaks) and recognizable quartz peaks. The three XRD patterns (see Appendix II, Fig. 8A) of the 29.24 m illustrate a sharp peak of chlorite (002) and (004) which may have a thick crystallites in the absence of kaolinite (Moore and Reynolds 1989)..

Quartz dominates the non-clay fraction mineralogy along the depth of the GD core. Within the rhythmic stratified clay-silt at depth about 8 m, quartz reaches the highest concentration of 25.5 percent. Within the clay-silt diamicton at depth about 31

m, quartz lowest concentration of 0.98% was found. The other non-clay minerals (plagioclase, K-feldspar, calcite, siderite and pyrite) were found in trace amounts.

Clay Fraction Mineralogy in the DC Core

As it was in the HP and GD cores, the dominant clay mineral in the DC core is illite (Table 5; Fig. 11). Although, there is a general decrease in illite concentration from near surface to about 13 m depth, there are actually two populations with a significant break at 13 m. The break at 13 m corresponds closely to a substrate change from the rhythmic stratified clay-silt to clay-silt diamicton. Chlorite is second in abundance in the clay fraction of the DC core. Above the 13 m and within the rhythmic stratified clay-silt, chlorite shows a decrease in concentration. At depth 13 m, chlorite and all other minerals (illite, kaolinite, illite/smectite and quartz) experience abrupt change in their concentrations. Chlorite highest concentration (35 percent) was found at 13 m depth.

Kaolinite distribution mirrors chlorite. With depth, kaolinite concentrations increase except at 13 m where kaolinite is not present. As in kaolinite, Illite/smectite and smectite concentrations increase with depth and, at 13 m, illite/smectite highest concentration was found. Below 13 m, illite/smectite concentrations decreas with depth.

Quartz dominates the non-clay fraction mineralogy over the length of the DC core. Quartz concentrations are constant along depth with few exceptions over the length of the core and the highest concentration was found at the bottom, which may corresponds to a substrate change. The XRD patterns (see Appendix II, Fig. 9A and 10A) of depths 13

Table 5. Normalized mineral concentration (%) in the clay-sized fraction of core-DC

Sample #	Core depth (m)	Smectite	Illite	Chlorite	Kaolinite	Illite/Smectite	Quartz
DC5	5.78	0.24	65.23	21.74	9.17	1.44	2.18
DC6	7.98	0.77	62.86	20.90	9.98	2.67	2.84
DC7	9.39	0.99	63.47	18.05	11.58	3.49	2.41
DC8	10.31	0.97	60.42	18.60	13.99	3.47	2.54
DC9	12.7	0.28	65.62	16.39	14.48	1.72	1.51
DC10	13.1	0.79	56.21	35.27	0.00	6.98	0.76
DC11	15.7	0.54	65.43	22.16	6.87	1.78	3.21
DC12	16.05	0.68	65.45	16.71	11.60	2.72	2.84
DC13	17.95	0.62	68.17	19.05	9.35	1.73	1.08
DC14	19.2	0.36	63.23	16.41	12.86	1.72	5.42

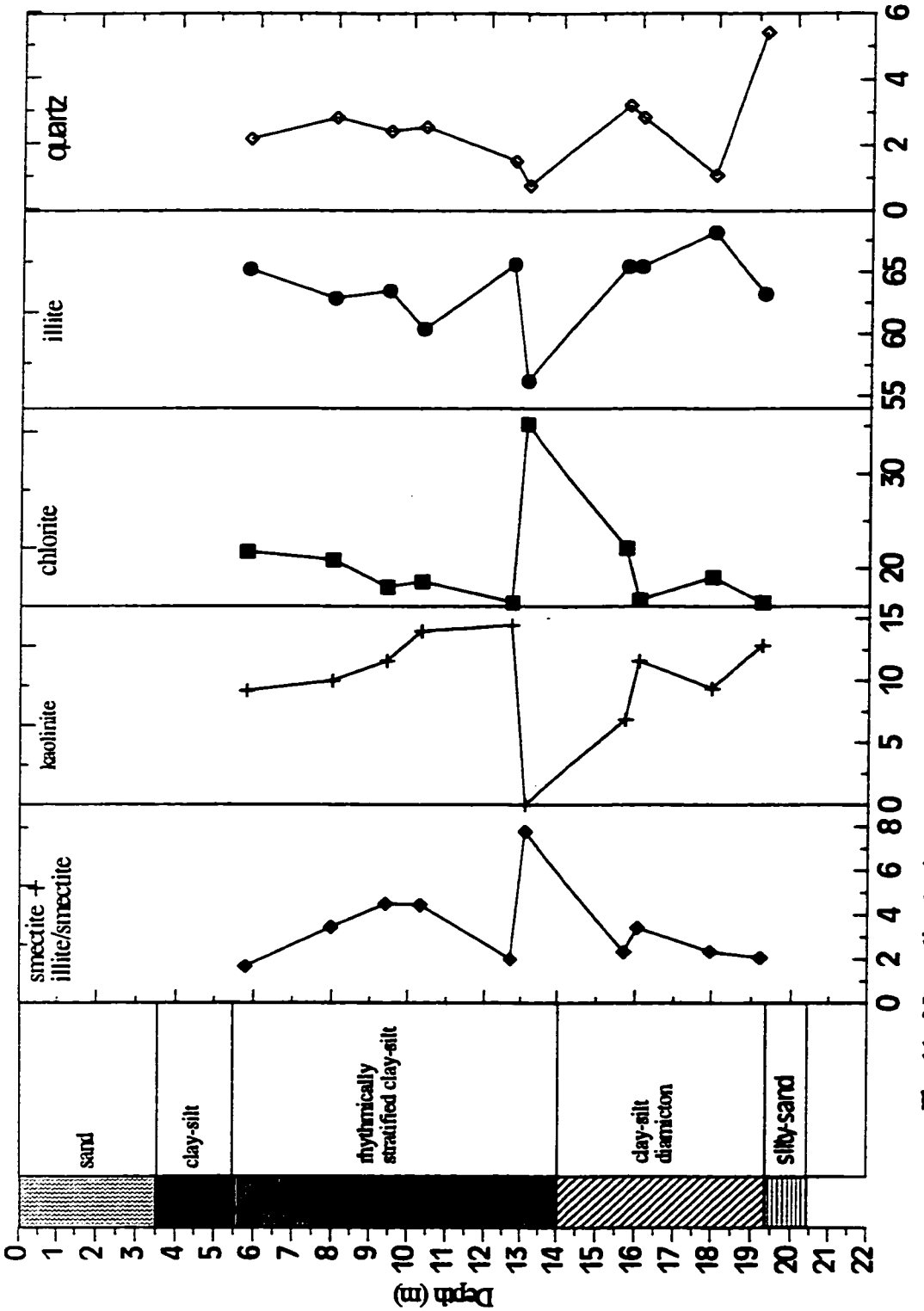

Fig. 11. Normalized mineral concentrations (%) in the clay-size fraction of core DC.

and 19 m show a vary sharp peak of chlorite (002) and (004) which usually coincide with kaolinite (001) and (002).

CHAPTER 5

DISCUSSION

Paleoenvironment of Walpole Island Sedimentation

The late Wisconsinan tills deposited in southern Ontario represent the Labrador Sector of the Laurentide Ice Sheet, which originated in the Labrador and Quebec highlands, spread southward and occupied southern Ontario (Prest 1984; Fulton 1989). The tills of the Labrador Sector are underlained by sedimentary rocks in the Great Lakes-St. Lawrence Lowlands (Barnette 1992).

The Quaternary sediments of southern Ontario were deposited by meltwaters of the Laurentide Ice Sheet (Karrow 1989). The sources of these sediments are Great Lakes basin glaciolacustrine sediments which went through alteration and reworking during the Laurentide Ice Sheet advance (Ambrose 1964). Thus the clayey tills were derived from reworked glaciolacustrine sediments (Barnett 1992). Seven units were identified in the three cores with grain size, textures, and mineralogy each representing a stage of deposition associated with a specific event.

Mineralogic Variation

Significant features regarding the depositional history can be inferred from the clays by applying the following information:

1) Because the three clay minerals illite, smectite and chlorite are 2:1 layer type with a charge of less than 1, they all have transitional capabilities one to another (Moore and Reynolds 1989).

2) Illite is formed in moderate- to low-rain environments where waters have high K^+/H^+, K^+/Na^+, K^+/Mg^{2+}, Si/Al ratios (Garrels and Christ 1965). High illite values occur in both continental and marine environments.

3) Chlorite is formed in environments with low K^+/Mg^{2+} waters ratio (Weaver 1973), and environment of formation is similar to that of illite.

4) Kaolinite forms in humid, acidic environments, where alkali and alkaline earth metals are leached from the weathered material.

Mineralogy of the HP, GD and DC Cores

Near surface sediments (3.5, 3.64 and 5.78 m in the HP, GD and DC cores, respectively) are composed of fine to coarse sandy deltaic. Sufficient clay fractions were not recoverable for x-ray analysis.

The distribution of clay minerals over the length of the three cores are dominated by illite. Illite is stable and generally is formed in environment where the waters have a high K^+/H^+ ratio (Garrels and Christ 1965). The K^+/Na^+ and K^+/Mg^{2+} ratios are equally important because the abundance of K^+ ion tends to be fixed in the interlayer positions of the three-layer clay to form illite.

Chlorite is second in abundance with depth in the three cores. The structure of chlorite is similar to that of illite with addition of a brucite layer ($Mg(OH)_2$). Keller (1956) suggests that chlorite may form through the absorption of Mg^{2+} by a degraded three-layer clay mineral such as illite. Moreover, the occurrence of chlorite at depth may relate to the abundance of Mg^{2+} ions from source area indicating the breakdown

of a more Mg-rich material such as dolomitic limestone. High concentraions of Mg^{2+} ion were found in porewater analysis of the three cores by Cumming (1995).

The existence of kaolinite in an environment can define the environment of formation of clay fractions. Where the concentrations of kaolinite increase, it can be used as indication of humid, acidic conditions and the alkali and alkaline earth metals are leached from the weathered material leaving Al^{3+} to combine with hydrated silica and form hydrous aluminum silicate.

The expandable clay present is essentially all mixed-layer illite/smectite. Sparse smectite (< 1%) was found in the three cores. The observed relationship between smectite and illite/smectite is: where smectite is present in a significant amount (7% in the DC core at depth 13 m), mixed-layer clay is generally sparse (0.79% in the same core at same depth); conversely, where mixed-layer clay is abundant, smectite is sparse or absent (Furlong 1968). Grim (1951, 1958) stated that smectite may, over a period of time, lose its adsorbed water and be converted first to mixed-layer clay and then to illite or chlorite.

All non-clay minerals are absent or in trace amount, except for quartz which occurs in variable concentration over the length of the three cores. The solubility of silica minerals is a function of pH; as the pH value increases (9.0-9.5), the solubility of silica increases sharply. The high Al:Si ratio may be a consequence of precipitation of silica to form quartz or release of silica by mineral reactions, including clay minerals or dissolution of feldspars (Boggs 1992).

Paleoenvironment of the HP Core

The origin of Southern Ontario tills can be related to the Canadian Shield debris which were carried during the initial arrival of ice and are regarded to be a 'parent till' (Karrow 1989). With later ice advanced into Southern Ontario, these tills were reworked and became finer and incorporated carbonates and fine clastic detritus from the Devonian limestone and black shale which make up the local bedrock. The St. Clair clay plains were deposited during the several advance and retreat of the Laurentide Ice Sheet in the Great Lakes region. During the retreat of the ice, glacial lakes were formed and deposited fine-grained lacustrine sediments. On ice advancments, these fine-grained lake sediments were incorporated into the glacial deposits and reworked, resulting in the deposition of thick clay-rich sediments (Karrow 1989).

The paleoenvironment of the HP sediments can be subdivided into two environments of deposition; the upper and the lower zones, disregarding the recent deltaic sediments.

The upper zone environment (3.5 to 14 m) is comprised of lacustrine and glaciolacustrine sediments. In the first two metres, lacustrine clay-silt sediments were deposited during the late Wisconsinan (after the final retreat of the ice sheet) stage of glaciation and early Holocene (9 000 to 5 000 B.P.) (Dyke and Prest 1987). An unconformity due to non-deposition and subaerial exposure occurred prior to late Wisconsinan and early Holocene date and lasted for a thousand years (10 000 to 9 000 B.P.) (Soderman and Kim 1970). The prevailing climate of the one thousand years

hiatus was dry with low lake levels. Under the humid and warm conditions of late Wisconsinan and early Holocene, the surfaces of fine-grained organic matter probably were oxidized and caused neutralization or slightly alkaline glacial lake waters. Under these conditions, silica solubility is enhanced and the remaining silica reacted with alumina to give rise to kaolinite formation. A probable intense weathering caused a break up of chlorite and reduced its concentration within the lacustrine unit. Illite was stable under these conditions and presumably was formed where the waters have a high K^+/H^+ ratio. Smectite and illite/smectite were found in low concentrations through out the zone and may be the result of chlorite break up.

The following unit in the upper zone is the glaciolacustrine sediments (with almost 8 m in thickness). Laminated sediments were deposited during the late Wisconsinan ice sheet oscillations from the following glacial lakes events (Cumming 1995): Maumee IV during Early Mackinaw Interested (13 900 B.P), Whitely during the Port Huron Stade (13 000 B.P), Warren (12 800 B.P.), Grassmere (12500 B.P.), and Lundy (12 400 B.P.) during the Two Creeks Interstade (12 200 B.P.). The glaciolacustrine sediments are found as varve-like or laminated deposits, which represent different seasonal (freezing and melting) particle precipitation. During the spring, melting of ice and snow brings in a large influx of sediments and the coarser sediments (silt to fine sand) are deposited first from low density water creating the light varve. The finer grained materials (clay to fine silt) are deposited during winter creating the darker colored layer. The variable distribution of clay fractions within this unit confirm the different seasonal deposition. In the warm dry environments from the

Early Mackinaw Interestade through to the Two Creeks Interestade, leaching did not take place because of the lowering in water budget. The alkalis and alkaline earths were, however, available to form slightly higher concentration of illite and chlorite. Kaolinite reaches lowest value within the glaciolacustrine unit at a depth (the significant minerals break at 14 m depth) where illite and chlorite experienced the highest concentrations. The significant minerals break at 14 m confirms the dry, warm climate. The highest concentrations of quartz were found above the significant minerals break which may relate to fine sand drifts from the water circulation of Lake St. Clair.

Below 14 m, the lower zone comprises clay-silt diamicton. These lower zone sediments are massive glacial tills with a grain size dominated by silt. The matrix is poorly sorted, sediments size ranges from clay to pebbles (Cumming 1995). These tills were deposited subaqueously beneath an ice sheet (Karrow 1989). The waters of the formation environment may have more potassium available along depth, which may give rise to the K^+/H^+, K^+/Mg^{2+}, K^+/Na^+ ratios to form a higher illite percentage (Garrels and Christ 1965). The high values of the K^+/H^+, K^+/Mg^{2+}, K^+/Na^+ ratios may result from an intensive weathering of parent tills (aluminosilicate minerals in particular K-feldspar), which were carried by ice from the Precambrian Shield. Furthermore, with the passage of time, smectite tends to convert to illite as it loses its absorbed water and the K^+ ion become available. Although chlorite is second in abundance, its concentrations are approximately 20 percent and its existence may relate to the intensive weathering of dolomitic limestone, which was carried from the

Devonian limestone and black shale that make up the local bedrock (Karrow 1989). Kaolinite concentrations increase gradually along depth, which confirms the probable arrival of detrital kaolinite with the advanced ice sheet or arrival of fine sand. Other clay fractions (smectite and illite/smectite) maintain low concentrations along the lower horizon due to the insuitability of formation factors and their transition characterization. Quartz follows same pattern in its low concentrations which may relate to the removal of silica to form illite and chlorite.

Paleoenvironment of the GD and DC Cores

The paleoenvironment of the central and the southern part of the study area, which contains both the GD and DC cores, is characterized by different events from that of the northern part. The existence of the green clay at the top of the GD core and evidence of fracturing and normal faulting at high degree within the DC core and to a lesser degree in the GD core. On the other hand, the nature of the formation and depositional environment of Cores-GD and DC are close to that of the Core-HP.

All clay fractions (including illite, chlorite and kaolinite) of the GD core experienced abrupt concentration changes which divide the sediment columns into upper and lower zones. The upper zone starts near surface and extends to 24 m and the lower zone (15 m thickness) extends to the freshwater aquifer. The first metre of the upper zone is distinguished by green-coloured sediments, which are specialized by the lack of carbonate minerals and silt-sized grains. The green clay sediment was deposited during an early Holocene dry climate, low levels in Lake Stanley (10 00 B.P.), and a reducing

environment. The low lake level ended during the next 5 000 years because isostatic uplift of the North Bay outlet raised water levels in the Port Huron and Chicago basins. This period of rising water was termed the Stanley-Nipissing transition by Hough (1958). During this transition, the topographically lower areas were filled by stagnant waters creating small ponds (McFarlane 1995). The absence of green clay unit in both the HP and DC cores confirms that the green clay was formed only locally in small contained areas. The green colour of this unit may relate to the existence of ferrous iron (Fe^{2+}) and the dry climate can be inferred from the complete absence of kaolinite and the high percentage of illite and chlorite which form upon retention of metal ions K^{+}, Mg^{2+} and Ca^{2+}. Smectite and illite-smectite were found in low concentrations within the green clay unit and may be due to their transitional state in the clay. During the dry climate, silica might have been added to the area as drift sand resulting in moderate quartz concentrations. The lacustrine and glaciolacustrine deposition of the sediments of the GD and DC cores follows that of the HP core except that, in the GD and DC cores, sediments are brown colored and overconsolidated. The overconsolidated sediments of the GD and DC cores were interpreted by Soderman and Kim (1969) as a result of the lowering of the groundwater elevation due to the dry climate and the low level of Lake Stanley. The brown colour may relate to the retention of decayed and oxidized organic matter during the low groundwater level.

Within the lacustrine and the glaciolacustrine sediments and below the green clay of the upper zone, illite and chlorite follow same concentration patterns. The variable concentrations may relate to climatic changes and eventually a change in Mg^{2+} and K^{+} ions

retention. Below the green clay, kaolinite shows an abrupt increase, a gradual decrease, and a rapid increase depths with lowest concentrations of illite and chlorite. The variation in kaolinite concentration within the upper horizon confirms a variable climate and a variable chemistry of the environment. The humidity and wetting increase leaching and removing of Ca^{2+}, Mg^{2+}, K^{+} and Fe^{2+} and Fe^{3+} ions and excess of H^{+} due to excess of precipitation to form a highest kaolinite concentration within the abrupt minerals change. Both illite/smectite and smectite maintain low concentrations along the upper zone because of their transition in the clay. Low quartz concentrations were found along the upper horizon with few exceptions and the highest concentration which co-exists with the high concentration of probable arrival of detrital kaolinite or sand with the advancing ice.

The lower zone is characterized by a higher concentrations of illite which may result from the availability of K^{+}. Potassium higher concentrations may have resulted from break up of detrital sediments clay to form illite, similar to the depositional environment of the lower part of the HP core.

The DC core environment, which represents the modern Great Lakes Stage form 3 500 B.P. to present, is quite similar to that of the HP core. Two main categories of environments prevailed; the upper (7 m thickness) and the lower (6 m thickness) horizon environments, which has similar characterization regarding to the presence of clay fractions. Although, illite and chlorite are the dominant clay fractions in the shallow environment a general decrease in the concentrations with depth is observed. Kaolinite and quartz reveal increasing in concentrations with depth. All minerals including illite, chlorite, kaolinite and quartz experienced a drastic change at same depth of the HP core.

The lower environment horizon starts below the minerals breaking change depth (the 13 m). The lower horizon is characterized by a general increase in illite, kaolinite and decrease in chlorite and quartz concentration.

Correlation of Cores

Correlation can be made among the three cores on the basis of mineralogy. The upper zones of the three cores are consistent. The variation in illite and chlorite in the cores-HP and GD confirm oscillation values of K^{+}, Ca^{2+} and Mg^{2+} ions reflect variable climatic conditions during deposition. The lamina observed in the three cores within this zone may be caused by the variations of clay fractions. Varve-like deposits represent a temperature variation and the lacustrine deposits of dry warm summer of the Early Mackinaw Interestade through the Greatlakean stade represent the clay fraction variation of the Late Wisconsinan. The DC core upper zone shows almost a constant distribution of clay mineral fractions and the general mineral distribution is consistent with that of the HP and GD core. A significant change in mineral concentrations is observed at the same horizon was found in the HP and DC cores. It was found in the GD core at a different depth and with different sediment thicknesses.

Illite, chlorite and kaolinite dominate the mineralogy of the lower zone sediments. Although the thicknesses of the horizons sediment are different in the three cores, clay minerals appear to be formed and deposited under same events. MacFarlan (1995) correlated the three cores from the stratigraphic point of view. The stratigraphic correlation was based on the deposition of deltaic sediments. Part of the HP core is

located within the premodern delta and the GD and DC cores are located within the modern delta. MacFarlan (1995) correlated the brown clay and related it to the low groundwater elevation in both the HP and GD cores, which is not present in the HP core.

CHAPTER 6
GEOCHEMISTRY
OF GROUNDWATER

Introduction

Two sites in Walpole Island were selected for groundwater geochemical and isotopic investigations: (1) in an active landfill and (2) in an abandoned landfill. The two sites are located in the centre of Walpole Island at the leading edge of the Nipissing Great Lakes Stage Delta and close to the GD-Core.

Five wells were chosen for ground water studies in the active landfill site. These were drilled by Burnside Environmental Limited in December, 1995. The present investigation was conducted in May of 1996. The wells (Fig. 12) are OW1, OW2, OW4 and OW5d and OW5s. The active landfill site is located in the centre of Walpole Island. This site is surrounded by tall grass and a 2 m long berm that separates the active land from the grass. The active landfill site is flat and all residences have an access at all time with no restriction on garbage dump, therefore, a variety of wastes are found. Seven buried waste trenches were excavated randomly in the site with different shape and size and average depth of about 4 m. The waste is deposited below the water table and is covered by silty sand.

The abandoned landfill site with wells OW1A, OW2A and OW3A is also located on the west side of Walpole Island about 180 m east of the St. Clair River (Fig. 12) and to

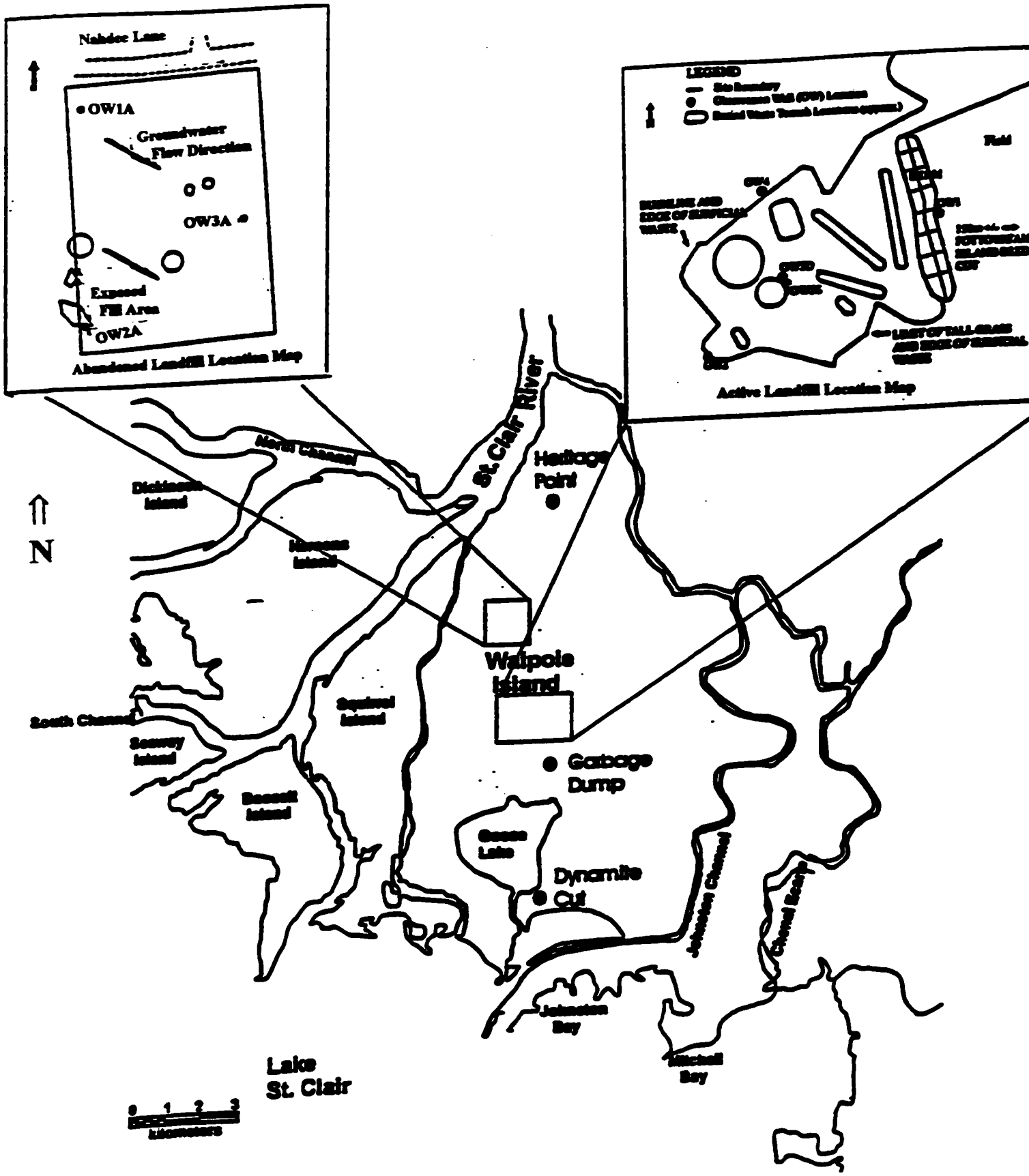

Fig. 12. Map of Lake St. Clair Delta area showing the active and the abandoned landfill location.

the south of Nahdee lane. This site was open to the public for garbage disposal and received a variety of waste in an excavated pit for the time between 1944 and 1976.

Chemical Evolution of Natural Groundwater

Groundwater Chemistry

The source of the surface and ground water in Walpole Island is principally from precipitation, which average 750 mm per year distributed more or less evenly through out the year (Ecologistic 1979). The chemistry of percolating rain and snowmelt water is subject to alteration during the infiltration through soil. The soil zone has a greater carbon-dioxide concentration than the atmosphere, because of organism decay and root respiration. Because rainwater is in equilibrium with atmospheric CO_2 it becomes enriched with CO_2 as it percolates downward. This enrichment increases the CO_2 partial pressure of the water and enables it to dissolve more soil carbonates. Thus the HCO^{3-}, Ca^{2+} and Mg^{2+} contents of groundwater depend on the CO_2 concentration in soil zone, the solubility of calcite and dolomite and the partial pressure of carbon dioxide (P_{CO2}). The equilibrium equations for the carbonate system are:

$$CO_2 + H_2O = H_2CO_3 \quad (1)$$

$$H_2CO_3 = H^+ + HCO_3^- \quad (2)$$

$$HCO_3^- = H^+ + CO_3^- \quad (3)$$

$$k_{CO2} = [H_2CO_3] / [H_2O]P_{CO2} \quad (4)$$

$$k_1 = [H^+][HCO_3^-] / [H_2CO_3] \quad (5)$$

$$k_2 = [H^+][CO_3^-] / [HCO_3^-] \quad (6)$$

The replenishment of CO_2 gas also controls surface water chemistry as it percolates downward. The amount of CO_2 that can be dissolved in water will depend on the geochemistry of the recharge area, in particular water pH and carbon dioxide partial pressure (P_{CO2}), which can be controlled in soils by organism decay and root respiration. In an open system, the P_{CO2} remains constant upon continuous replenishment of CO_2 gas.

Organic acids can also be created in the soil zone if the soil zone is carbonate-, organic- and humus-rich. Humic (a substances that is insoluble in water at pH 2 but becomes soluble at higher pH) and fluvic (the fraction that is soluble under all pH conditions) acids may also be involved during rain and snowmelt water percolation.

Natural water contains a variety of dissolved species which can be classified into three categories. Major (greater than 5 mg/L) constituents are Ca^{2+}, Mg^{2+}, Na^{+}, K^{+}, HCO_3^{-}, SO_4^{2-} and Cl^{-}. Minor constituents (0.01-10.0 mg/L) NO_3^{2-}, Fe^{3+}, F^{-}, Sr^{2+} and K^{+}. Trace constituents (less than 0.1 mg/L) are ions of the following metals Al, As. Cd, Co, Cu, Mn, Pb, V, Zn, Bi, Cr, Ni and Sb. Several sources contribute the above constituents to groundwater and also control the concentrations. These sources include natural sources such as the leaching of rocks and soil, dissolution of silicate and carbonate minerals, surface water, geochemical processes (adsorption and solubility) as well as contribution from human activities e.g. leaching of landfills. In addition to the natural and human activities contributions of these metals, there can be constituents removal by groundwater flushing.

Sedimentary minerals such as gypsum and anhydrite release SO_4^{2-} anion when they encounter groundwater according to the following.

$$CaSO_4.2H_2O = Ca^{2+} + SO_4^{2-} + H_2O \quad (7)$$

The dissolution of some mineral e.g. halite, sylvite, clay minerals, feldspars, sewage and industrial waste, and oil field drainage can release certain ions e.g. Na^+, K^+ and Cl^-. On the other hand, a decrease in SO_4^{2-} concentration may occur owing to either groundwater flushing which remove this anion or biochemical SO_4^{2-} reduction. The biochemical SO_4^{2-} reduction process occurs in an anaerobic groundwater environment when the oxidation of organic matter is accomplished through the reduction of SO_4^{2-}.

Rocks and soils are the largest sources of heavy metals in natural waters. The concentrations of heavy metals varies with the rock type and mineral content. Leaching of clastic sediments contribute Ti, V, Cr, Fe, Co and Ni to natural waters. These elements occur in residual mineral grains remaining after weathering of the other rock constituents (Rubin 1974). Soil and clay minerals contain significant amounts of V, Ni, Cu, Fe, and Zn. Soils, that are rich in organic matter, are able to bind trace metals by forming metal complexes which are pH dependent. Furthermore, the existence of hydrous oxides of iron, manganese and titanium in the soil and clays will adsorb metals selectively (Rubin 1974). Both hydrous manganese oxides and hydrous iron oxides occur in soils and sediments in the normal Eh-pH range and as coating around silicate grains or as discrete grains of oxide mineral (Drever 1988).

In order to evalute the sources of the dissolved constituents in waters and any modification to the water as it passes through an area e.g. regolith or other earth

materials, a graphical techinque was developed by Piper (1944). The diagram (Fig. 13) consists of three fields: two triangular fields and intervening diamond-shaped field. In the triangular field at the lower left (Mg^{2+}, Ca^{2+}, $Na^{+}+K^{+}$) are plotted. The anion groups (SO_4^{2-}, HCO_3^{-}, Cl^{-}) are plotted likewise in the triangular field at the lower right. Two points on the diagram: one in each of the two triangular fields indicate the relative concentrations of the several dissolved constituents of a natural water. The central diamond-shaped field is used to show the over-all chemical character of the water by a third single-point plotting, which is at the intersection of lines projected from the plotting of cations and anions

Groundwater Stable Isotope Chemistry

The process that influences stable isotope composition in water is the evaporation-condensation cycle, which in turn is controlled by many parameters e.g. elevation, precipitation quantities, distance from the ocean and climate. For all practical purposes, rainwater is derived from evaporation from the surface of the ocean, mostly in subtropical regions. Evaporation process starts in the subtropical regions and the vapor, which becomes lighter in δ D and $\delta^{18}O$, moves towards the poles where condensation and precipitation occur (Arthur *et.* al., 1983). Craig (1961) plotted the δ D and $\delta^{18}O$ values in fresh waters as a straight line,

$$\delta D = 8\delta^{18}O + 10 \qquad (8)$$

where D is deuterium or ^{1}H and ^{2}H. The position of a sample along this line (the meteoric water line) depends on the amount of the precipitation during the time that

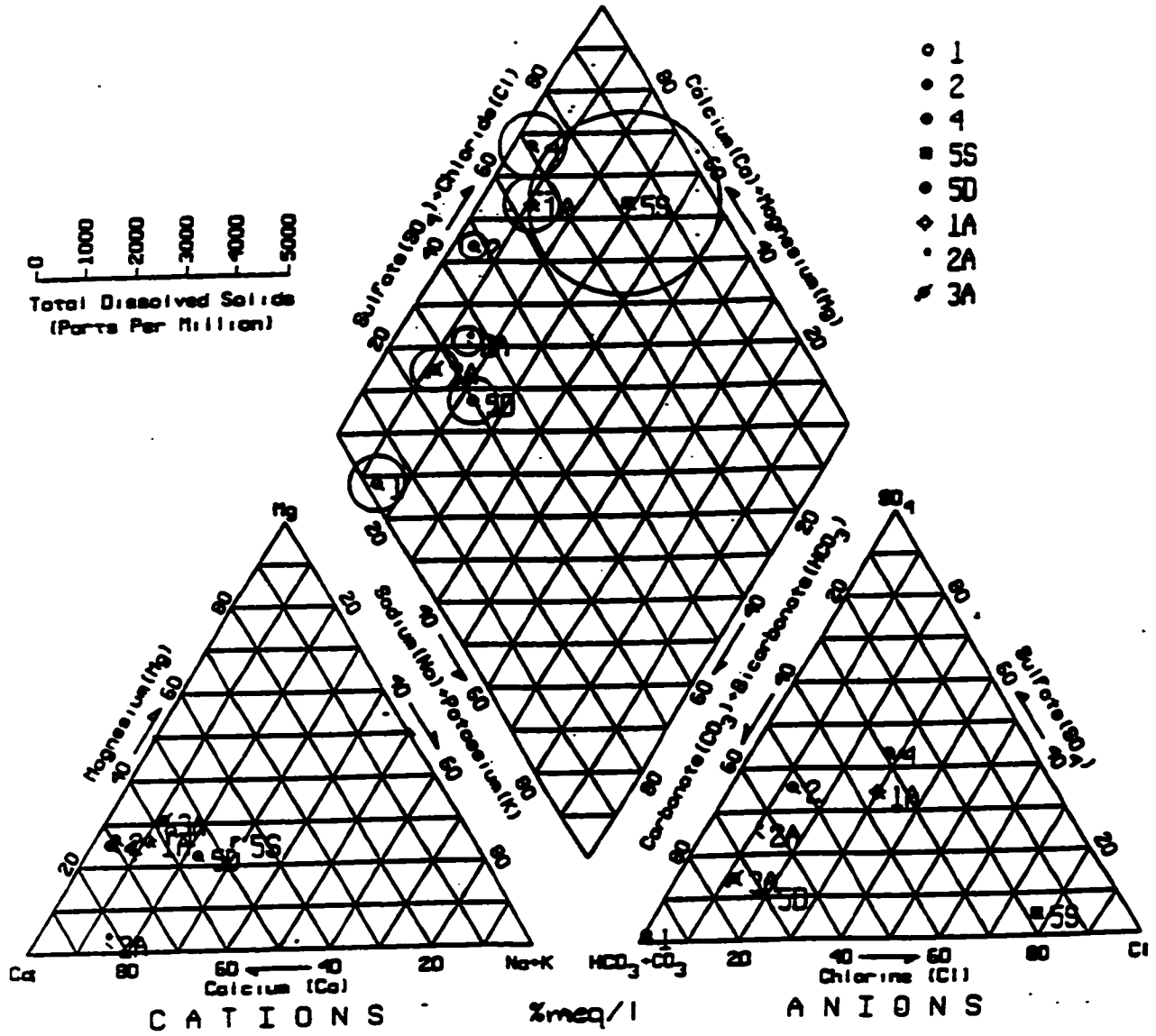

Fig. 13. Piper diagram used to classify water on the basis of its chemical composition. Where: 1 = OW1, 2 = OW2, 4 =OW4, 5S =OW5s, 5D = OW5d, 1A = OW1A, 2A = OW2A, and 3A = OW3A.

vapour left the ocean and the time of rainfall. As a consequence, rain becomes lighter in $\delta^{18}O$ as it reaches the poles from the equator. Several factors control the evaporation-condensation processes such as temperature, altitude and latitude. Because of the differences in mass of atoms, light stable isotopes can be fractionated by natural processes at low temperature. Such isotope fractionation leads to variability in the isotopic ratios in certain phases and certain regions (Drever, 1988). For example, the $^{16}O/^{18}O$ ratio in rain water is different from that in seawater. There are several factors control isotope fractionation. These are: 1) the differences in the masses of the isotopes and molecules affect the rates of some physical and chemical processes like dissociation, 2) evaporation and diffusion (velocities differences of isotopic molecules), 3) the temperature (more fractionation at low temperature), and 4) the chemical bond strength (the lighter the isotopes the weaker the bound). Isotope composition of a sample is defined by the delta (δ) notation in per thousand (‰). The ratio, which is the difference between a standard and a sample, are reported as follows

$$\delta ‰ = \frac{R_{sample} - R_{standard}}{R_{standard}} * 10^3 \qquad (9)$$

Where: R_{sample} is the isotope ratio of the sample.

$R_{standard}$ is Standard Mean Ocean Water (SMOW).

Isotope fractionation factors for the reaction of phases A and B are expressed on the basis of isotope ratios (Fritz and Fontes 1980)

$$\alpha_{A\text{-}B} = R_A/R_B \qquad (10)$$

and by using (δ) definition

$$\alpha_{A\text{-}B} = 10^3 + \delta_A / 10^3 + \delta_B \quad (11)$$

Thus, a relationship between fractionation factor (α) and fractionation equilibrium (K) occur when the isotopes are distributed randomly in a compound and it can be written as:

$$\alpha = K^{1/n} \quad (12)$$

where n is the number of atoms exchanged (Fritz and Fontes 1980).

For the purpose of studying groundwater isotope concentrations oxygen, and carbon are usually examined. Oxygen has three stable isotopes: ^{16}O, ^{17}O and ^{18}O with natural abundances of 99.76%, 0.037% and 0.1%, respectively. For practical uses absolute abundance of individual isotope is not measured. It is easier to use the relative difference in the abundance ratio of the heavy isotope to the light isotope of the same sample with respect to a reference standard. The $\delta^{18}O$ contents of precipitation are linearly related to mean annual temperature and, therefore, ^{18}O contents of groundwater usually reflect the mean annual temperature of the groundwater at the time of infiltration (Intera 1989).

Carbon has two stable isotopes: ^{12}C and ^{13}C with abundance of 99.984% and 0.015% respectively and one unstable ^{14}C isotope. ^{14}C is radioactive and decays with a half-life of 5,730 years into ^{14}N. Carbon dioxide of the atmosphere has $\delta^{13}C$ -7 to -10‰ with respect to PDB standard, marine carbonate rocks of Phanerozoic age are close to 0‰, and nonmarine carbonate rocks are -4.93‰ (Faure 1991). The sources of dissolved inorganic carbon (DIC) in groundwater can be from dissolution of carbonate minerals; oxidation of organic matter (soil CO_2), soil CO_2 resulted from the

methanogenesis of organic matter, atmospheric CO_2 (Fig. 14) and volcanic or metamorphic CO_2. Studying DIC sources in groundwater is significant because of the strong reaction between $CO_{2(aq)}$ and $HCO_3^-{}_{(aq)}$ and the highly fractionating effects of photosynthesis. Isotopic composition of carbon is governed by a variety of process such as photosynthesis, diagenesis, and metamorphism (Deines 1980). During all the chemical and biological reactions, isotopic fractionation of ^{13}C occurs with different fractionation factor, $\in$, at different temperatures as in the following reactions (Salomons and Mook 1986) (Table 6).

$$CO_{2\,g} + H_2O = H_2CO_3 \quad (13)$$

$$H_2CO_3 = H^+ + HCO_3^- \quad (14)$$

$$HCO_3^- = H^+ + CO_3^{2-} \quad (15)$$

$$CO_3^{2-} + Ca^{2+} = CaCO_3 \quad (16)$$

Table 6. ^{13}C fractionation factors for the carbonate open system (Salomons and Mook 1986).

Temp°C	$\in CO_{2g}$-HCO3	$\in CO_{2g}$-CO_{2aq}	$\in CO_{2aq}$-$HCO3^-$	$\in HCO3^-$-$CO3^{2-}$	$\in HCO3^-$-CaCO3
5	-10.25	-1.15	-11.35	-0.6	-0.11
15	-9.02	-1.1	-10.12	-0.49	+0.41
25	-7.92	-1.06	-8.97	-0.39	+0.91
35	-6.88	-1.02	-7.9	-0.29	+1.37

Although, terrestrial plants fix atmospheric CO_2 during photosynthesis, its $\delta^{13}C$ is low in a comparison with the source CO_2 (Arthur, *et.* al. 1983). The depletion of ^{13}C in land plants is caused by fractionation during the photosynthesis process when the atmospheric CO_2 gas diffuses into the green cell of plants and causes internal CO_2 to be depleted in ^{13}C. The CO_2 will be converted into two kinds of acids depending on the

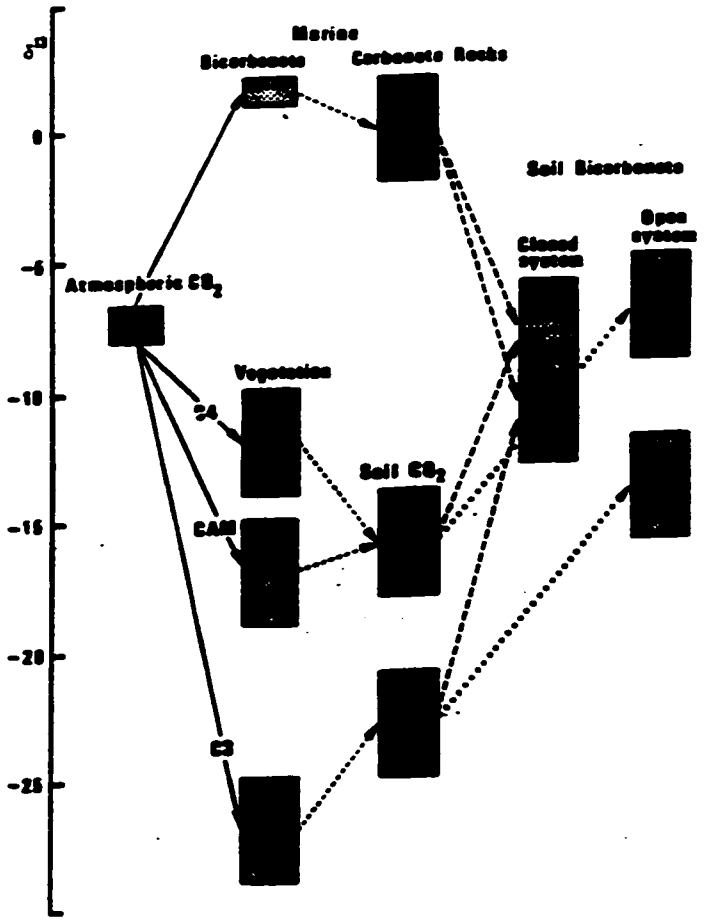

Fig. 14. Schematic diagram showing $\delta^{13}C$ values in the atmosphere, biosphere and hydroshere (from Salmons and Mook 1986).

number of C atoms; the phosphoglyceric acid which contains three C atoms (Calvin cycle) or the dicarboxylic acid with four C atoms (Hatch-Slack cycle) (Faure 1991). Lerman (1972), Throughton (1972), and Allaway *et.* al. (1974) classified plants according to their ^{13}C content. The carbon isotopic composition of the various plants ranges from ranges between -23 to -33‰ with average of -26‰ in the Calvin cycle (C3). The carbon isotopic composition of Hatch-Slack (C4) plants ranges from -9 to -16‰ and average of -13‰ The carbon isotopic composition of the CAM (Crassulacean Acid Metabolism) plants cover the whole range of C3 and C4 plants under varying conditions (Deines 1980). The C3 plants dominate temperate regions, C4 plants dominate tropical region and CAM plants dominate very arid regions.

Groundwater Trace Metal Chemistry

Trace metals are elements occurring in natural waters at concentrations of less than 1 mg/L. They may be derived from the weathering of rocks and minerals or from human activities. In natural waters many processes regulate the trace metal concentrations. These may be speciation, organic matter and complex formation, equilibrium solubility control and adsorption and coprecipitation controls.

In electrolyte solutions, the resultant ions or uncharged molecules have a different characterization from the original constituent of the solution. The solubility of gibbsite is an example of a complex process because the dissolved aluminum can exist in several forms: Al^{3+}, $Al(OH)^{2+}$, $Al(OH)_2^{+}$, $Al(OH)_3^{0}$ and $Al(OH)_4^{-}$ in solution

(Drever 1988). The solubility of gibbsite is very low except at pH approximately 4 to 9.

The presence of organic matter in groundwater can control trace metal concentration. Complex formation by organic matter is higher in fresh water than in the seawater because of the competition between the organic and inorganic ligands, the latter being more concentrated in ocean waters. The presence of organic matter in solution modifies the adsorption of trace metals by oxide and silicate surfaces.

One of the most important processes that regulates the concentration of trace metal in solution is equilibrium with respect to a solid phase containing the element as a major constituent. To determine whether or not a solution is in equilibrium with the solid phase, the activity of electrons (pe/Eh) of the solution must be known by calculating the activities of a redox pair (Drever 1988).

Adsorption and coprecipitation are other factors that regulate and control the concentration of trace metal in groundwater and reduce their concentration. The adsorption process, which is pH dependent, occurs because of the attachment of ions to the surface of solid phases. On the other hand, coprecipitation occurs when there is co-operation between dissolved ions as a minor component and a solid phase as it precipitates.

Results and Discussion

Major Element Distribution

Chemical data for groundwater samples is reported in Table 7 and shown in the Piper diagrams (Fig. 13)

The calcium concentrations of all the water samples range between 82-267 mg/L; while waters close to carbonate rocks may range from 30 to 100 mg/L; seawater concentrations are usually 400 mg/L and brines may contain up to 75 000 mg/L (Environment Canada 1979). A drinking water limit of 200 mg/L has been proposed by Department of National Health and Welfare (1969). The sources of calcium in groundwater may related to the solution of calcium carbonate (calcite and aragonite), calcium sulfate (anhydrite and gypsum) and transformation of plagioclase to kaolinite or other clay minerals or leaching from soil or human activities such as sewage and industrial wastes.

Magnesium ranges from 20 to 91 mg/L in all the well samples and natural surface waters contain between 1.0 to 100 mg/L, seawater has approximately 1000 mg/L, and brines may contain up to 57 000 mg/L (Environment Canada 1979). The maximum acceptable value in drinking water is 150 mg/L (Department of National Health and Welfare 1969). The source of magnesium in natural water derives from the weathering of igneous rocks and dolomitic sedimentary rocks or from industrial waste.

Sodium ranges between 6 to 172 mg/L in both the acitive and the abandond water samples. Seawater has approximately 10 500 mg/L and brines may range from 25 000 to 100 000 mg/L (Environment Canada 1979). The acceptable limit of sodium

Table 7. The chemical analysis data of the active and abandoned landfill well

	Wells #							
Parameters (mg/L)	OW1	OW2	OW4	OW5d	OW5s	OW1A	OW2A	OW3A
Ca	161	97	154	82	267	137	110	103
Mg	49	23	33	20	91	35	20	34
Na	44	6	8	1	37	21	20	15
K	1	0.5	1.5	1	37	10	3	15
*T.A. as $CaCO_3$	300	82	170	254	344	159	105	217
SO4	5	44	200	30	80	120	33	34
Cl	30	11	94	41	870	77	10	20
As	0.003	0.041	0.053	0.031	0.014	0.002	0.008	0.008
Fe	1	2.2	0.11	0.5	0.023	0.36	0.24	1
Mn	0.66	0.18	0.25	0.2	0.58	0.28	0.26	0.21
Al	0.011	0.002	0.005	0.007	0.28	0.005	0.005	0.006
Cd	0	0	0	0	0.001	0	0	0
Co	0.01	0.003	0.005	0.005	0.004	0.003	0.004	0.003
Cu	0	0.002	0.004	0.001	0.001	0.001	0	0
Pb	0.002	0.02	0.006	0.002	0.002	0.28	0.26	0.21
V	0.001	0.004	0.002	0.002	0.002	0.001	0.002	0.001
Zn	0.002	0.005	0.005	0.003	0.006	0.004	0.007	0.004
Cr	0.002	0.001	0.001	0	0.001	0	0.001	0.006
Ni	0.002	0.002	0.005	0.002	0.004	0.001	0.002	0.003
Sb	0.03	0.034	0.003	0.034	0.43	0.04	0.03	0.036
pH	6.81	6.7	6.66	6.8	6.37	6.61	6.74	6.55
TDS	80	2.95	383	292	1440	417	285	373
*C (U.S. gal/day/ft^2	243	600	763	595	2.84 (m	846	520	729
Well depth (m)	3	3.9	3.7	6.5	3.7	4.27	3.66	4.2
O^{18} (SMOW)	-	-8.96	-8.29	-9.29	-8.48	-8.71	-9.37	-9.51
C^{13} (PDB)	-	-14.9	-15.81	-12.41	-15.62	-15.12	-15.04	-15.47

*T.A = Total Alkalinity

*C = Conductivity

in drinking water is less than 270 mg/L (Hart 1974). The sources of sodium in natural water include igneous rocks, clay minerals, feldspar, and evaporite minerals such as halite. Potassium ranges from 0.5 to 37 mg/L in the well water samples. Seawater contains approximately 380 mg/L, natural surface waters less than 10 mg/L, and brines may contain up to 25 000 mg/L. No recommended limit has been prescribed for potassium (Environment Canada 1979). The sources of potassium in natural waters are evaporatec deposits, feldspar, clay minerals and industrial effluents. The common salts of potassium are highly soluble in water and they resist separation from water by natural processes other than evaporation (Ontario Ministry of Environment 1991).

Alkalinity as $CaCO_3$ ranges between 82 to 344 mg/L in Walpole Island groundwater samples. In natural surface waters, alkalinity rarely exceeds 500 mg/L. The acceptable limit of alkalinity in drinking water is less than 500 mg/L (Department of National Health and Welfare 1969).

Sulfate ranges from 5 to 200 mg/L in the well water samples. While surface water ranges from a few to thousands of milligrams per liter, brines can contain 200 000 mg/L and seawater contains 2650 mg/L. Drinking water should contain less than 500 mg/L (Department of National Health and Welfare 1969). The sources of sulfate in natural waters are the leaching of sedimentary rocks, organic materials, industrial discharges. Sulfate is produced from the final oxidation stage of sulfides, sulfites and thiosulphate. Sulfate, under anaerobic conditions, can be reduced to hydrogen sulfide which is highly corrosive (Ontario Ministry of Environment 1991).

Chloride ranges from 10 to 870 mg/L in both the acitive and the abandond water samples. Concentrations of chloride vary by climatic regions, surface water in humid regions contains low chloride concentrations (< 10 mg/L). In smi-arid regions, surface water contains several hundred milligrams per litre (Environment Canada 1979). Seawater may contain up to 200 000 mg/L and drinking water should contain less than 250 mg/L (Department of National Health and Welfare 1969). The largest sources, that contribute chloride to groundwater, can be domestic sewage discharge, municipal storm drainage, road salting, and industrial wastes (Ontario Ministry of Environment 1991).

OW2 is located in an elevated location of the waste area and its major constituents are low in a comparison with the other well water samples and with other natural waters; it is considered here to represent the background groundwater quality at both sites. The low concentrations of both sodium and chloride give an indication of no impact of the landfill and the surface waste on water quality

OW1 is located at the lowest elevation of the site and shows slightly elevated major elements concentration in a comparison with the OW2. The high alkalinity value may relate to the presence of carbonates, bicarbonates, and hydroxides. The minor impact of the wast leachate on the indicator parameter (in particular chloride and sodium) may relate to the natural dilution.

OW4 is located on the edges of the waste area within about 10 m of buried waste cells (Burnside Environmental LTD Report 1995). Again, there seem to be no sharp impact of the leachate contamination on the indicator parameters (chloride and

sodium). However, sulfate is above the background and this high value may be due to oxidation of organic matter.

OW5s and Ow5d are located in the centre of the site and surrounded by the buried waste pits and surface waste. The highest concentrations of all the major constituents are found in OW5s in a comparison with the background (OW2). The deepest well is OW5d and its samples contain the lowest concentrations in a comparison with the background groundwater quality. The lowest concentrations of OW5d may suggest that the landfill leachate impacts are restricted to the upper sand unit and the low permeability of the silty clay unit (Burnside Environmental LTD Report 1995).

Water analysis in the abandoned landfill wells indicate that the impact of the leachate contamination on the indicator parameters (chloride and sodium) and all other's were found exceeding the background groundwater quality (OW2). The OW1A, OW2A and OW3A wells are located close to each other and water parameters are high in a comparison with the background quality. Parameters such as chloride, sodium are considered a good indicator of leachate contamination. Chloride is a conservative ion in groundwater and is considered to be a good indicator of leachate contamination.

In the cation triangle of the Piper diagram (Fig. 13), most water samples of both areas are located within the calcium-dominated hydrochemical facies. The exception, the OW5s water, is located in the mixed-ions facies. The location of water samples in the calcium-dominated facies confirms that a possible ion-exchange occurred during the infiltration. The source of shallow groundwater of all wells, as it was

inferred from ^{18}O analysis (discussed later), is a young recharge and most likely related to rainfall. During the infiltration, ions were adsorbed on colloidal particles because these particles have a large electrical charge relative to their surface area. The surface charge may result from the ionic substitutions within the crystal structure or chemical dissociation reactions at the particle surface (Freez and Cherry 1979). The solubility of calcium is another factor for calcium domination in groundwater.

In the anion triangle, water samples of OW1, OW2, OW5d, OW2A and OW3A are located in the bicarbonate dominated facies, suggesting a possible reduction of SO_4^{2-} to H_2S and then to HCO_3^- in anaerobic environment. Sulfate has much lower concentrations in all water samples in a comparison with natural waters content and drinking water limit. When all the dissolved oxygen in groundwater is consumed, oxidation of organic matter can still occur by oxidizing agents such as SO_4^{2-}. As the oxidizing processes continue, the oxidizing agents will be consumed, the environment will be converted to a reducing environment, and the organic matter may undergo anaerobic degradation. The reaction for this process can be written as (Freez and Cherry 1979)

$$CH_2O + 1/2SO_4^{2-} = 1/2HS^- + HCO_3^- + 1/2H^+ \quad (17)$$

Water samples of OW4 and OW1A are located in the mixed ions and the OW5s water is located in chloride-dominated facies, which confirm a leachate of chloride from waste side.

In the diamond-shaped field (Fig. 13), all water samples are located within the area which has the alkaline earths (Ca^{2+} and Mg^{2+}) exceeding the alkalis (K^+ and

Na^{+}), confirming the exchange reactions occuring between ions in the water and ions adsorbed on the medium during the infiltration. Potassium is the ion most affected by the exchange reactions because potassium does not form salts unless it exists in a very high concentrations. Because all samples are dominated by the alkaline earths (Ca^{2+} and Mg^{2+}), the alkali ions (in particular potassium) were removed. Water samples of OW4, OW5S and OW1A are located in the area where the strong acids (sulfate (SO_4) and chloride (Cl)) exceed the weak acids (bicarbonate (HCO_3)) and water samples of OW1, OW2, OW5d, OW2A and OW3A are located in the area where the weak acids exceed the strong acids. The evolution of the strong acids of the first three wells may be related to the release of SO_4^{2-} and Cl^- ions from soil to the percolating rainwater. The SO_4^{2-} and Cl^- ions are released upon dissolution of sulfate- or chloride-bearing minerals such as gypsum or halite, respectively. The high concentrations of the bicarbonate in the OW1, OW2, OW5d, OW2A and OW3A wells can be explained by dissolution of carbonate minerals as aresult of water carbon dioxide-rich infiltrating through the soil zone. As H_2CO_3 is consumed in the soil zone, oxidation of organic matter and root respiration is a source of replenishment of CO_2 to the soil air. The continuous reactions between the percolating water and CO_2 will continue to produce H_2CO_3. Sulfate reduction is another source for producing bicarbonate. Sulfate reduction can be defined as a bacterial reaction in which bacteria use the oxygen in the SO_4^{2-} to oxidize organic matter to CO_2, producing sulfide species as by-product (Drever 1988). The reaction can be written as

$$SO_4^{2-} + 2C_{organic} + H_2O = H_2S + 2HCO_3^- \qquad (18)$$

The pH of water samples from all wells is 6.37-6.81 (Table 7) and is in the acceptable range value of 6.5 to 8.3 according to Water Quality Guidelines (Environment Canada 1979).

Trace Metal Distribution

Thirteen trace metals were determined for the purpose of characterizing groundwater contamination in both the active and abandoned landfill (Table 7). Generally, all samples concentrations are below the Water Quality Guidelines (Environment Canada 1979).

Arsenic ranges were found between 0.002-0.28 mg/L in Walpole Island groundwater samples. Fresh water may contain as high as 0.010 mg/L arsenic (Environment Canada 1979). In seawater, arsenic concentrations is between 0.00015 and 0.006 mg/L (Woolson 1975; Bowen 1966). The recommended permissible limit of arsenic in drinking water is 0.05 mg/L (Environment Canada 1979). Elemental arsenic is insoluble in water but many arsenates are highly soluble (Ontario Ministry of Environment 1991). Because arsenic can exist in the valence states of -3, 0, +3, and +5, it can form a wide range of compounds with a large number of anions. The high concentration of As in OW5s may come from the waste since this well is located in the central area of the waste disposal site.

Iron concentration values range between 0.023 and 2.2 mg/L in the water samples. In surface water, iron concentration is usually less than 0.5 mg/L (Environment Canada 1979). Iron is one of the most abundant elements in the earth's

crust and it is a constituent of many industrial wastes. Iron can exist as Fe-oxides which are slightly soluble in water depending of the pH. The solubility of Fe-oxides limits their stability in natural environments because they may be removed by acidic water. Fe-carbonate is another form of iron in natural environment. Because of the dominance of Fe^{2+} over Fe^{3+} in most environments, the most common Fe-carbonate may be as $FeCO_3$ (siderite) rather than $Fe_2(CO_3)_3$. In well OW2, which has the lowest alkalinity, sulfate and the highest iron concentration, siderite may form from saturated solutions which are in equilibrium with CO_2 gas or contain fixed amount of carbonate ions as a result of prior interaction with rocks or minerals (Faure 1991). Siderite may precipitate under strongly reducing environment from basic solution and its stability restricted to its solubility in water. Iron can change from the ferrous to the ferric state when it exists in water in sufficient amounts in the form of chloride, nitrate or sulfate salts (Ontario Ministry of Environment 1991). Both OW1 and OW2 have the highest concentration, which may come from the corrosion of iron, steel and scrap metal of the waste active site.

Manganese concentration range from 0.2 to 0.66 mg/L in well samples. In surface water, Mn is usually present in quantities of 0.2 mg/L (Environment Canada 1979). The acceptable level of Mn in drinking water is 0.05 mg/L (Department of National Health and Welfare 1969). Manganese occurs in soils as manganic and manganous compounds (Ontario Ministry of Environment 1991). Under anaerobic conditions the maganic ion is reduced to soluble nitrate, sulfate, and chloride salts and is leached along with iron, into ground and surface waters. The existence of

manganese may indicate domestic or industrial pollution. The highest concentrations of Mn were found in wells OW1 and OW5s, 0.66 and 0.58 mg/L, respectively, which may come from the waste dump site.

Aluminum ranges from 0.003 to 0.053 mg/L in the well samples. Most natural waters contain less than 1.0 mg/L of Al and seawater concentrations average 0.01 mg/L (Environment Canada 1979). The sources of aluminum are mostly aluminosilicate minerals in igneous and sedimentary rocks as well as soils.

Cadmium concentrations are 0.0001 mg/L in Walpolw Island groundwater samples. Natural waters contain only traces of cadmium, in the range of 0.0001 to 0.01 mg/L and seawater concentration is 0.0001 mg/L (Environment Canada 1979). The permissible limit of Cd in drinking water is 0.01 mg/L (Department of the Environment 1972; Department of National Health and Welfare 1969). Cadmium is insoluble in water but carbonate and hydroxide are slightly soluble. Cadmium occurs in nature as a sulfide salt and in zinc-lead ores (Ontario Ministry of Environment 1991).

Cobalt ranges between 0.003 to 0.01 mg/L in the well samples. Cobalt concentration in natural surface water is < 0.0001 mg/L and in seawater concentration is about 0.0005 mg/L. There are no water quality guidelines for cobalt in drinking water (Environment Canada 1979).

Copper ranges from 0 to 0.004 mg/L in the well samples. Copper concentration in natural surface waters is up to 0.05 mg/L and in seawater ranges from 0.001 to 0.025 mg/L (Environment Canada 1979).

Lead ranges between 0.002 to 0.02 mg/L in the well samples. Lead concentration in natural surface waters is 0.04 mg/L and in seawater ranges from 0.001 to 0.025 mg/L (Environment Canada 1979). Although lead is insoluble at normal groundwater pH level, lead salts such as acetate and chloride, are soluble. Therefore, lead does not remain long in natural waters (Ontario Ministry of Environment 1991).

The vanadium ranges between 0.001 to 0.004 mg/L in all samples. Vanadium concentration in natural surface waters is 0.3 mg/L and seawater contains 0.003 mg/L (Environment Canada 1979).

Zinc ranges between 0.002 to 0.007 mg/L in all samples. The zinc concentration in natural surface waters is less than 0.05 mg/L and seawater contains 0.01 mg/L (Environment Canada 1979). The zinc ion is believed to adsorb strongly and permanently on fine particles (silt) which settles from suspension (Ontario Ministry of Environment 1991).

Chromium ranges between 0 to 0.006 mg/L in all samples. The chromium concentration in natural surface waters is < 0.001 mg/L and seawater contains 0.00005 mg/L (Environment Canada 1979). Drinking water supplies should not exceed 0.05 mg/L chromium. Chromium is present in rocks and soils as insoluble chromic oxide which is strongly sorbed to fine particles (Ontario Ministry of Environment 1991).

Nickel ranges between 0 to 0.006 mg/L in all samples. The nickel concentration in North American rivers is 0.1 mg/L and seawater ranges between 0.005 to 0.007 mg/L (Environment Canada 1979). The toxicity of nickel is very low, therefore, no drinking water guidelines. Nickel is insoluble but as a salt (ammonium

sulfate, nitrate, and chloride) is highly soluble (Ontario Ministry of Environment 1991).

Antimony ranges between 0.03 to 0.04 mg/L in all samples. The antimony concentration in natural surface waters is in trace amount and in seawater 0.0005 mg/L (Environment Canada 1979). No guidelines for antimony concentrations have been proposed for drinking water, but the level should be low not to exceed 0.01 mg/L (Tai 1970)

Stable Isotope Distribution

The stable isotopes $\delta^{18}O$ and $\delta^{13}C_{DIC}$ were measured to determine the source and flow direction of subsurface water and to assess and identify its contamination (Table 7). Desaulniers *et* al. (1981) examined the $\delta^{18}O$ of the groundwater in the southwestern Ontario clay till and he concluded that concentrations ranged from a water-table value of -10‰ to deep (20-40 m) groundwater values of -14 to -17‰. The shallow groundwater values are indicative of present day precipitation. The deeper values represent cooler, glacial waters (^{14}C > 8000 years). Desaulniers (1986) used $\delta^{18}O$ present-day enrichment to identify groundwater flow directions in the clay till of southwestern Ontario. Desaulniers (1986), Sklash *et* al. (1986), Scott (1986), Erdmann (1987) and Williams (1988) used $\delta^{18}O$ in studies of the freshwater aquifer in Ontario and Michigan. They inferred the flow direction of groundwater in directions of $\delta^{18}O$ depletion. Long *et* al. (1988) determined isotopic composition of shallow saline (< 100 m depth) groundwater in the east-central Michigan basin and they found the range was

from -9 to -19‰. Fritz *et* al. (1975) measured the $\delta^{18}O$ contents of shells and mollusks from a basal till unit beneath Lake Erie. The isotopic composition of shells and mollusks ranged between -18 to -20‰ with emplacement occurring between 12800 and 13800 B.P. These results confirm that deep groundwaters are a mixture of modern meteoric water and water that recharged the fresh water aquifer system during a cooler time period. The $\delta^{18}O$ concentrations range of both the active landfill and abandoned wells are from -8.29 to -9.51‰ (Table 7). These values are close to the porewater ^{18}O concentration range (-8.65 to -9.33‰) of the GD-Core at shallow depth (8.84-10.57 m). The data represent a young recharge (< 10000 B.P) which is similar to the present day rainfall (-9‰ to -11‰) (Sklash *et.* al. 1986; Desaulniers *et* al. 1981). Other possible sources of shallow groundwater may be the infiltration of St. Clair River water ($\delta^{18}O$ = -7.2‰) or infiltration of waters from deeper geologic formations which have $\delta^{18}O$ value of -10 to 0‰ (Dollar *et* al. 1987). The flow directions of shallow groundwaters are toward southeast of the study area and follow the same pattern of fresh water movement beneath the clay till deposits. Crnokrak (1991) studied the flow direction of fresh water in the St. Clair River, Lake St. Clair and Detroit River (Fig. 15) drainage basin. The flow direction of fresh water is southeast in areas (Oakland, Macomb and St. Clair) located to the west of St. Clair River, Lake St. Clair and Detroit River with an isotope range from -9 to -11‰. Further depletion (-16 to -17‰) is found toward St. Clair River and representing waters of glacial origin. In areas located east of St. Clair River (Lambton County), groundwater flow direction is

Fig. 15. Contour map of $\delta^{18}O$ in the freshwater aquifer (from Crnokrak 1991).

westward toward the St. Clair River with isotope concentrations of -8.5 to -10‰ and more depletion (-17‰) toward the river. The Kent County flow regime is southward with -9 to -10‰ with further depletion (-18‰) toward Lake Erie. Results inferred form this study indicate that the flow regime of the St. Clair delta groundwater toward southeast in both the active landfill and the abandoned landfill sites.

The concentration of ^{13}C of most shallow wells located in both the active and abandoned landfill areas range from -14.86 to -15.81‰ (Table 6). The OW5d at 6.5 m depth has a ^{13}C of -12.41‰. The source of ^{13}C of both the active and the abandoned landfill can be related to the C3 plants or Calvin cycle. The plants of the C3 cycle are isotopically light and the soil-CO_2 has low ^{13}C values (-20 and -25‰) as well (Fritz and Fontes 1986). The aqueous form of this CO_2 will have enrichment in ^{13}C value which can be explained by the preferential uptake of ^{12}C during the photosynthesis and the release of ^{13}C which enriched the respiration CO_2 (Park and Epstein 1960). The 10 cm isotopically light -25‰ humus layer (Arthur *et* al. 1983), which was found at the surface of the GD-Core and the abundant vegetation are consistent with the organic source of the dissolved inorganic carbon. The source of the OW5d may relate to a mixing of dissolved inorganic carbon from pre-existing carbonate rocks that are generally heavier in ^{13}C from +1 to +2‰ and dissolved organic matter. Generally, groundwaters have a wide range of ^{13}C values (-30 to +3‰; average -10‰) because of the interaction between the isotopically light organic matter and the isotopically heavy carbonate minerals (Arthur *et* al. 1983).

CHAPTER 7
CONCLUSIONS AND RECOMMENDATION

Conclusions

The conclusions which can be drawn from this study are:

(1) The clay assemblages in Walpole Island Quaternary sediments contain illite, chlorite, kaolinite, illite/smectite and smectite. The dominant non-clay mineral tends to be quartz and plagioclase, K-feldspar, calcite, siderite and pyrite are found in small amounts.

(2) The concentrations of illite in the three cores is less than 65 percent, chlorite concentrations are around 20 percent, kaolinite concentrations are around 10 percent, mix-layered clay concentrations do not exceed 3 percent, trace amounts of smectite do not exceed 1 percent, and quartz concentrations are approximate 4 percent.

(3) The clay assemblages profiles for Cores-HP and GD indicate that the concentrations of illite, chlorite and kaolinite increased with depths and the other minor constituents including illite/smectite and smectite have a variable concentrations with depth.

(4) The paleoenvironment of the area has been subdivided into upper and lower horizons of having variable thicknesses.

(5) The analysis of shallow groundwater samples indicate that three possible sources for ^{18}O: 1) a young recharge (< 10 000 B.P.), which is similar to present day rainfall and snowmelt; 2) the infiltration of St. Clair River water; 3) and the infiltration of waters

from deeper geologic formations. Rainfall and snowmelt are the most important and the main sources.

(6) The flow direction of shallow groundwaters are towards southeast of the study area.

(7) The analysis of ^{13}C indicate that the source of carbon in groundwater can be related to the C3 plants or Calvin cycle.

(8) The analysis of major element in water samples indicate that chloride concentrations (10-870 mg/L) are above the drinking water limit (< 250 mg/L).

(9) Trace metal analysis indicate that arsenic (0.002-0.28 mg/L), iron (0.023-2.2 mg/L), and manganese (0.18-0.66 mg/L) show elevated concentrations which exceed the drinking water limit (0.05, < 0.05, and 0.05 mg/L, respectively).

(10) The low concentrations of most trace metals and major elements may be related to groundwater flushing.

Recommendations

Based on the results and conclusions described in this study, the following may be important to take into consideration for future study:

(1) The Quaternary sediments here have never been exposed to industrial contamination, further study of trace metals and organic matter must be undertaken to determine the relationship between mineralogy and its natural levels of major and minor elements. This may help to determine the nature of clay sediments in fixation and release of contaminants into surrounding area.

(2) The present waste disposal practices should be improved to prevent future degradation of the environment in the active landfill site. The uncovered surface waste should be compacted and properly covered and all waste deposited at the active landfill should be regularly covered.

(3) Access to the site should be controlled to ensure only acceptable wastes are deposited. This may be accomplished by a road gate, fencing, and the presence of operator to control the dump of the waste quality.

References

Al-Aasm, I.S., W.H. Blackburn, T.M. White, R.L. Thomas and M.A. Racz 1995. Sedimentologic and isotopic studies of St. Clair Delta sediment, Ontario. Geol.Ass. Can. / Min. Ass. Can. Abstracts, 20:A-1.

Allaway, W.G., Osmond, C.B. and Throughton, J.H., 1974. Environmental Regulation of Growth, Photosynthetic pathway and carbon isotope discrimination ratio in plants capable of Crassulancean acid metabolism. In: R.L. bieleski, A.R. Ferguson and M.M. Cresswell (Editor), Mechanisms of Regulation of Plant Growth. R. Soc. N.Z., Bull., 12: 1965-202.

Ambrose, J.W., 1964. Exhumed paleoplains of the Precambrian Shield of North America; American Journal of Science, v.262, p.817-857.

American Public Health Association, American Water Works Association and Water Pollution Control Fedration (APHA-AWWA-WPCF) 1975. Standard Methods for the Examination of Water and Wastewater 14th edition.

Arthur, M.A., T.F. Anderson, I.R. Kaplan, J. Veizer and L.S. Land 1983. Stable Isotopes in Sedimentary Geology. SEPM Short Course No. 10, Dallas.

Bailey, S.W. ed. 1988. Hydrous phyllosilicates (exclusive of micas): Vol. 19 in Reviews in Mineralogy: Mineralogical Sociaty of America, Washington, 584p.

Barnett, P.J. 1979. Glacial Lake Whittlesey: The probable ice frontal Position in the eastern end of the Erie basin; Canadian Journal of Earth Sciences, v.16, p.568-574.

Barnett, P.J 1992. Quaternary Geology of Ontario. In Geology of Ontario, Ontario Geological Survey Special Volum 4(1).

Benner, M.M., 1971. Variation in the $^{13}C/^{12}C$ ratio of plants in relation to the pathway of photosynthetic carbon dioxide fixation. Phytochemistry, 10: 1239-1244.

Bhattachary, J.P., and R.G., Walker 1992. Daltas. in R.G., Walker and James N.P., eds., Facies Models: Response to Sea Level Change. Geological Association of Canada.

Biscay, P.E. 1965. Mineralogy and Sedimentation of Recent Deep-Sea Clay in the Atlantic Ocean and Adjacent Seas and Oceans. Geological Society of America Bulletin, v. 76, p. 803-832.

Boggs, S. Jr. 1992. Petrology of Sedimentary Rocks. Macmillan Publishing Company, New York, Maxwell Macmillan Canada, Toronto, Maxwell Macmillan International, New York, Oxford, Singapore, Sydney.

Bowen, H.J.M. 1966. Trace Elements in Biochemistry. Academic Press, London and New York.

Brigham, R.J., 1971. Structural Geology of Southwestern Ontario and Southeastern Michigan. Ontario Dept. Mines and Northern Aff., Petro. Res. Sect. Paper 71-2, 110 p..

Burnside Environmental LTD. Report, 1995. Environmental Issues Inventory. Draft Report, Walpole Island First Nation.

Burst, J.F., 1958. Mineral heterogeneity of "glauconite" pellets. Am. Miner., 43:481-497.

Chamley, H. 1989. Clay Sedimentology. Springer-Verlag Berlin Heidelberg New York London, Paris Tokyo Hong Kong.

Champman, L.J. and D.F. Putnam 1951. The Physiography of Southern Ontario. Univ. of Toronto Press, Toronto. 284 p.

Christensen, M.D., 1993. Acoustic Investigation and New Depositional Model for the Devolopment of the St. Clair Delta, Ontario, Canada.Unpubl. M.Sc. thesis. University of Windsor, Windsor, Ontario. 121 p.

Cole, L.J. 1903. The delta of the St. Clair River. Geol. Surv. Michigan, 19: 1-28.

Craig, H. 1961. Isotopic variations in meteoric waters. Science, 133: 1702-1703.

Crnokrak, B. 1991. An Environmental Isotope and Computer Flow Model Investigation of the Freshwater Aquifer in the Lake Huron to Lake Erie Corridor. Ontario, Canada. M. Sc. Thesis, University of Windsor, Windsor, Ontario. 250p.

Cumming, J.D. 1995. Sedimentology and Porewater Isotope Chemistry of Quaternary Deposits from the St. Clair Delta, Walpole Island, Ontario, Canada. M.Sc. Thesis, University of Windsor, Windsor, Ontario. 122p.

Cumming, J.D. and I.S. Al-Aasm 1996. Sedimentology and Porewater Isotope Chemistry of Quaternary Deposits from the St. Clair Delta, Walpole Island, Ontario, Canada. Department of Earth Sciences, University of Windsor.

Deines, P. 1980. The isotopic composition of reduced organic carbon. In: Handbook of Environmental Isotope Geochemistry, P. Fritz and J.C. Fontes (eds.), V. 1, The Terrestrial Environment, A, Elsevier, p. 329-406.

Department of National Health and Walfare, 1969. Canadian Drinking Water Standards and Objectives 1968.

Desaulniers, D.E. and J.A. Cherry and P. Fritz 1981. Origin, age and movement of pore water in argillaceous Quaternary deposits at four sites in southwestern Ontario. J. Hydrology, 50: 231-257.

Desaulniers, D.E. 1986. Groundwater Origin, Geochemistry and solute Transport in Three Major Glacial Clay Plains of East-Central North America. Ph. D. Thesis, University of Waterloo, Waterloo, Ontario, 444 p.

Dollar, P., S.K. Frape, R.H. McNutt, P. Fritz, and R.W. Macqueen 1987. Grant 249. Geochemical Studies of Formation Waters from Paleozoic Strata, Southwestern Ontario. In: Geoscience Research Grant Program, Summury of Research, 1986-1987. Ontario Geol. Surv. Miscellaneous Paper 136, pp. 57-65.

Dominion Soil Investigation Inc. 1977a. Soil Investigation for Proposed Water System, Walpole Island, Ontario. 10p.

Dominion Soil Investigation Inc. 1977b. Soil Investigation for Proposed Access Road to Pump Installation No. 1., Walpole Island, Ontario. 5p.

Dorr, J.A. and D.F. Eschman 1971. Geology of Michigan. Ann Arbor, University of Michigan Press. p. 167.

Dreimanis, A. 1961. Tills of southern Ontario; in Soils of Canada, Royal Society of Canada, Special Publiction, no. 3, p.80-96.

Drever, J.I. 1973. The preparation of oriented clay speciemens for x-ray diffraction analysis by a filter-memberance peel technique. Am. mineral. 58: 553-554.

Drever, J.I. 1988. The Geochemistry of Natural Waters. Printice Hall, New York.281p.

Dwyer, C.F. 1997. Sedimentologic and Mineralogic Studies on Channel Sediments of the St. Clair Delta, Ont. Canada. Unpubl. B.Sc. thesis, University of Windsor, Ontario. 74p.

Dyke, A.S. and V.K. Prest 1987. Late Wisconsinan and Holocene history of the Laurentide Ice Sheet. Geographic Physique et Quaternaire, 41: 237-263.

Ecologistics Ltd. 1979. Biophysical Survey of the Walpole Island Indian Reseve. Unpubl. 106 p.

Environment Canada 1979. Water Quality Sourcebook. A Guide to Water Quality Parameters. Inland Water Directorate, Water Quality Branch, Ottawa, Canada. 89 p.

Epstein, S. and T.K. Mayeda 1953. Variation of the $^{18}O/^{16}O$ ratio in natural waters. Geochim. Cosmochim. Acta, 4:213-222.

Erdmann, R. 1987. An Environmental Isotope Study of the Fresh Water Aquifer in St. Clair and Macob Counties, Michigan. B.A.Sc. Thesis, Department of Geology, University of Windsor, Ontario, 71 p.

Faure, G. 1991. Principles and Applications of Inorganic Geochemistry. Macmillan Publishing Company, New York, Collier Macmillan Canada, Toronto, Maxwell Macmillan International, New York, Oxford, Singapore, Sydney. 626 p.

Flint, R.F. 1971. Glacial and Quaternary Geology. John Wiley and Sons, New York. p. 296-311.

Freez, R.A. and J.A. Cherry 1979. Groundwater. Printice Hall, New Jersey. 604 p.

Fritz, P., T.W. Anderson and C.F.M. Lewis, 1975. Late quaternary trends and history of Lake Erie form stable isotope studies. Science, Vol. 190, pp. 267-269.

Fritz, P.and J.C. Fonts 1980. Introduction. In: Fritz, P. and J.C. Fonts, eds., Handbook of Environmental Isotope Geochemistry: Vol. 1: The Terrestrial Environment. Elsevier, Amsterdam. 545 p.

Fullerton, D.S., 1980. Preliminary Correlation of Post-Erie Interstadial Events (16 000-10 000 B.P.), Central and Eastern Great Lakes Region, and Hudson, Champlain, and St. Lawrence Lowlands, United States and Canadian: United States Geological Survey Professional Paper 1089, 52 p.

Fulton, R.J., 1989. Summary: Quaternary Stratigraphy of Canada. In: Quaternary Stratigraphy of Canada: A Canadian Contribution to IGCP Project 24. Geol. Surv. Can., Paper 84-10, p. 1-5.

Furlong, R.B. 1968. Clay Minerals in the Gypsum Spring and lower Sundance Formations, Eastern Big Horn Mountains. WGA Earth Science Bulletin. p. 5-16.

Garrels, R.M. and C.L. Christ 1965. Solutions, Minerals and Equilibri. Harper and Row, New York, N.Y., 450pp.

Gilbert, G.K., 1890. Lake Bonneville. U.S. Geol. Survey, Monograph No. 1, pp. 438.

Grabar, E.R. and P. Aharon 1991. An improved microextraction technique for measured dissolved inorganic carbon (DIC), $\delta^{13}C_{DIC}$ and $\delta^{18}O_{H2O}$ from milliliter-size water samples. Chem. Geol. (Isot. Geosc. Sect.) 94: 137-144.

Grim, R.E 1951. The depositional environment of red and green shales: Jour. Sed. Pet., v. 21, p.226-232.

Grim, R.E. 1958. Concept of diagenesis in argillaceous sediments: Am. Assoc. Pet. Geol. Bull., v. 42, no. 2, p. 246-253.

Grim, R.E. 1968. Clay Mineralogy. McGraw-Hill, New York, 596p.

Hart, B.T. 1974. A Complation of Australian Water Quality Criteria. Caulfield Institute of Technical Paper No. 7. Australin Government Publishing Servece, Canberra.

Hough, J.L., 1958. Geology of the Great Lakes: Urbana, Illinois, University of Illinois Press, 313 p.

Intera Technologies Ltd. 1989. Hydrologic study of the Fresh Water Aquifer and Deep Geologic Formations Sarnia, Ontario. Volum 1. Report Prepared for Ontario Ministry of the Environment Detroit/St. Clair/St. Mary's Rivers Project by Intera Technologies Ltd. Ottawa, Ontario.

Jiwani, R.N. (1983). Contaminant Hydrogeology of the Walpole Island Indian Reserve Lambton County, Ontario, Canada. M.Sc. Thesis, University of Windsor, Windsor, Ontario. 250p.

Johnson, M.D., D.K. Armstrong, B.V. Sanford, P.G. Telford and M.A. Rutka (1992). Paleozoic and Mesozoic geology of Ontario. In: Thurston, P.C., H.R. Williams, R.H. Sutcliffe and G.M. Scott, eds., Geology of Ontario, Spec. Vol. 4(2): 907-1008.

Karrow, P.F. 1989. Quaternary geology of the Great Lakes subregion. In: Quaternary Geology of Canada and Greenland. Goel. Surv. Can., (1): 326-350.

Keller, W.D. 1956. Clay Minerals as influenced by environments of their formations: Am. Assoc. Pet. Geol. Bull., v. 40, p. 2689-2710.

Lerman, J.C. 1972. Soil-CO_2 and groundwater: carbon isotope compositions. Proc. 8th Int. Conf. Radiocarbon Dating, Wellington, 1972, 1: D93-D105.

Leverett, F. and Taylor, F.B., 1915. The pleistocene of Indiana and Michigan and the History of the Great Lakes: United States Geological Survey Monograph 53, 529 pp.

Lewis, C.F.M., 1969. Late Quaternary History of Lakes Levels in the Huron and Erie Basins: Proceedings 12th Conference on Great Lakes Recearch, International Association for Great Lakes Research, p. 250-270.

Lewis, C.F.M., 1970. Recent Uplift of Manitoulin Island: Canadian Journal of Earth Sciences, v. 7, p. 665-675.

Long, D.T., T.P. Wilson, M.J. Takacs and D.H. Rezabek 1988. Stable isotope geochemistry of saline near-surface groundwater. East-central Michigan basin. GSA Bull. vol. 100, pp.1568-1577.

MacFarlane, B. 1995. Grain Size Distribution and Mineralogy of the St. Clair River Delta Sediment. B.Sc. Thesis, University of Windsor, Windsor, Ontario. 45 p.

MacGregor, J.D. 1980. Petroleum Evaluation of the Walpole Island Indian Reserve No. 46. Unpubl. 31p.

Moore, D.M. and R.C. Reynolds, Jr. 1989. X-Ray Diffraction and the Identification and Analysis of Clay Minerals. Oxford New York, Oxford University Press.

Ontario Ministry of the Environment, 1991. Water Quality Data, Ontario Lakes and Streams 1987. Vol. XXIII, Southwestern Region.

Orion Research Incorporated Laboratory Product Group. Model 94-17B Chloride Electrode and Model 96-17B Combination Chloride Electrode Instruction Manual. p. 2-13

Park, R. and Epstein, S., 1960. Carbon isotope fractionation during photosynthesis. Geochim. Cosmochim. Acta, 21: 110-126.

Pezzetta, J.M., 1968. The St. Clair River Delta. Ph.D. Dissertation, Dept. Geol., Univ. of Mich., 193 p.

Pezzetta, J.M., 1973. The St. Clair River Delta: Sedimentary Characteristics and Depositional Environment. Journal of Sedimentary Petrology, Vol. 43, No. 1, pp. 168-187

Piper, A.M. 1944. A graphic procedure in the geochemical interpretation of water analysis. Trans. Amer. Geophys. Union, 25, pp.914-923.

Prest, V.K. 1984. The Late Wisconsinan glacier complex; in Quaternary Stratigraphy of Canada-A Canadian Contrivution to IGCP project 24, Geological Survay of Canada Paper 84-10, p.21-36.

Racz, M.A. 1994. Grain Size and Mineralogic Study of Channel Sediments, St. Clair Delta, Ontario. B.Sc. Thesis, University of Windsor, Windsor, Ontario. 66p.

Raphael, C.N., and E. Jaworski 1982. The St. Clair River delta: a unique lake delta. Geographical Bullten 21: 7-28.

Rubin, A.J. 1974. Aqueous-Environmental Chemistry of Metals. Ann Arbor Science Publishers INC., Ann Arbor, Michigan. 390 p.

Salomons, W. and W.G. Mook 1986. Isotope geochemistry of carbonates in the weathering zone. In: Fritz, P. and J.C. Fontes, eds., Handbook of Environmental Isotope Geochemistry: Volume 2: The Terrestrial Environment. Elsevier, Amsterdam. Ch. 6, p. 239-269.

Scott, S. 1986. An Oxygen-18 and Tritium Survey of the Fresh Water Aquifer, Lambton County, Ontario. B.A.Sc. Thesis, Dept. of Geology, University of Windsor, Ontario, 72 p.

Shilts, W.W., Aylsworth, J.M., Kaszycki, C.A. and Klassen, R.A. 1987. Canadian Shield; in Geomorphic System of North America, Geological Sociaty of America, Centinnial Special V. 2, P119-161.

Sklash, M.G 1984. Groundwater Quality Survey: ST. Anne Island, Walpole Island Indian Reserve, Ontario. Occasional Paper No. 2 (a) August 1984.

Sklash, M.G., S. Mason and S. Scott 1986. An Investigation of the quantity, quality and sources of groundwater seeping into the St. Clair River, near Sarnia, Ontario, Canada. Water Poll. Res. J. Canada, vol. 21, No 3, pp. 351-367.

Soderman, L.G. and Y.D. Kim 1970. Effect of groundwater levels on stress history of the St. Clair clay till deposit. Canadian Geotechnical Journal, 7, 173(1970).

Tai, W.K.Y. 1970. Water Hardness, Toxicity of Metals and Their Relationship to Cardiovascular Disease. National Health and Welfare, Public Health Division.

Throughton, J.H., 1972. Carbon isotope fraction by plants. Proc. 8th Int. Conf. Radiocarbon Dating, Wellington, 1972, 2: 421-437.

Tuker, M.E. 1981. Sedimentary Petrology. Blackwell Publishing London, 260 p.

Weaver, C.E. and L.D. Pollard 1973. The Chemistry of Clay Minerals. Elsevier, New York, 213p.

White, T. 1993. A Reconnaissance Isotope Chemistry Investigation of Carbonates from Goose Lake, Johnston Bay and Lake St. Clair, Ontario. B.Sc.Thesis. University of Windso, Windsor, Ontario. 69p.

Wightman, R.W. 1961. The St. Clair Delta. M.A. thesis Dep. of Geogr., Univ. of Western Ontario., London. 140 p.

Williams, T.J. 1988. An Environmental Isotope Survey of the Buried Bedrock Valley Near Sarnia, Ontario. B.A.Sc. Thesis, Department of Geology, University of Windsor, Ontario, 56 p. and Appendices.

Woolson, E.A. 1975. Bioaccumulation of aresenicals. In Aresenical Pesticides. Edited by E.A. Woolson, American Chemical Sociaty Symposium Series, Washington, D.C. pp. 97-107.

APPENDIX I

METHODOLOGY AND PRECISION TABLES

Chloride Determination

The measurement was performed by using the following required materials: pH/MV meter, magnetic stirrer, magnetic plate, 85 g of 5M of sodium nitrate ($NaNO_3$) as Ionic Strength Adjuster (ISA), standard solutions of sodium chloride (1000 μg/mL Cl) which was prepared by dissolving 1.6485 g/L NaCl in Milli-Q water, and four standards (1000, 100, 10, 1 μg/mL Cl) were prepared from the 1000 μg/mL Cl by taking 500, 50, 5 μg/mL, respectively for the first three standards and 5 μg/mL from the 10 μg/mL to prepare the 1 μg/mL standard. The analytical procedure was performed by using a millivolt meter readout and according to the following procedure. Each standard solution was brought up to 500 mL, the meter was calibrated with standard solution of 4 pH, 100 mL of the each standard solution was used and mixed with 2 mL of the ISA, stirred well and the voltage was recorded by placing the millivolt electrode in the each sample. A curve was plotted on semilogarthmic scale for all the standards (Fig. 1A). The same procedure of the standards was applied for each sample and the recorded voltage for all samples were plotted by using the calibration curve and the unknown Cl concentrations were determined.

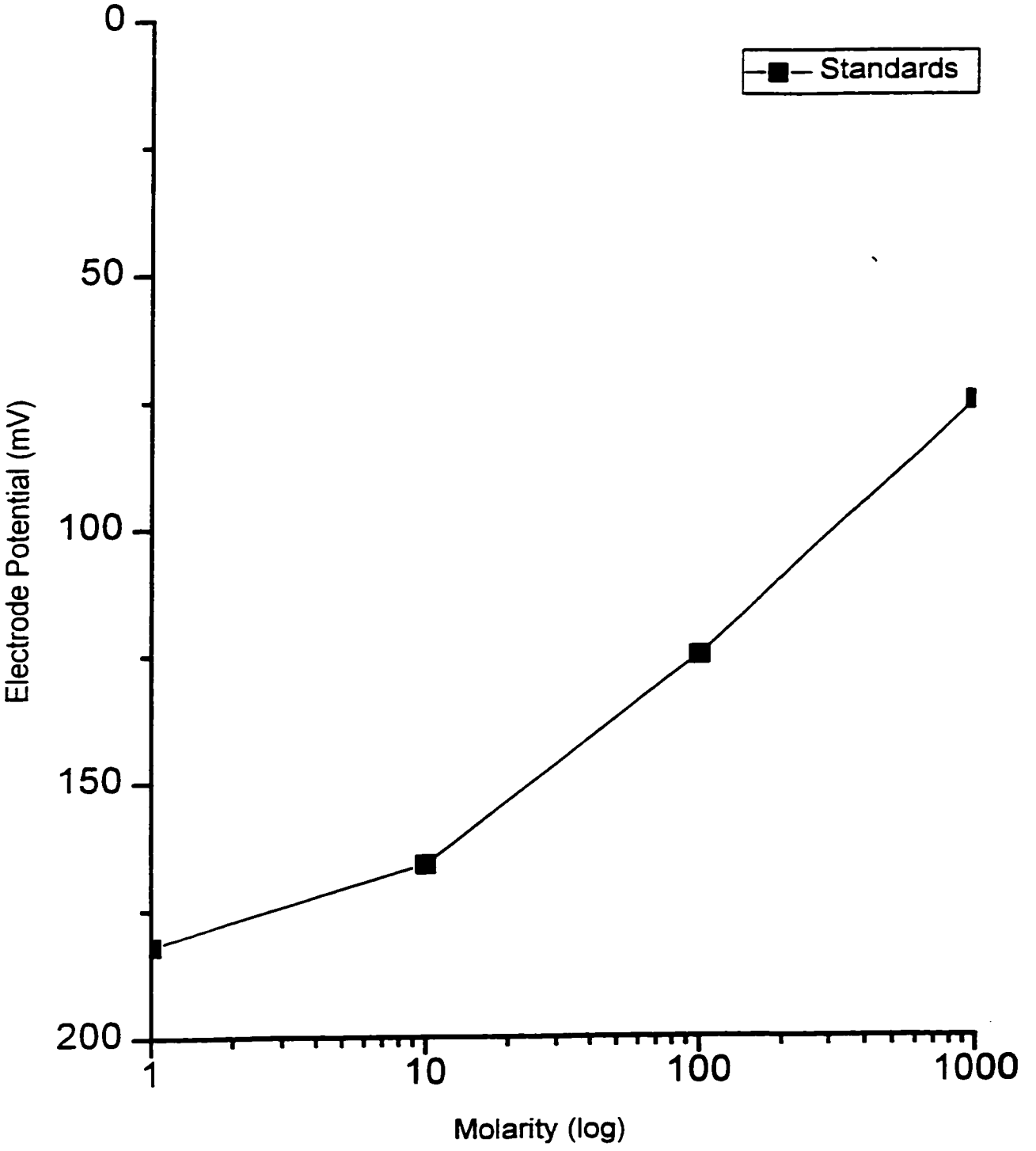

Fig. 1A. Chloride calibration curve.

Sulfate Determination by Turbidimeter Method

The required materials are: anhydrous sodium sulfate to prepare stock solution of 1000 μg/L by placing a 2 g of anhydrous sodium sulfate in an oven of 110°C for 2 hours, the dry sample was cooled in dissecator for 20 minutes and a weight of 1.4787 g of the dry sample dissolved in 1000 mL of Milli-Q water. Barium chloride was needed to prepare standards of 10, 20, 30, 40, 50, 60, 70, and 80 ug/mL and the volume for each standard was 2, 4, 6, 8, 10, 12, 14, and 16 mL of 1000 μg/L, respectively.

By pipetting the calculated volume for each standard from the stock solution into a well washed, 200 mL dry flask and each standard was placed in the spectrophotometer's cuvete to be analyzed and the result was plotted to get a calibration curve (Fig. 2A). The analytical procedure was performed by pipetting a specific volume of each sample in a 50 mL dry flask and brought up with Milli-Q water to volume, a 25 mL of the diluted sample was taken and mixed with barium chloride, stirred well and transferred to the spectrophotometer cell for analyzing. The cell has to be clean, facing the light of the spectrophotometer and a careful reading was recorded.

Each reading was plotted on the prepared calibration curve and the sulfate concentration was calculated as

$SO_4 = F * N$

Where F = flask volume (mL)/ sample volume (mL) and

N = the reading from the calibration curve.

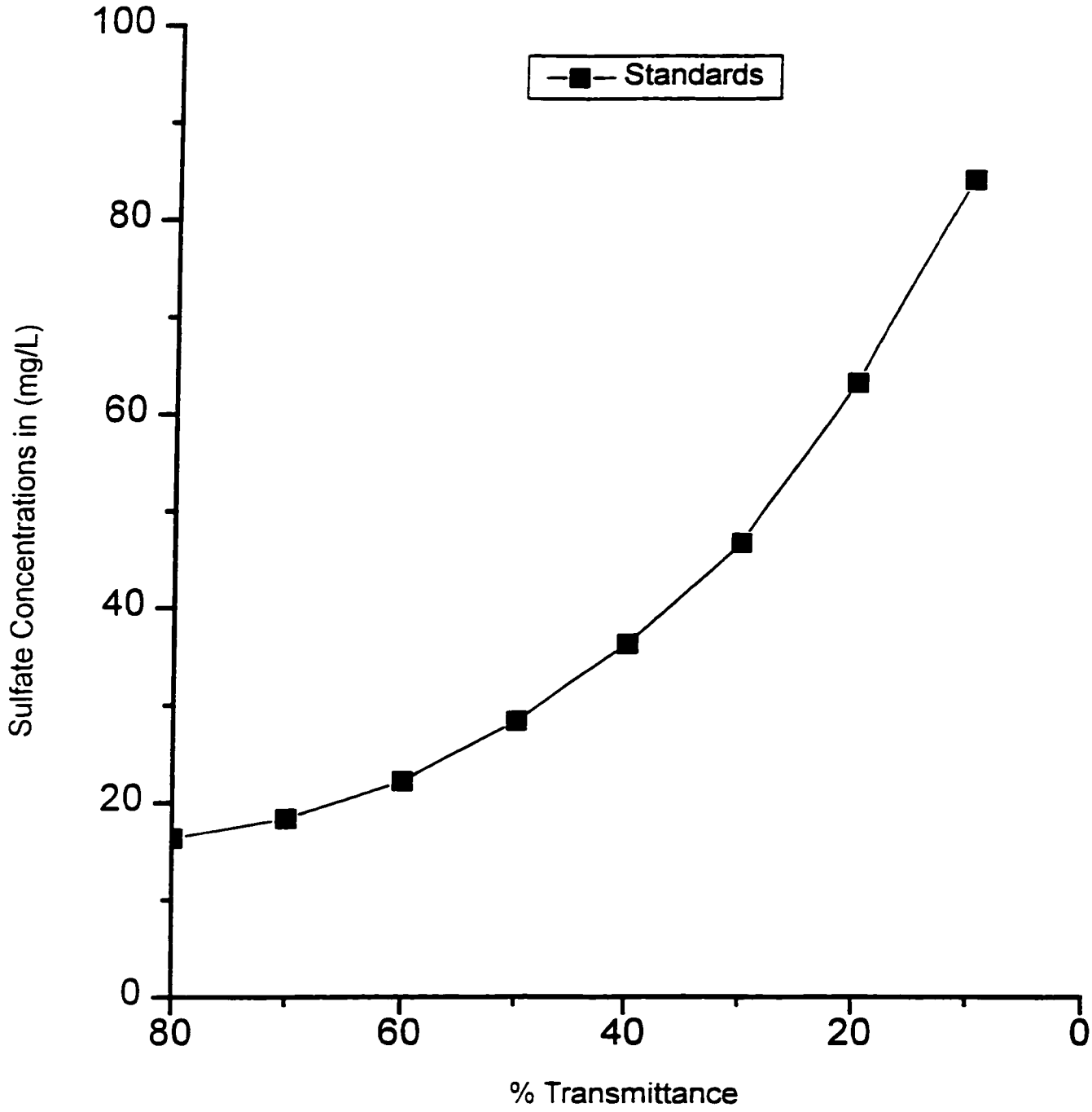

Fig. 2A. Sulfate calibration curve.

Alkalinity Determination

The materials, that were used to perform the analysis, are: indicators (phenolphthalein solution and mixed bromocresol green-methyl red indicator solution), 0.1N hydrochloric acid, 0.02 N hydrochloric acid, 0.02N sodium carbonate, 0.1N sodium hydroxide and 10% barium chloride. The phenolphthalein indicator was prepared by dissolving 0.5 g of the phenolphthalein in 25 mL 95% ethyl alcohol in 50 mL volumetric flask and the solution was brought up to volume by Milli-Q water. The bromocresol green-methyl red indicator solution was prepared by dissoving 0.02 g methyl red sodium salt and 0.1 g bromocresol green, respectively in 100 mL 95% ethyl alcohol. To prepare a 1 litre stock solution of 0.1N hydrochloric acid, 9.5 mL concentrated Hcl was required. The 0.02N hydrochloric acid was prepared by diluting 200 mL of the 0.1N the stock solution to 1 liter with Milli-Q water. The 0.02N sodium carbonate was prepared by dissolving 1.06 g in 1 liter Milli-Q water. The 0.02N hydrochloric acid was standardized against the 0.02N sodium carbonate by using the identical volumes of final solution. All water samples did not reach the phenolphthalein endpoint, therefore, the total alkalinity to pH 4 was calculated as follows:

Total alkalinity as $CaCO_3$ (mg/L) = B * N * 50 000 / mL sample

Where B = total mL titration for sample to reach second endpoint and,

N = normality of acid.

Table 1A. The analytical precision of trace metals and major ions

Well #	Ca (ppb)	%RSD	Mg (ppb)	%RSD	Na (ppb)	%RSD
OW1	161119	104	48497	90.7	44183	10.6
OW2	97195	1.47	22655	0.05	6204	0.24
OW4	153560	0.67	33034	0.18	8438	0.28
OW5s	267365	0.87	90777	2.1	171982	1.2
OW5d	81945	0.92	20292	0.55	38322	1.5
OW1A	137149	0.86	34604	0.75	20914	1.94
OW2A	110153	1.4	20011	0.48	20413	0.24
OW3A	103406	1.2	33574	0.8	14888	1.2
Method of analysis	ICP		ICP		ICP	
Limit of Detection (LOD)	25.6		106		17.5	

Well #	K (ppm)	%RSD	Fe (ppb)	%RSD	Al (ppb)	%RSD
OW1	1.1	0.94	1201		3.11	72.6
OW2	0.46	4.13	2204	0.3	40.81	5.23
OW4	1.45	0.79	106.07	6.8	52.66	8.9
OW5s	37.23	0.7	22.63	6	13.99	33.4
OW5d	0.91	1.1	498.29	1	30.93	9.4
OW1A	9.96	0.7	359.82	0.94	5.43	20.4
OW2A	2.55	0.53	239.5	1.2	5.46	25.1
OW3A	15.04	0.41	976.48	4.1	5.77	59.9
Method of analysis	ICP		ICP			
Limit of Detection (LOD)	0.16		1.01			

Well #	As (ppb)	%RSD	Cd (ppb)	%RSD	Co (ppb)	%RSD
OW1	11.4	94.7	0.22		8.72	173
OW2	2.2	71.1	0.13	173	2.95	67.5
OW4	5.37	78.3	0		4.62	23.8
OW5s	28.02	16.2	0.54	69.6	4.22	24.2
OW5d	7.04	51.2	0		5.22	22.6
OW1A	1.99	103	0		3.14	36.1
OW2A	7.83	43.4	0.04	173	4.2	38.2
OW3A	7.75	49.7	0.09	74.9	3.33	44.6
Method of analysis	ICP		GFAA		GFAA	
Limit of Detection (LOD)	17.91		0.01		0.14	

Table 1A. The analytical precision of trace metals and major ions

Well #	Cu (ppb)	%RSD	Mn (ppb)	%RSD	Pb (ppb)	%RSD
OW1	0	67.4	658.63		2.42	173
OW2	2.38	13.2	175.42	0.26	16.26	20.2
OW4	3.56	14.1	253.4	0.35	5.74	167.9
OW5s	0.63	82	583.58	0.47	1.88	90.7
OW5d	1.07	61.9	195.53	0.11	2.03	173
OW1A	1.06	30.9	276.66	0.27	1.45	173
OW2A	0		257.96	0.13	3.35	173
OW3A	0		212.93	0.17	2.68	173
Method of analysis	GFAA		ICP		GFAA	
Limit of Detection (LOD)	0.05		0.38		0.07	

Well #	V (ppb)	%RSD	Zn (ppb)	%RSD	Cr (ppb)	%RSD
OW1	0.91	65.2	1.78	46.1	0.22	109
OW2	3.53	15.2	5.25	4.1	0.48	86.9
OW4	1.94	34.7	4.65	5.1	0.99	14.8
OW5s	2.23	13.7	5.95	2.7	0.94	67.5
OW5d	1.87	12.8	2.79	2.4	0.14	173
OW1A	1.11	47.9	4.04	3	0	
OW2A	2.12	26.7	7.02	2.7	0.83	106
OW3A	0.88	74.2	4.17	8.2	0.61	165
Method of analysis	ICP		ICP		GFAA	
Limit of Detection (LOD)	1.22		1.06		0.09	

Well #	Ni (ppb)	%RSD	Sb (ppb)	%RSD
OW1	1.83	173	32.87	85.2
OW2	1.54	70.5	35.44	74.2
OW4	5.28	9.8	33.32	87.1
OW5s	4.24	24.2	43.05	76.2
OW5d	1.77	32.3	33.76	86.9
OW1A	1.22	60.5	35.11	84.7
OW2A	2.3	39.8	32.01	87.2
OW3A	2.68	63.4	35.83	86.8
Method of analysis	ICP		ICP	
Limit of Detection (LOD)	2.99		153	

APPENDIX II

XRD GRAPHS

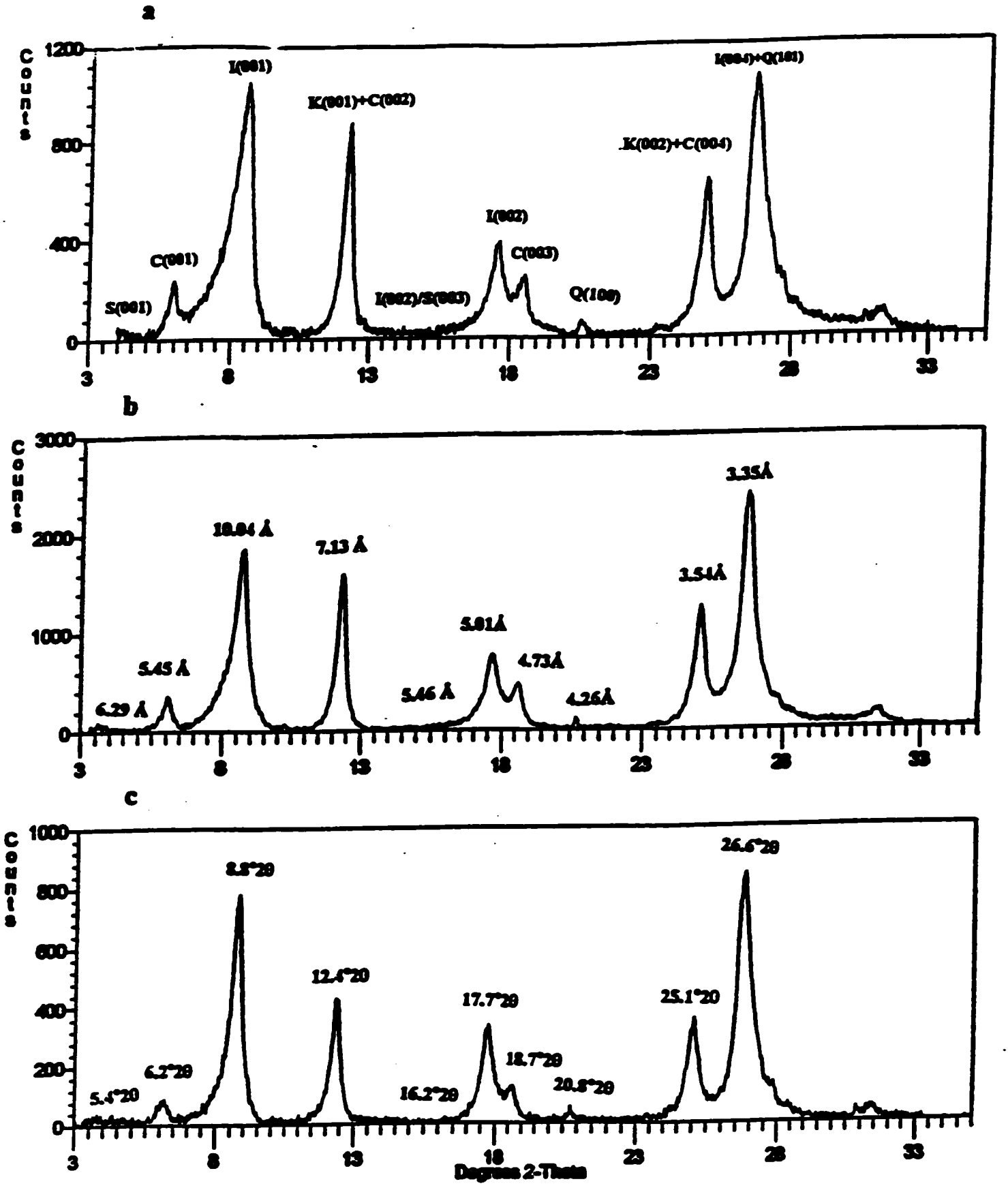

Fig. 1A. X-ray diffractogram pattern showing (a) air dried scan of clay minerals with their peaks. (b) glycolation scan of clay minerals with their d-space. (c) heat scan of clay minerals with 2θ values. Where I = illite, S = smectite, C = chlorite, and K = kaolinite.

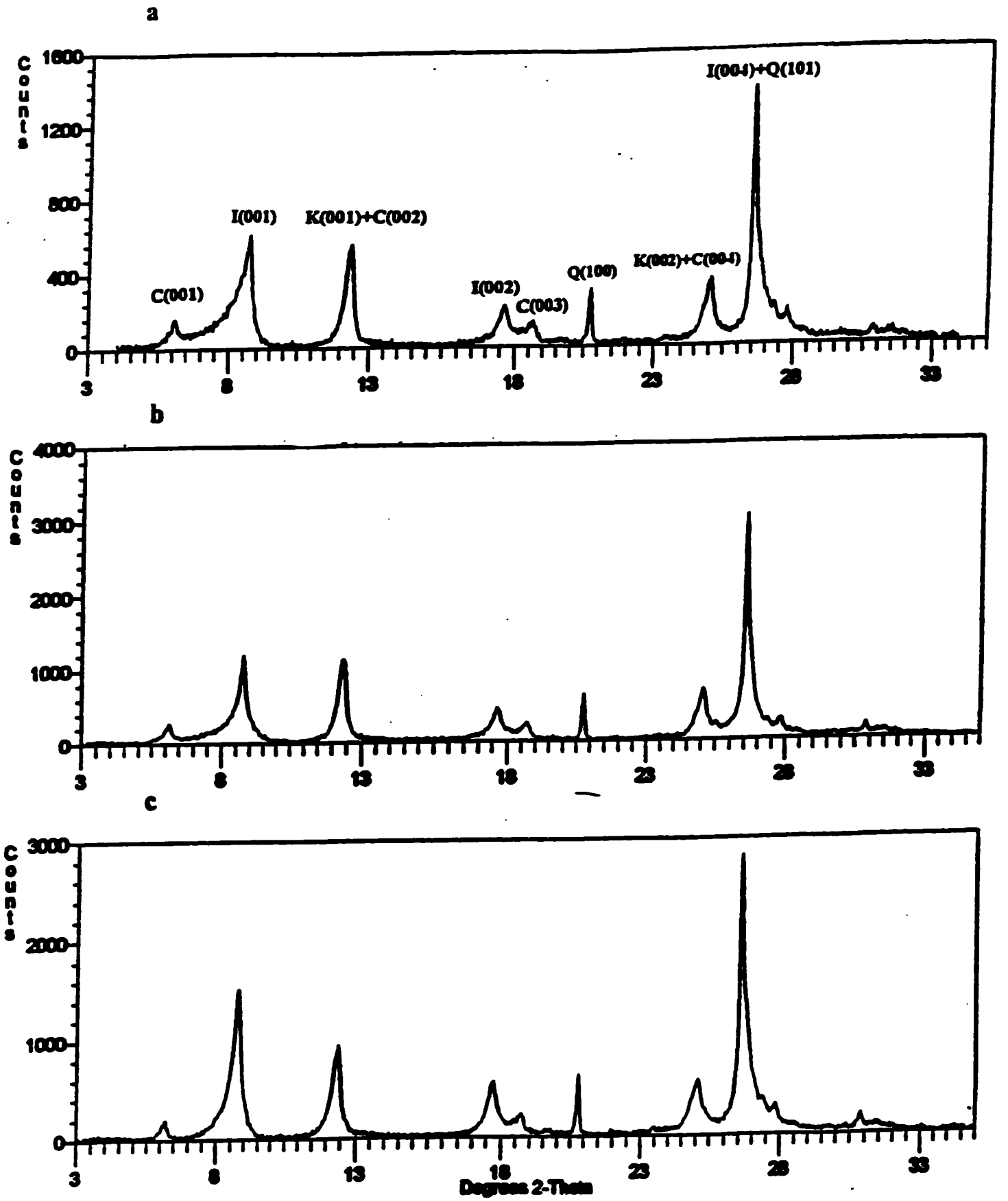

Fig. 2A. X-ray diffractogram pattern of core-HP8 at depth 11.5 m, the depth of highest quartz concentration showing (a) air dried scan. (b) glycolation scan. (c) heat scan. Where I = illite, S = smectite, C = chlorite, and K = kaolinite.

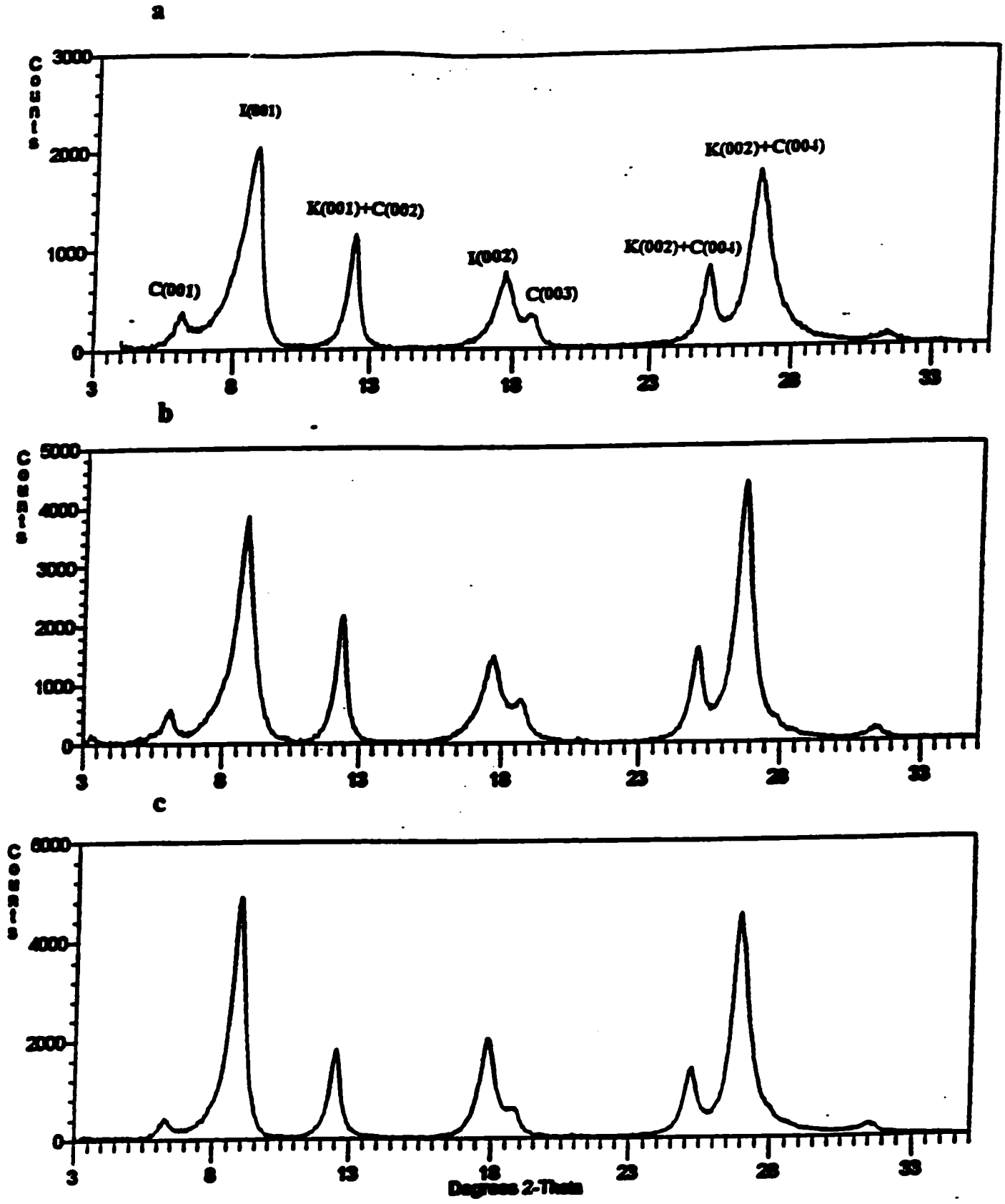

Fig. 3A. X-ray diffractogram pattern of core-HP10 at depth 13.74 m, the depth of minerals change with highest illite concentration showing (a) air dried scan. (b) glycolation scan. (c) heat scan. Where I = illite, S = smectite, C = chlorite, and K = kaolinite.

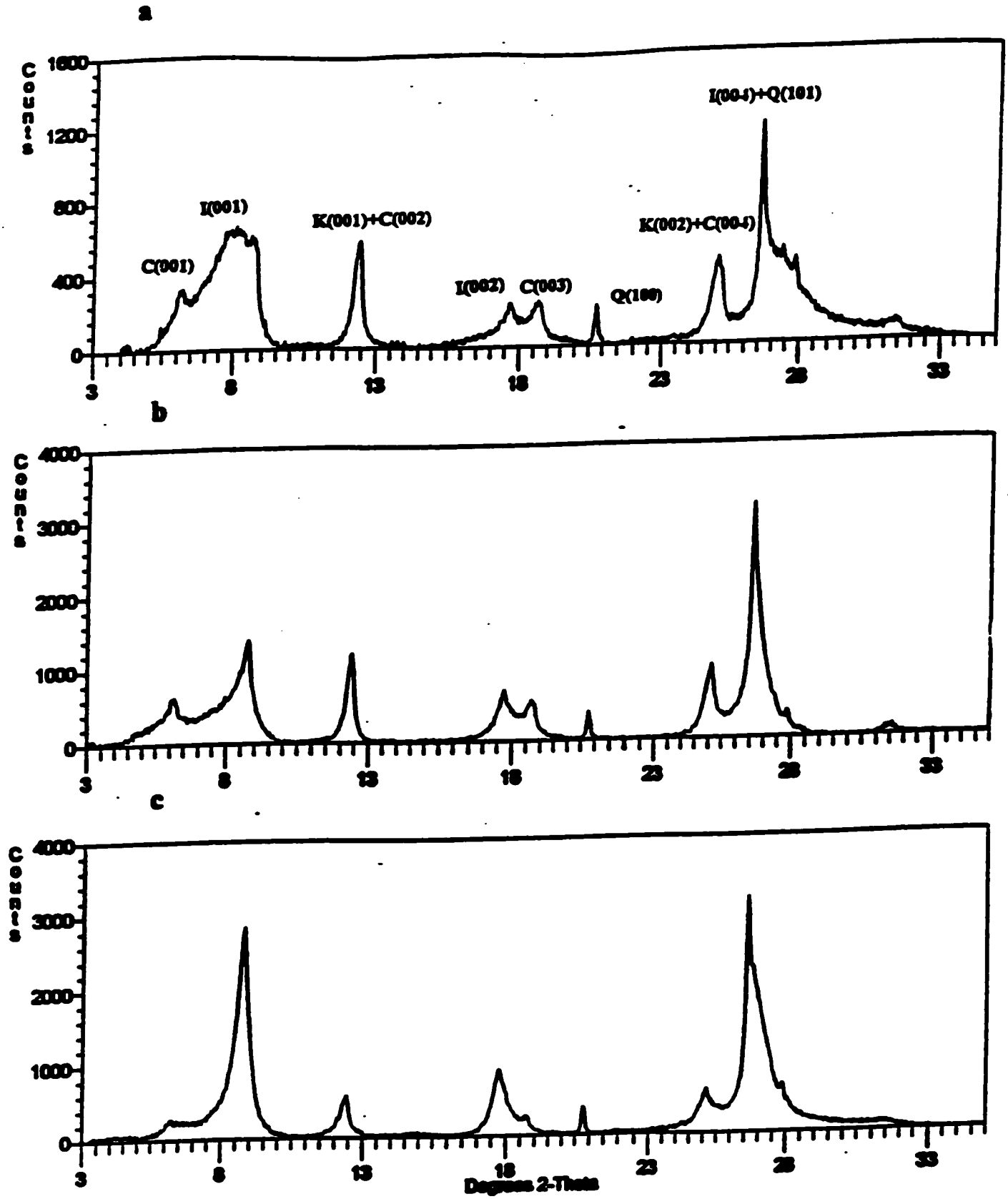

Fig. 4A. X-ray diffractogram pattern of core-GD3 at depth 3.64 m, the depth of green clay with no kaolinite and highest chlorite concentration showing (a) air dried scan. (b) glycolation scan. (c) heat scan. (a) and (b) pattern are showing the broad chlorite and illite peaks. Where I = illite, S = smectite, C = chlorite, and K = kaolinite.

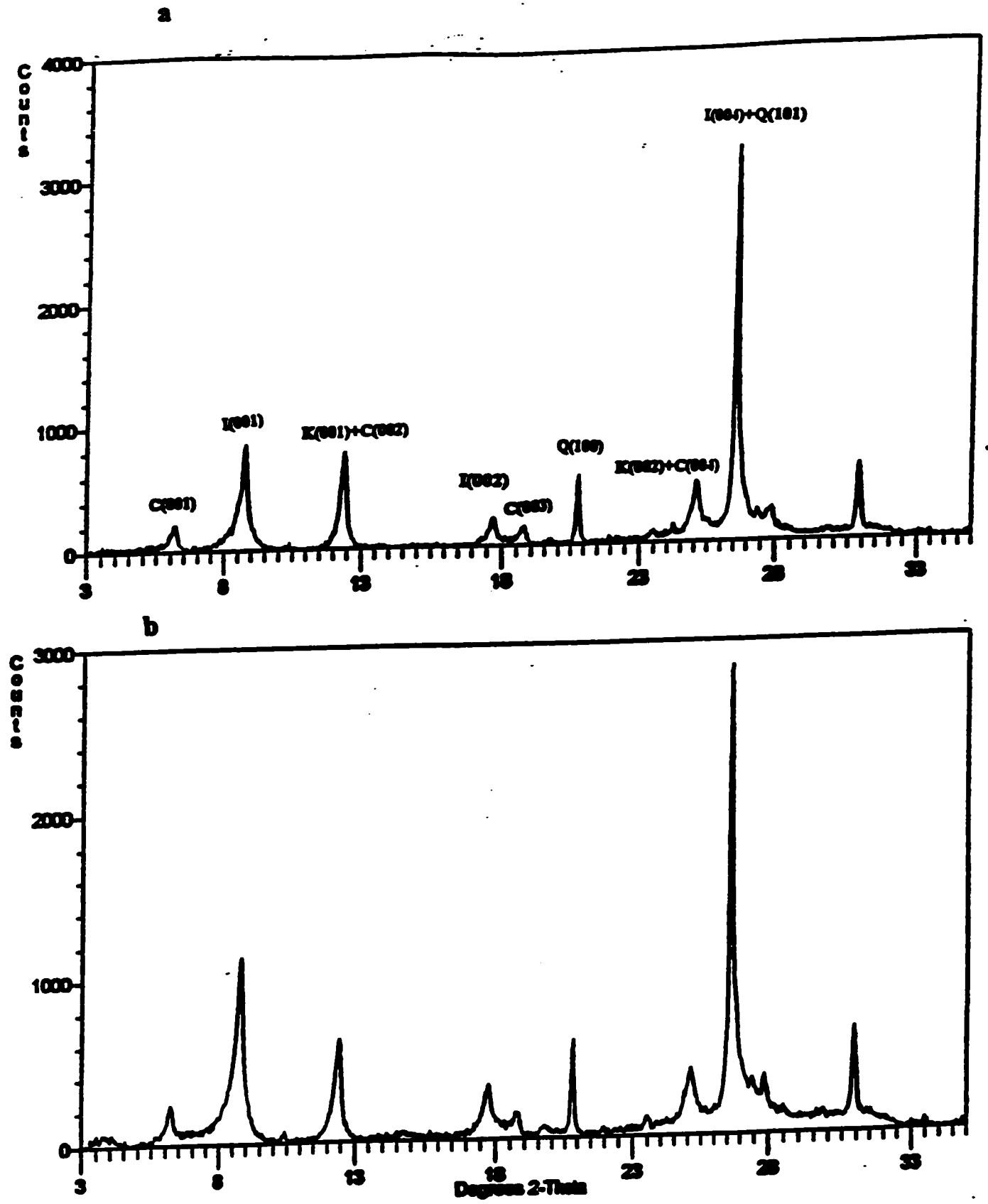

Fig. 5A. X-ray diffractogram pattern of core-GD6 at depth 7.71 m, the depth highest quartz concentration showing (a) air dried scan. (b) glycolation scan.

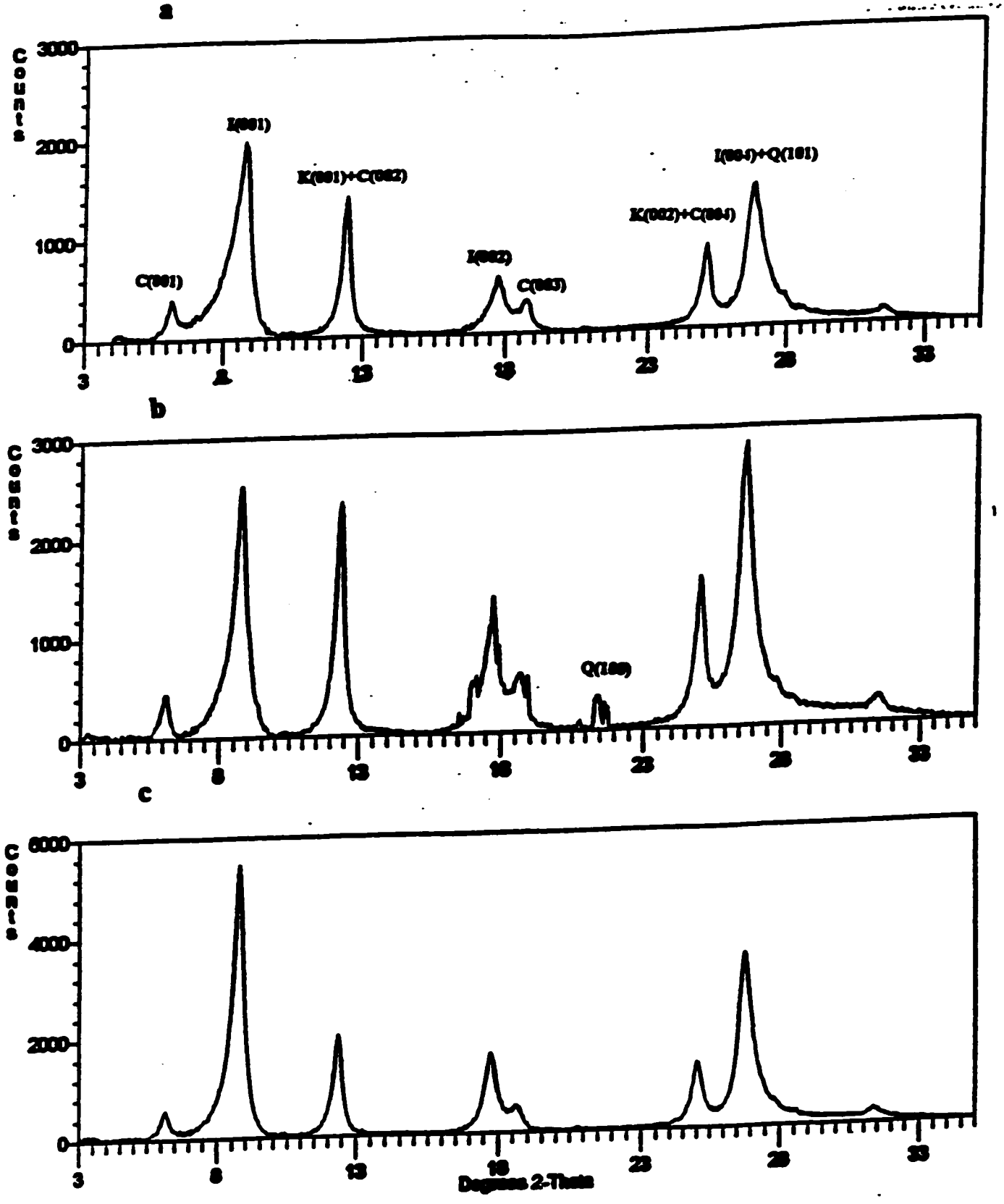

Fig. 6A. X-ray diffractogram pattern of core-GD13 at depth 16.78 m, the depth of highest illite and chlorite concentrations showing (a) air dried scan. (b) glycolation scan. (c) heat scan. Where I = illite, S = smectite, C = chlorite, and K = kaolinite.

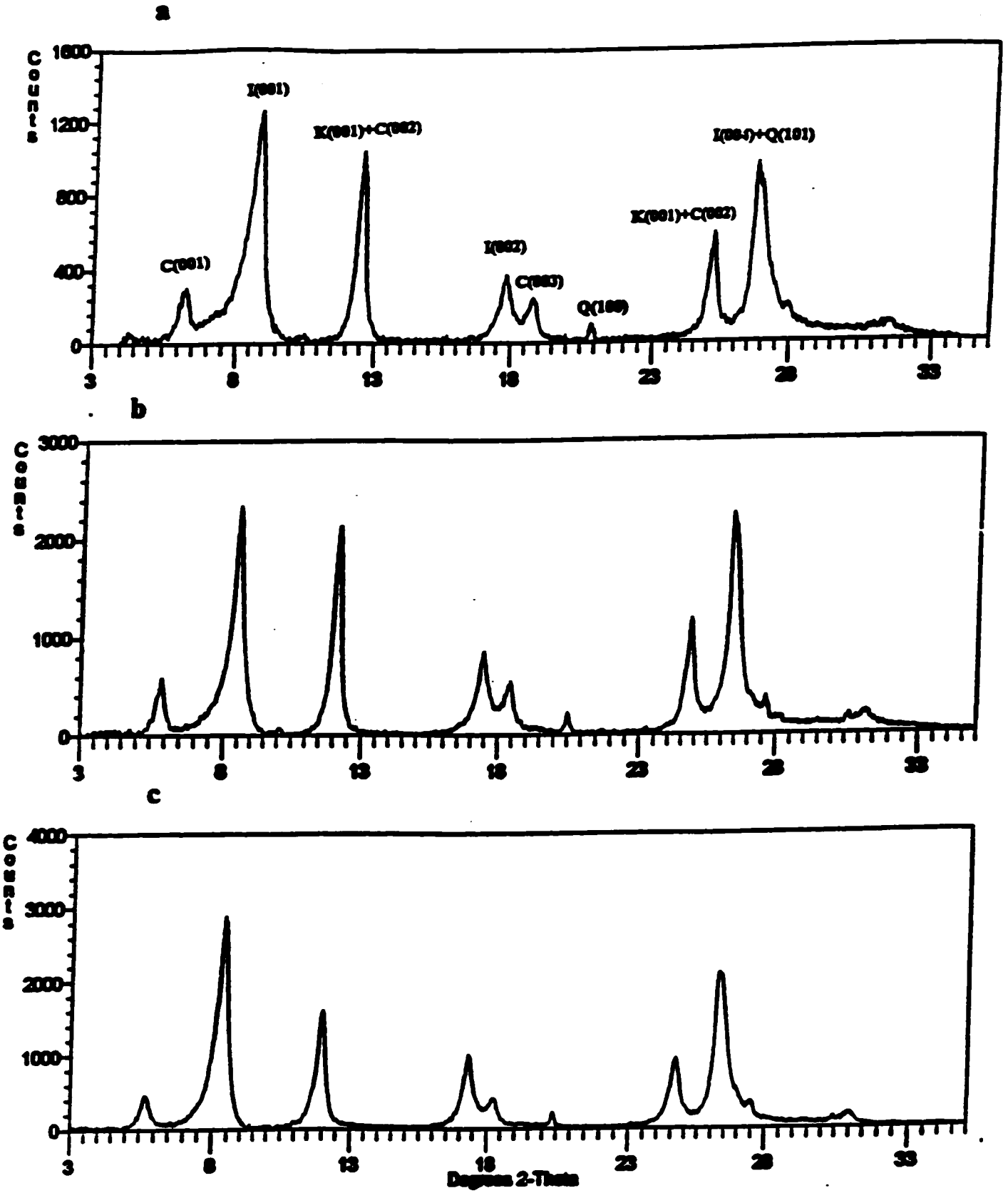

Fig. 7A. X-ray diffractogram pattern of core-GD18 at depth 24.31 m, the depth of highest kaolinite and lowest illite and chlorite concentrations showing (a) air dried scan. (b) glycolation scan. (c) heat scan. Where I = illite, S = smectite, C = chlorite, and K = kaolinite.

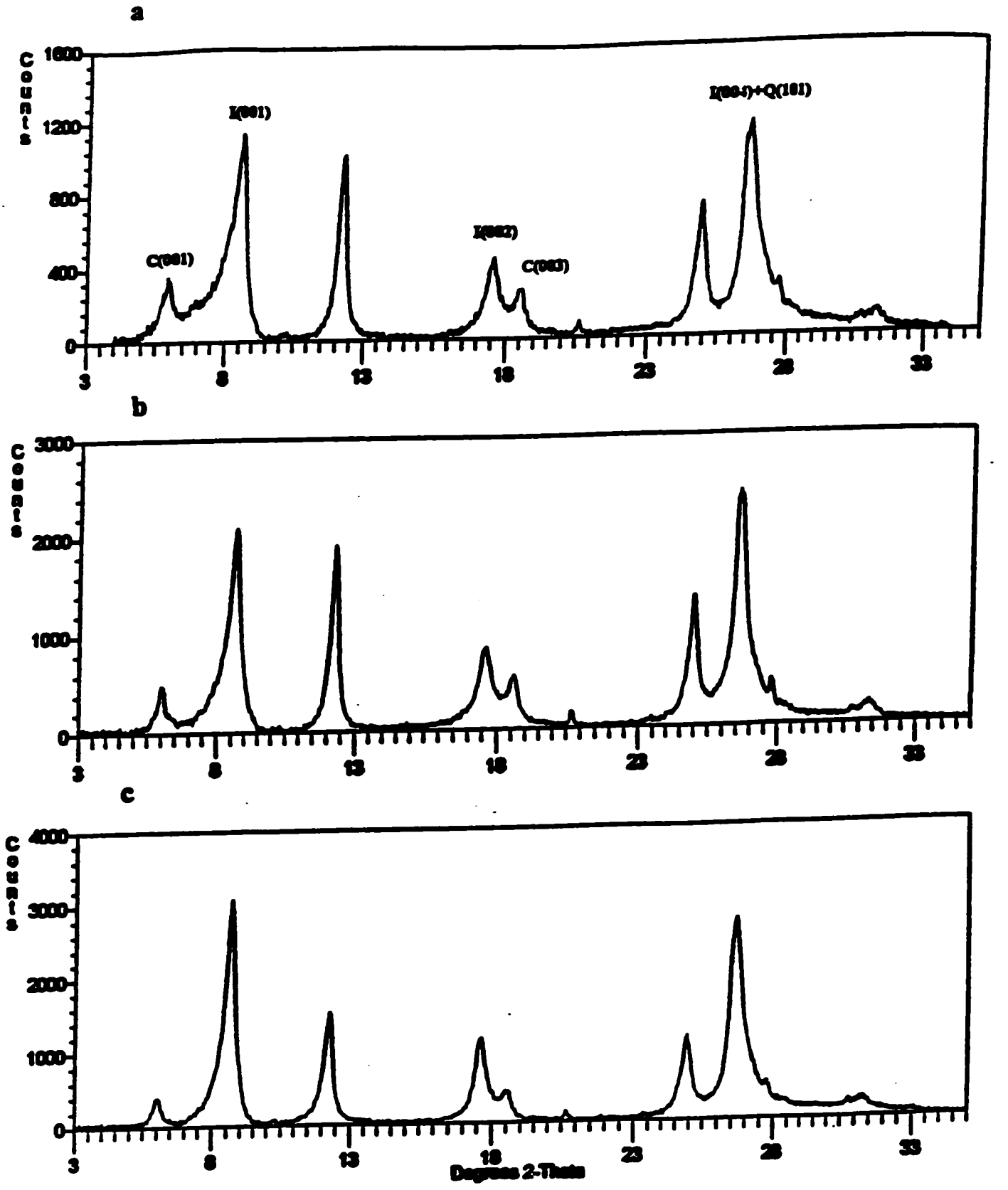

Fig. 8A. X-ray diffractogram pattern of core-GD21 at depth 29.24 m, the depth of no kaolinite and high illite and chlorite concentrations showing (a) air dried scan. (b) glycolation scan. (c) heat scan. Where I = illite, S = smectite, C = chlorite.

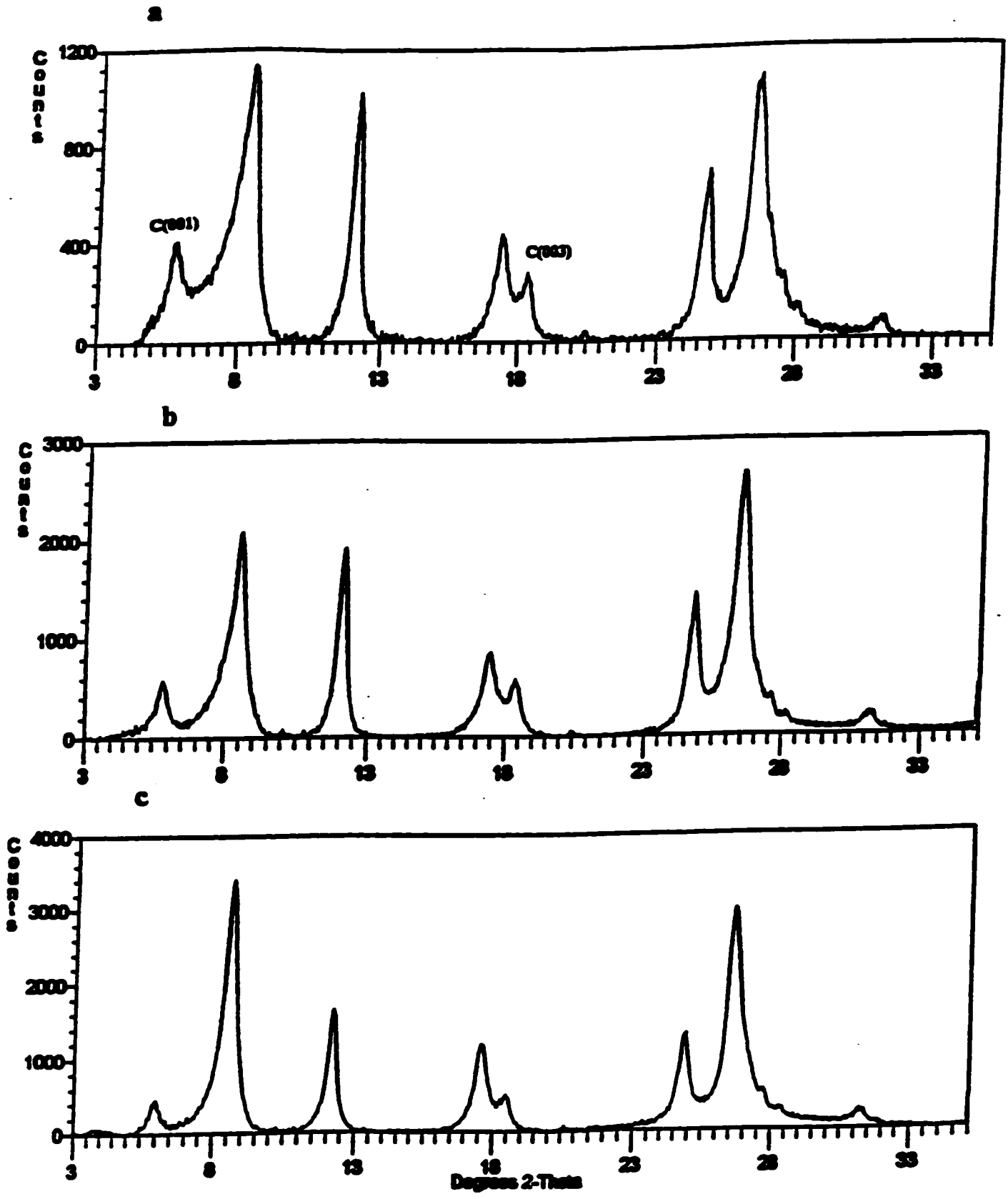

Fig. 9A. X-ray diffractogram pattern of core-DC10 at depth 13.1 m, the depth of no kaolinite, lowest quartz and highest chlorite concentrations showing (a) air dried scan. (b) glycolation scan. (c) heat scan.

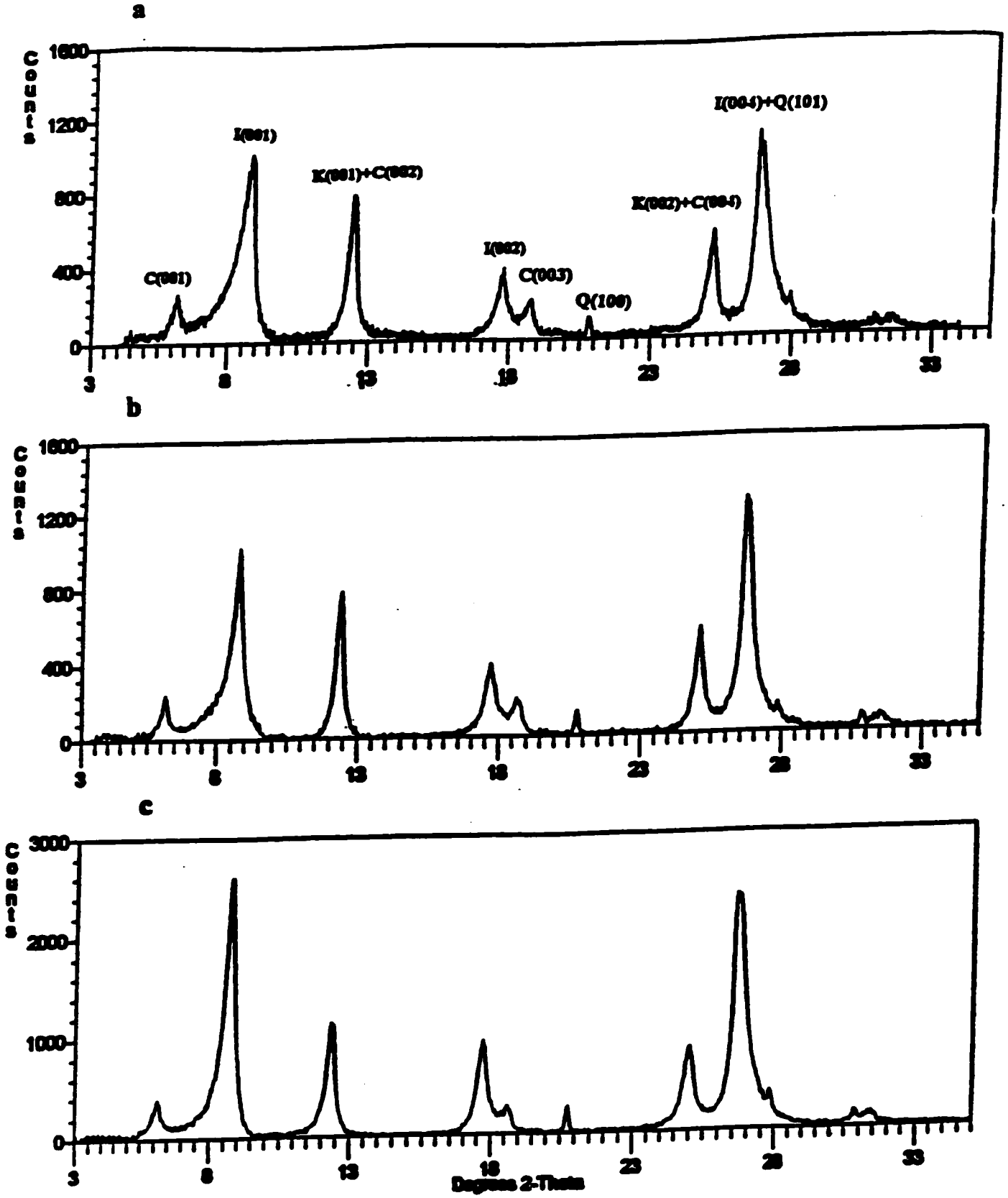

Fig. 10A. X-ray diffractogram pattern of core-DC14 at depth 19.2 m, the depth of high illite, chlorite, kaolinite,and quartz concentrations showing (a) air dried scan. (b) glycolation scan. (c) heat scan. Where I = illite, S = smectite, C = chlorite, and K = kaolinite.

APPENDIX III

CORE DESCRIPTION

Core	Depth from surface (m)	Core Description
HP1S1	0.00-0.78	Lithology: 1- Mineralogy: peat's, quartz; 2-Color: between pale yellowish brown 10YR 8/6 to dark yellowish orange 10YR 6/6. Texture: 1- grain size: medium sand; 2-grain shape: rounded 3-sorting/distribution: well sorted; 4- fabric/grain packing: tangential; 5- bedding: visible
HP1S2	0.78-0.99	Lithology: 1- Mineralogy: quartz; 2-Color: between dark yellowish brown 10YR 4/2 to light olive gray 5Y 5/2. 2-Texture: 1- grain size: fine sand; 2-grain shape: angular 3-sorting/distribution: poorly sorted; 4- fabric/grain packing: concave; 5- bedding: visible with angular inclusion pebbles and shales.
HP2S1	0.99-1.45	Lithology: 1- Mineralogy: quartz and mineral fragments; 2-Color: between pale yellowish brown 10 YR 6/2 to grayish orange 10 YR 7/4. Texture: 1- grain size: fine to coarse sand; 2-grain shape: angular to sub-rounded. 3-sorting/distribution: poorly sorted; 4- fabric/grain packing: concave; angular. 5- bedding: visible
HP2S2	1.45-2.51	Lithology: 1- Mineralogy: quartz; 2-Color: between light olive gray 5 Y 6/1 to greenish gray 5 GYM 6/1. Texture: 1- grain size: fine to coarse sand; 2-grain shape: angular to sub-rounded. 3-sorting/distribution: poorly sorted; 4- fabric/grain packing: concave; 5- bedding: loose sediment
HP3	2.51-4.04	Lithology: 1- Mineralogy: quartz, carbonate and organic material; 2-Color: between light olive gray 5 Y 6/1 to greenish gray 5 GY 6/1. Texture: 1- grain size: fine sand rich with pebble inclusion; 2-grain shape: well-rounded. 3-sorting/distribution: well sorted clast support; 4- fabric/ grain packing: concave; 5- bedding: massive bedding (ungraded)
HP4	4.04-5.56	Lithology: 1- Mineralogy: quartz and carbonate ; 2-Color: light olive gray 5 Y 6/1. Texture: 1- grain size: clayey-silt with fine to medium sand; 2-grain shape:well-rounded;3-sorting : well sorted; 4- fabric/grain packing: point contact;5- bedding: massive bedding
HP5	5.56-7.09	Lithology: 1- Mineralogy: quartz and carbonate ; 2-Color: light olive gray 5 Y 6/1 Texture: 1- grain size: clayey-silt; 2-grain shape:well-rounded;3-sorting: well sorted 4- fabric/grain packing: point contact;5- bedding: massive bedding

Table A2. Core-HP descriptions.

HP6	7.09-8.61	Lithology: 1- Mineralogy: quartz and carbonate ; 2-Color: light olive gray 5 Y 6/1
		Texture: 1- grain size: clayey-silt with fine sand; 2-grain shape: well-rounded; 3- sorting: well sorted;
		4- fabric/grain packing: point contact; 5- bedding: massive bedding
HP7	8.61-10.13	Lithology: 1- Mineralogy: quartz and carbonate ; 2-Color: medium bluish gray 5 B 5/1;
		light olive gray 5 Y 6/1 to greenish gray 5 GY 6/1. Texture: 1- grain size: clayey-silt with fine sand;
		and pebble inclusion 2-grain shape: well-rounded; 3- sorting: well sorted; 4- fabric/grain packing:
		point contact; 5- bedding: rhythmically layered with thickness of 3 to 5 mm; varve darken with depth
HP8	10.13-11.66	Lithology: 1- Mineralogy: quartz and carbonate ; 2-Color: dark greenish gray 5 G 4/1;
		Texture: 1- grain size: clayey-silt with fine sand;2-grain shape: well-rounded;
		3- sorting: well sorted; 4- fabric/grain packing: point contact;5- bedding: rhythmically layered.
HP9	11.66-13.18	Lithology: 1- Mineralogy: quartz and carbonate ; 2-Color: olive gray 5 Y 4/1;
		Texture: 1- grain size: sandy clayey-silt. 2-grain shape: well-rounded;
		3- sorting: well sorted; 4- fabric/grain packing: point contact. 5: bedding: rhythmically layered.
HP10	13.18-14.71	Lithology: 1- Mineralogy: quartz and carbonate ; 2-Color: light olive gray 5 Y 6/1;
		Texture: 1- grain size: clayey-silt. 2-grain shape: well-rounded;
		3- sorting: well sorted; 4- fabric/grain packing: point contact. 5: bedding: rhythmically layered.
HP11	14.71-16.23	Clayey-silt; carbonate rich; olive gray 5 Y 6/1; massive texture; non-sorted; shale claste and sand inclusions
HP12	16.23-17.75	Clayey-silt; carbonate rich; olive gray 5 Y 6/1; massive texture; non-sorted; shale claste and sand inclusions
HP13	17.75-19.28	Clayey-silt; carbonate rich; olive gray 5 Y 6/1; massive texture; non-sorted; shale claste and sand inclusions
HP14	19.28-20.8	Clayey-silt; carbonate rich; olive gray 5 Y 6/1; massive texture; non-sorted; clay inclusions
HP15	20.8-22.33	Clayey-silt; carbonate rich; olive gray 5 Y 6/1; massive texture; non-sorted.

Table A2. Core-HP description.

HP16	22.33-23.85	Clayey-silt; carbonate rich; olive gray 5 Y 6/1; massive texture; non-sorted, clay inclusions, carbonate and shale clasts
HP17	23.85-25.37	Clayey-silt; carbonate rich; light olive gray 5 Y 4/1; massive texture; non-sorted, clay inclusions, carbonate and shale clasts
HP18	25.85-26.9	Clayey-silt; carbonate rich; light olive gray 5 Y 4/1; massive texture; non-sorted, clay inclusions, carbonate and shale clasts
HP19	26.9-28.42	Clayey-silt; carbonate rich; light olive gray 5 Y 4/1; massive texture; non-sorted, clay inclusions, carbonate and shale clasts

Table A2. Core-HP description.

Core	Depth from surface (m)	Core description
GD1	0.00-1.22	Lithology: 1- Mineralogy: quartz and carbonate; 2-Color: dark yollowish brown 10YR 4/2.
		2-Texture: 1- grain size: medium to fine sand; 2-grain shape: subrounded to rounded.
		3-sorting/distribution:very well sorted; 4- fabric/grain packing: concave-convex; 5- bedding: visible with
		angular inclusions pebbles and shales.
GD2	1.22-2.74	Lithology: 1- Mineralogy: quartz and carbonate; 2-Color: dark yollowish brown 10YR 4/2.
		2-Texture: 1- grain size: fine sand matrix supported; 2-grain shape: subrounded
		3-sorting/distribution: well sorted; 4- fabric/grain packing: concave-convex; 5- bedding: visible with
		angular inclusions pebbles and shales.
GD3	2.74-4.27	Green clay from 3 to 4 m depth; lithology: 1- Mineralogy: carbonate-free; 2-Color: light olive 10 Y 5/4.
		Texture: massive; above the green clay, interlayered silt and fine sand.
		Below the green clay, clayey silt and concretions. Carbonate rich, well sorted .
GD4	4.27-5.18	Clayey-silt; lithology 1- mineralogy: carbonate rich, well sorted. 2- color: light olive gray 5 Y 6/1.
		texture: massive with shell fragments.
GD5	5.18-6.71	Clayey-silt; lithology 1- mineralogy: carbonate rich, well sorted. 2- color: greenish gray 5 G 6/1.
		texture: rhythmically thin layers (15 mm thickness) start at 5.5 m depth
GD6	6.71-8.23	Clayey-silt; lithology 1- mineralogy: carbonate rich, well sorted. 2- color: brownish gray 5 YR 4/1.
		texture: rhythmically layers with variable thickness (dark with depth), wet.
GD7	8.23-9.75	Clayey-silt; lithology 1- mineralogy: carbonate rich, well sorted. 2- color: brownish gray 5 YR 4/1.
		texture: rhythmically layers with variable thickness (10 mm), wet.
GD8	9.75-11.28	Clayey-silt; lithology 1- mineralogy: carbonate rich, well sorted. 2- color: brownish gray 5 YR 4/1.
		texture: rhythmically layers with variable thickness (5 mm), wet.

Table A3. Core-GD description.

GD9	11.28-12.8	Clayey-silt; lithology 1- mineralogy: carbonate rich, well sorted. 2- color: brownish gray 5 YR. 4/1.
		texture: rhythmically layers with variable thickness (4 mm), wet.
GD10	12.8-14.32	Clayey-silt; lithology 1- mineralogy: carbonate rich, well sorted. 2- color: light brownish gray 5 YR 6/1.
		texture: rhythmically layers with variable thickness (10 mm), wet, clay inclusions.
GD11	14.32-15.85	Clayey-silt; lithology 1- mineralogy: carbonate rich, well sorted. 2- color: brownish gray 5 YR 4/1.
		texture: rhythmically layers with variable thickness (5 mm), wet, clay inclusions.
GD13	15.85-17.37	Clayey-silt; lithology 1- mineralogy: carbonate rich, well sorted. 2- color: brownish gray 5 YR 4/1.
		texture: rhythmically layers with variable thickness (4 mm), wet, clay inclusions.
GD14	17.37-18.9	Clayey-silt; carbonate rich, non sorted, light brownish gray 5 YR 6/1. massive texture, wet, clay inclusions.
GD15	18.9-20.42	Clayey-silt; carbonate rich, non sorted, light brownish gray 5 YR 6/1, massive texture, wet.
GD16	20.42-21.91	Clayey-silt; carbonate rich, non sorted, light brownish gray 5 YR 6/1, massive texture, wet with small shale clasts.
GD17	21.91-23.47	Clayey-silt; carbonate rich, non sorted, light brownish gray 5 YR 6/1, massive texture, wet, with small chert clasts.
GD18	23.47-25.00	Clayey-silt; carbonate rich, non sorted, light brownish gray 5 YR 6/1, massive texture, wet, with clay inclusions

Table A3. Core-GD description.

GD19	25.00-26.52	Clayey-silt; carbonate rich, non sorted, light brownish gray 5 YR 6/1, massive texture, wet.
GD20	26.52-28.04	Clayey-silt; carbonate rich, non sorted, light brownish gray 5 YR 6/1, massive texture, wet with clay inclusions.
GD21	28.04-29.57	Clayey-silt; carbonate rich, non sorted, light brownish gray 5 YR 6/1, massive, wet with clay inclusions.
GD22	29.57-31.09	Clayey-silt; carbonate rich, non sorted, light brownish gray 5 YR 6/1, massive texture, wet with clay inclusions (5 mm).
GD23	31.09-32.61	Clayey-silt; carbonate rich, non sorted, light brownish gray 5 YR 6/1, massive, wet, with clay inclusions.
GD24	32.61-34.14	Clayey-silt; carbonate rich, non sorted, light brownish gray 5 YR 6/1, massive texture, wet, with clay inclusions (10 mm in length)
GD25	34.14-35.66	Clayey-silt; carbonate rich, non sorted, light brownish gray 5 YR 6/1, massive texture, wet, with clay inclusions (10 mm in length)
GD26	35.66-37.19	Clayey-silt; carbonate rich, non sorted, light brownish gray 5 YR 6/1, massive texture, wet, with clay inclusions.
GD27	37.19-38.71	Clayey-silt; carbonate rich, non sorted, light brownish gray 5 YR 6/1, massive, wet, with clay inclusions.
GD28	38.71-40.23	Clayey-silt; carbonate rich, non sorted, light brownish gray 5 YR 6/1, massive texture, wet with clay inclusions and angular shale.
GD29	40.23-41.75	Bedrock: black shale, fissile.

Table A3. Core-GD description.

Core	Depth from s	Core description
DC4	4.27-5.28	Sand: lithology: 1- Mineralogy: quartz rich; 2-Color: pale yellowish brown 10 YR 6/2.
		2-Texture: 1- grain size: medium to fine sand; 2-grain shape: very well rounded.
		3-sorting/distribution:very well sorted. 4- fabric/grain packing: point contact. 5- bedding: visible with
		clay inclusions and shales fragments.
DC5	5.28-6.78	Clayey-silt, lithology: 1-mineralogy: carbonate rich. 2- Color: light brownish gray 5 YR 6/1.
		texture: well sorted, well rounded, massive texture to very small lamina, and shell fragment.
DC6	6.78-8.31	Clayey-silt, lithology: 1-mineralogy: carbonate rich. 2- Color: dusky yellowish brown 10 YR 2/2.
		texture: well sorted, well rounded, rhythmically layered with thickness of 10 mm.
DC7	8.31-9.83	Clayey-silt, lithology: 1-mineralogy: carbonate rich. 2- Color: dark yellowish brown 10 YR 4/2.
		texture: well sorted, well rounded, rhythmically layered with thickness of 10 mm.
DC8	9.83-11.35	Clayey-silt, lithology: 1-mineralogy: carbonate rich. 2- Color: dark yellowish brown 10 YR 4/2.
		texture: well sorted, well rounded, rhythmically layered with thickness of 2 mm.
DC9	11.35-12.88	Clayey-silt, lithology: 1-mineralogy: carbonate rich. 2- Color: dark yellowish brown 10 YR 4/2.
		texture: well sorted, well rounded, rhythmically layered with thickness of 2 mm, clay inclusions, normal faulting.

Table A4. Core-DC description.

DC10	12.88-14.4	Clayey-silt, carbonate rich, dark yellowish brown 10 YR 4/2, well sorted, well rounded, rhythmically layered (1 mm.)
DC11	14.4-15.93	Clayey-silt, carbonate rich, dark yellowish brown 10 YR 4/2, massive, wet, normal faulting feature.
DC12	15.93-17.45	Clayey-silt, carbonate rich, dark yellowish brown 10 YR 4/2, massive to crudely stratified, wet, several chert clasts.
DC13	17.45-18.97	Clayey-silt, carbonate rich, dark yellowish brown 10 YR 4/2, massive to crudely stratified, wet, clay inclusions.
DC14	18.97-20.45	Clayey-silt, carbonate rich, dark yellowish brown 10 YR 4/2, massive-crudely stratified, wet, clay inclusions.
		The last metre of the core, coarse to medium-grained sand, compacted , wet and not sorted with angular shale clasts.
DC15	20.45-21.41	Bedrock : light greenish gray 5 GY 8/1 limestone.

Table A4. Core-DC description.

VITA AUCTORIS

NAME:	Jamilh Mohammad Mohsan Shareef
Birth:	Najaf, Iraq, 1958.
Education:	Diploma, Al-Mustansyria University, Baghdad, Iraq, 1979. B.Sc., Al-Mousal University, Mousal, Iraq 1981. M.Sc., University of Windsor, Windsor, Ontario, 1997.